Institutt for Bygg og Energiteknikk

Energi og Miljø i Bygg - Master

Master's thesis

MAEN 5900-1

Anders Strand - s315795

Supervisors

Moon Keun Kim

Ørnulf Kristiansen

2021

CANDIDATE NR.
100
AVAILABILITY
OPEN

Institutt for Bygg- og energiteknikk Telefon: 67 23 50 00

Postadresse: Postboks 4. St. Olavs plass, 0130 Oslo www.oslomet.no

Besøksadresse: Pilestredet 35, Oslo

Master's thesis

Master's thesis title	DATE
Comparative energy analysis and performance estimation of decentralized ventilation control strategies in local Norway climate	09.06.2021
AUTHOR	SUPERVISORS
Anders Strand	Moon Keun Kim Ørnulf Kristiansen
IN COLLABARATION WITH	CONTACT PERSON
OsloMet	Moon Keun Kim

SUMMARY

The work evaluates the decentralized ventilation technology and control strategy combinations in local Norway climate using a representative decentralized ventilation unit molded from scientific data and field measurements. The control strategy combinations are evaluated with respect to comfort and primary energy consumption. For this purpose a comprehensive comparative energy analysis is conducted based on a monthly time-step energy analysis and the dynamic simulation assessment tool IDA ICE. The results show that the control strategy based on temperature regulation with ventilation cooling is the recommended control strategy, as the low SFP of the decentralized ventilation unit can efficiently use ventilation as zone cooling.

3 KEYWORDS:
Decentralized ventilation
Control strategies
Comparative energy analysis

Acknowledgements

I would like to express my gratitude to my internal supervisor Dr. Moon Keun Kim for his guidance and constructive suggestions for improving my thesis. His willingness to give his time so generously has been very much appreciated.

Assistance, expertise and constant availability over e-mail provided by my external supervisor Ørnulf Kristiansen was also greatly appreciated.

Oslo Metropolitan University

Oslo, Juni 2021

Signature

Abstract

The present work evaluates different decentralized ventilation control strategy and supply temperature regulation strategy combinations in local Norway climate and is the main focus.

Field measurements on decentralized ventilation systems are utilized, which is further applied to mold a representative decentralized ventilation unit for evaluation of energy performance in a single-person reference zone. Evaluation is performed using a monthly time-step energy analysis, and the IDA ICE simulation tool for a comparative primary energy analysis on the strategy combinations, while simultaneously agreements of the national requirements are upheld. Primary energy comparison is conducted with respect to a centralized constant air volume (CAV) system, which is compared with all decentralized ventilation strategy combinations for a full comprehensive comparative analysis. The strategy combinations are assessed with respect to comfort criteria for a better understanding of the strategy potential. Assessment of the decentralized ventilation heat recovery unit applicability in local Norway climate is conducted based on seasonal energy analysis. Furthermore, the strategy combinations are tested with respect to higher occupancy zones, and also by using commercially available decentralized ventilation unit specifications for a wider understanding of the decentralized ventilation potential in local Norway climate.

The results of the evaluation show that the representative decentralized ventilation system has the greatest energy performance under demand controlled ventilation control strategies, as the lower heat recovery efficiency is less utilized in the cold climate, and the low specific fan power can efficiently be used for zone cooling in summer.

If the commercially available decentralized ventilation system does not exaggerate the given specifications, the decentralized ventilation technology has great potential in Norway climate due to the high heat recovery unit efficiency and low specific fan power, and supply air strategies such as natural fan-assisted ventilation and temperature regulation, in combination with the superior room-by-room/personalized ventilation control strategy possibilities.

Keywords – Decentralized ventilation, Control strategies, Comparative energy analysis

Sammendrag

Arbeidet evaluerer ulike desentraliserte ventilasjonskontrollstrategier- og tilluftstemperatur-reguleringskombinasjoner for lokalt Norsk klima og er hovedfokuset i oppgaven.

Feltmålinger på desentraliserte ventilasjonssystemer benyttes som videre brukes til å forme en representativ desentralisert ventilasjonsenhet for evaluering av energieffektivitet i en enkeltpersons referansesone. Evaluering utføres ved hjelp av en månedlig gjennomsnittlig energianalyse, og ved hjelp av IDA ICE-simuleringsverktøyet for en komparativ primær-energianalyse av strategikombinasjonene, samtidig som nasjonale krav opprettholdes. Primær-energisammenligning utføres med hensyn til et sentralisert system med konstant luftvolum (CAV), som sammenlignes med alle desentraliserte ventilasjons-strategikombinasjoner for en fullstendig omfattende komparativ analyse. Strategikombinasjonene blir vurdert med hensyn til komfortkriterier for bedre forståelse av strategipotensialet. Vurderingen av den desentraliserte ventilasjonenhetens varmegjenvinningsevne analyseres basert på sesongbaserte energianalyser. Videre testes strategikombinasjonene med tanke på soner med høyere personlaster, og også ved bruk av kommersielt tilgjengelige desentraliserte ventilasjonsenhets spesifikasjoner for en bredere forståelse av det desentraliserte ventilasjonspotensialet i det Norske klimaet.

Resultatene av evalueringen viser at det representative desentraliserte ventilasjonssystemet har best energieffektivitet under temperaturbehov-styringsstrategier, da den lavere varmegjenvinningseffektiviteten blir mindre utnyttet i det kalde klimaet, og den lave spesifikke vifteeffekten effektivt kan brukes til kjøling om sommeren.

Hvis det kommersielt tilgjengelige desentraliserte ventilasjonssystemet ikke overdriver de gitte spesifikasjonene, så har den desentraliserte ventilasjonsteknologien et stort potensial i det Norske klimaet på grunn av den høye varmegjenvinningseffektiviteten og den lave spesifikke vifteeffekten, og tilluftsstrategier som naturlig vifte-assistert ventilasjon og temperaturregulering, i kombinasjon med rom-til-rom/personlig ventilasjon kontrollstrategi muligheter.

Nøkkelord – Desentralisert ventilasjon, Kontrollstrategier, Komparativ energi analyse

Abbreviations and descriptions

ACH Air change per hour

AHU Air handling unit

AM 150 Commercially available decentralized ventilation unit from Airmaster

CASE Supply temperature regulation strategy (case 1, case 2 and case 3) inspired from SvalVent research

CAV Constant air volume

CO_2 Carbon dioxide (indoor air quality indicator)

D-CO_2 Dynamic/step-less proportional to CO_2 concentration ventilation control strategy

DCV Demand controlled ventilation

DeAL Evaluation study on decentralized ventilation systems (scientific article)

DV Decentralized ventilation

FTDVS Field tests decentralized ventilation system (scientific article)

HVAC Heating, ventilation and air conditioning

IAQ Indoor air quality

IDA ICE IDA Indoor Climate and Energy (building simulation software)

$L_{p,Aeq}$ A-weighted average sound pressure (A-weighted because it is how humans perceives sound)

$L_{p,AF,max}$ Highest measured A-weighted sound pressure in a given time interval

PIR Passive InfraRed (occupancy detection sensor)

PMV Predicted mean vote

PPD Percentage of dissatisfied

Representative DV unit A decentralized ventilation unit with specifications based on scientific literature and field measurements, which are used to produce main comparison findings for the DV unit technology control strategies

S-CO_2 Static/n-step proportional to occupancy load ventilation control strategy using CO_2 concentration upper limits

SFP Specific fan power

TEK 17 Norwegian building code

VAV Variable air volume

HRU Heat recovery unit

External references (articles, books etc) and internal references (figures, tables etc) are all hyperlinked (not including internal references directly below the reference itself). Decentralized ventilation units are hyperlinked to their respective webpage.

List of Figures

List of Tables

Table of contents

1 Introduction

1.1 Background

Buildings account for 40 % of the global energy consumption and one-third of global CO_2 emissions (Kim et al., 2014) (Hepbasli, 2012), and in Norway, it is estimated that around 45 % of the total energy usage to buildings are accumulated from commercial buildings (Grini et al., 2010). It is estimated that heating, cooling, and mechanical ventilation for residential and service buildings represent more than half of this energy consumption, where it is also estimated that infiltration and ventilation is one of the main contributors, although that percentage varies with climatic, building, and HVAC context (Santos and Leal, 2012). Progressively strengthening energy demands in the Norwegian building code are done to ensure as little energy waste as possible to reduce the amount of greenhouse gas emissions, reduce air pollution, and protect the future generations from not being able to cover their needs of energy. These energy demands come in the shape of better insulation of the building shell, higher heat recovery unit efficiencies, lower specific fan power values, lower thermal bridge values, and more airtight buildings which lowers infiltration rates. As these demands augment in strictness, the heat losses across the building envelope decreases, which has activated the need for better solutions and control strategies in the ventilation technology to further lower the building energy demand, while simultaneously satisfying the thermal and indoor air quality comfort demands.

With decentralized ventilation, the mechanically allocated air flows are directly transported through the façade rather than by a single centralized large air handling unit by transportation through a net of ductwork, so that concerning the stricter energy demands, decentralized ventilation units offer lower SFP values than a centralized ventilation system. This is because even though bigger fans are accompanied by greater fan efficiency, the missing ductwork leads to lower pressure losses and thus lower power consumption (Merzkirch et al., 2016). Missing ductwork also contributes to relative energy savings regarding occurring air leakages in the transportation from the air handling unit to its designated location in centralized systems which was found to be as high as 36 % (Modera, 2013).

The missing ductwork also brings the advantage of removing the false ceiling which is necessary for hiding and containing the centralized ventilation system. This reduction height can be 30 cm or more, which means an additional floor for every 10 floors, which will save building volume and increase the density efficiency of the area of each high rise building (Mahler and Himmler, 2008). Looking at the 20 tallest buildings in Oslo, there are a total of 377 floors, and if they were built with decentralized ventilation instead, it would save an entire 38 floors of building volume from a purely mathematical perspective if they were originally built with a centralized ventilation system. A study on wind loading found that by using a complex network topology of decentralized units, further energy savings concerning fan power can be achieved by manipulating the pressure gained by wind loading, which can be done through an overcapacity of fans (Baldini et al., 2008), allowing further advantage over centralized systems by manipulating natural forces.

An important energy-related advantage is the easier implementation of room-by-room/personalized ventilation control strategies as a decentralized system can individually ventilate single rooms, which can optimize the comfort aspects individually to each user without compromising the comfort for other users, as comfort is documented to be subjective, such as the difference between operative temperatures between women and men (Kingma and van Marken Lichtenbelt, 2015), and the differences in air velocity concerning the temperature (Schiavon et al., 2010). This could be individually controlled using active supply diffusers with variable slot opening permitting draught-free air rate adjustment with moving plates changing position (Rabani et al., 2019). Studies have shown that personalized ventilation may improve users' health, inhaled air quality, thermal comfort, user satisfaction, and productivity, while simultaneously having the potential for reduction of energy consumption (Schiavon et al., 2010) (Haynes, 2008).

Viewing the elimination of the centralized ductwork system from a construction perspective, the avoidance of multiple air distribution network components such as air ducts, fire dampers, and regulating dampers are achieved which further reduces the economic costs of maintenance, although the implementation of many DV units to replace these components are also followed with maintenance costs which are typically higher because of the high number of installed devices to fulfill the ventilation demands of the whole building (Bonato et al., 2020). In addition to this, solutions for effectively ventilating the core of the building and other areas far from the facade need to be implemented to fulfill the strict demands of the Norwegian building code. Another DV unit related issue is the noise emissions from the DV unit, as it is placed in the same room as the occupant, and the difficulty in regulating optimal indoor relative humidity as problems of too dry air has been noted during the winter season (Mahler and Himmler, 2008) (Gruner and Haase, 2012).

The profitability of ventilation control strategies is well documented concerning the centralized ventilation system (Mysen et al., 2005), although when considering the typical differences which are present in decentralized ventilation units, such as improved SFP, lower HRU efficiency, lower tolerance of maximum air rates due to noise emission and increased availability of controlling the supply air temperature, the control strategy comparison might reveal more interesting results. The investment costs of the DV system and equipment are also of importance, as better energy performing control strategies are typically more investment heavy (Mysen et al., 2003). The available variety of DV units are numerous, and so is the amount of different engineering designs to choose from, so that the best control strategy to choose will therefore heavily rely on the type of DV unit. This means that the cost-effectiveness of the ventilation control strategy is not always guaranteed, as it depends on both DV unit design, HVAC features, climate, zone type, and building use (Santos and Leal, 2012).

1.2 Aim and objective

The main question present in this thesis is:

- Which ventilation control strategy combination is best suited for the decentralized ventilation technology in local Norway climate concerning primary energy consumption?

The minor questions are:

- How does the decentralized ventilation technology fair concerning a conventional centralized CAV system in primary energy consumption?
- What are the consequences of decentralized ventilation control strategies concerning comfort?
- Of which significance is the HRU in the decentralized ventilation system in local Norway climate?

1.3 Limitations

Research and scientific literature does not always contain the specifics required for certain calculations such as SFP and HRU efficiencies at all air rates, with different filters, and such, which enforces simplifications to be made. These simplifications are made in the shape of constant values derived from field measurements, and dismissing certain complications which may impact energy consumption and ventilation demands, as they are not well enough documented. The energy-related commercially DV unit specifications cannot be guaranteed as it is stated in articles that these specifications are most often exaggerated optimistically (Merzkirch et al., 2016) (Carbonare et al., 2020), which limits the data available to scientific literature for energy performance estimations. The energy performance of each control strategy with a DV unit is investigated in a single-person office cell located at the perimeter of the building as a simplification to better investigate the unique options available, which are firstly analyzed by monthly time-step average calculations, then IDA ICE simulations. Concerning the assessment tools, assumptions, and boundary conditions used in the present work, it is important to match the conclusive strength to a similar level, as these are shown to greatly impact energy consumption results (Santos and Leal, 2012).

Furthermore, the comfort aspect of the DV unit technology is limited to literature-based assessment tools, in particular, «Results of the evaluation study DeAL Decentralized facade integrated ventilation systems» (Mahler and Himmler, 2008), which is further referred to as DeAL in the present work and is used to better discuss weaknesses and strengths of the relevant control strategies.

When analyzing DV systems, it is also important to have some connections to commercially available DV units in Norwegian climates. For this, the AM 150 from Airmaster (Airmaster, 2020a) is used as an inspiration for discussion of the availability of functions that are necessary for the described operational modes and other important aspects. Discussion on this specific product has been conducted with the sales manager of Airmaster. The product is further referred to as AM 150.

Calculations and simulations are divided into summer and winter season operation modes, which is typical to do in Norwegian climate (Thyholt et al., 2001).

1.4 Assessment tools

As aforementioned in the limitations chapter, literature-based assessment tools are of high importance in the present work as certain criteria's cannot be investigated personally, and certain DV unit specifics cannot be solely derived from manufacturer datasheets as these have been in found multiple articles to be positively exaggerated (Merzkirch et al., 2016) (Carbonare et al., 2020).

Comfort criteria are mainly derived from DeAL, which has investigated the DV technology in multiple buildings. A master thesis from NTNU «The Potential of Façade-Integrated Ventilation Systems in Nordic Climate» (Gruner and Haase, 2012), has also covered the comfort criteria of DV units using DeAL as an assessment tool, which is further used as inspiration. The DeAL study is from 2008, Germany, where the evaluation was conducted within a 2-year project in 10 buildings, where comfort, the satisfaction of user and operators, and energy efficiency were evaluated using interviews, surveys, and measurements.

The study «Field tests of centralized and decentralized ventilation units in residential buildings – Specific fan power, heat recovery efficiency, shortcuts, and volume flow unbalances» (Merzkirch et al., 2016), covers multiple important field measurements of different DV units aspects and is used as the main reference for determining which SFP values and HRU efficiencies to use, and also for argumentation of what should be included in specific DV unit calculations. The study is further referred to as FTDVS for «Field tests of decentralized ventilation systems». The study is from 2015, Luxembourg, where the measurements were conducted during the heating period of the years 2013/14 at outside temperatures between 0 and 4 °C.

Monthly calculations (monthly time-step energy analysis) are performed for the purpose of having further comparison data to the more accurate approach of building simulations. Doing calculations by hand also help better understand how and why different control strategies combinations differ in energy performance, as visualization can be made with a discreet number of zone balance scenarios during each day (see chapter 3.3.2, figure 3.5, 3.6 and 3.8).

The building simulation program IDA Indoor climate and energy or IDA ICE is used for seasonally energy performance estimations, which uses hourly data for accurate dynamic simulations. IDA ICE offers custom controls/schematics where the specific control strategies are already pre-customized or can be self-customized to run as preferred. The program allows for observation of certain indoor climate parameters such as operative temperature, relative humidity, and CO_2 levels and is run to ensure the best possible occupant comfort based on the input data. It further accurately models the inputs of the building, systems, and custom controllers, to ensure the lowest possible energy consumption.

IDA ICE is in the present work used for observing interesting patterns and logic in the primary energy consumption of each ventilation control strategy, and other analyses. The software only does what it is told, so any potential mistakes or illogical results produced must be observed through experience, as it is not always clear that the results are unreasonable. This gives a path for interesting discussion regarding the comparison of all control strategies and the other analyses so that weaknesses and strengths can be laid out. Only the primary energy consumption is extracted, for the sole reasoning of comparing the control strategies to each other. All inputs, custom controls, and simplifications are given in the present work so that if any results are illogical, the origin of the mistake is present. The current IDA ICE version used for simulation is version 4.8. The user manual version 4.5 is used for learning the software (EQUA Simulation AB, 2013).

1.5 Structure of the paper

The structure is divided into introduction, decentralized ventilation and comfort, methodology, results and discussion, conclusion, and then some further research recommendations, followed by the references and appendices.

Firstly, after the introduction, the decentralized ventilation system is described, covering the technology and other differences to the widely more used centralized ventilation system. An explanation of the analysis fundamentals is given, with visual demonstrations so ambiguity of the functions of each analysis is avoided. Comfort, demands, and requirements are also given as the energy performance of the ventilation system is kept in chains by maintaining these important limits, since the mechanical ventilation system would not even be necessary if comfort and health were not of vital importance in the first place. Comfort is evaluated from DeAL and other relevant field measurements are laid out.

Secondly, the methodology is described as this is important for the credibility and quality of the produced results. Boundary conditions, assumptions, and necessary simplifications are given here to ensure the reader an understanding of how the results are molded and produced, and to which caliber of credibility. Determination of DV unit specifications from existing data extracted from scientific peer-reviewed articles is given, following by a description of the control strategies and how the results are molded in each respective energy analysis.

Following the methodology, the results and discussion are presented, which contains the energy performance of the different energy analyses described in the methodology. The discussion is important to give the reader a guide through the results and to share one's own thoughts on the interesting parts of the results, and the how and whys for any irregularities which might be confusing at first glance. A conclusion fitting the level of the limitations and boundary conditions are given to show the results which are interesting from a scientific perspective and to lock out any findings which plausibility/quality are difficult to determine, as bringing these findings forth as interesting or credible could do more harm than good for the DV technology.

2 Decentralized ventilation and comfort

2.1 Decentralized ventilation system

2.1.1 General

There are multiple classes of decentralized ventilation systems, although they all have in common that the fresh air is supplied directly through the façade, with some having a centralized exhaust system and others discharging the exhaust air through the façade as well (Kim and Baldini, 2016). The relevant system is multifunctional by supplying and exhausting the air simultaneously through the façade, which is visualized in figure 2.1:

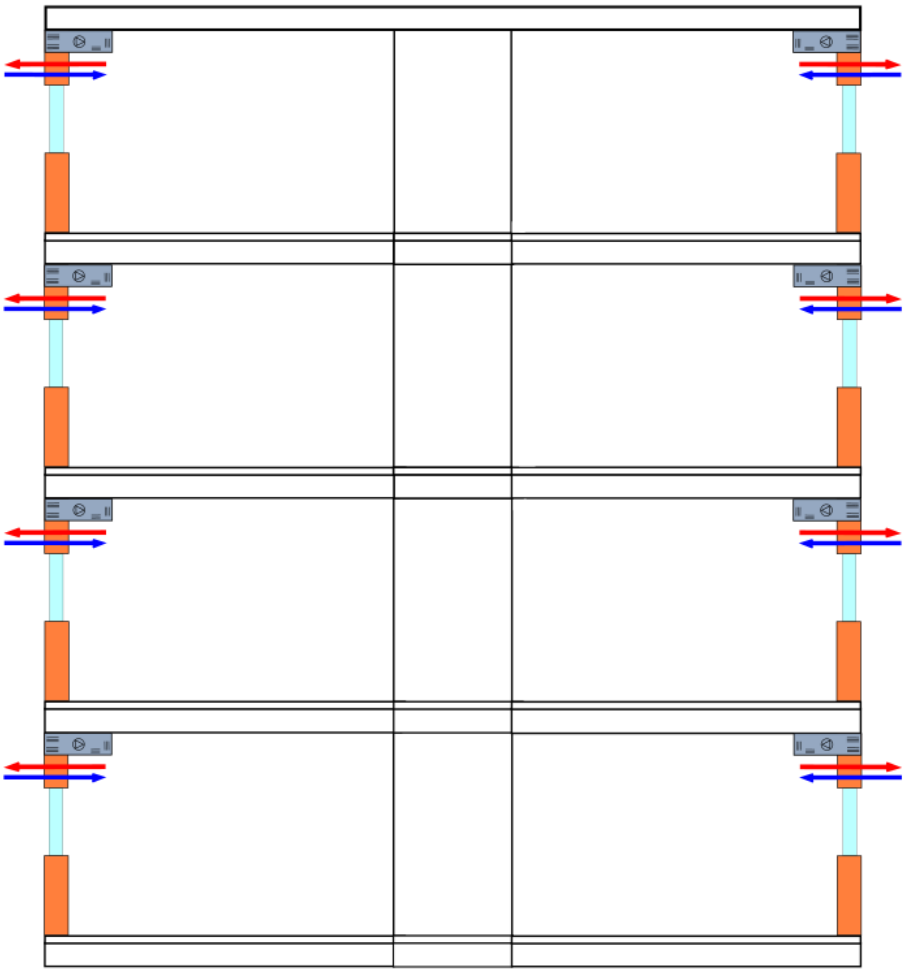

Figure 2.1: Visualization of supply and exhaust decentralized system through facade

In the present work, only DV units with façade supply and exhaust transportation are relevant, as they are widely accessible commercially in the Norwegian context, and therefore of higher interest (Eivind Ernstsen, Sales manager at Airmaster).

Furthermore, there are different setups for this design of DV units, such as façade integrated (part of the façade), floor type, floor-standing, and wall-mounted. These different designs of DV units are seen in figures 2.2 – 2.5 respectively (left figures directly extracted from the respective reference):

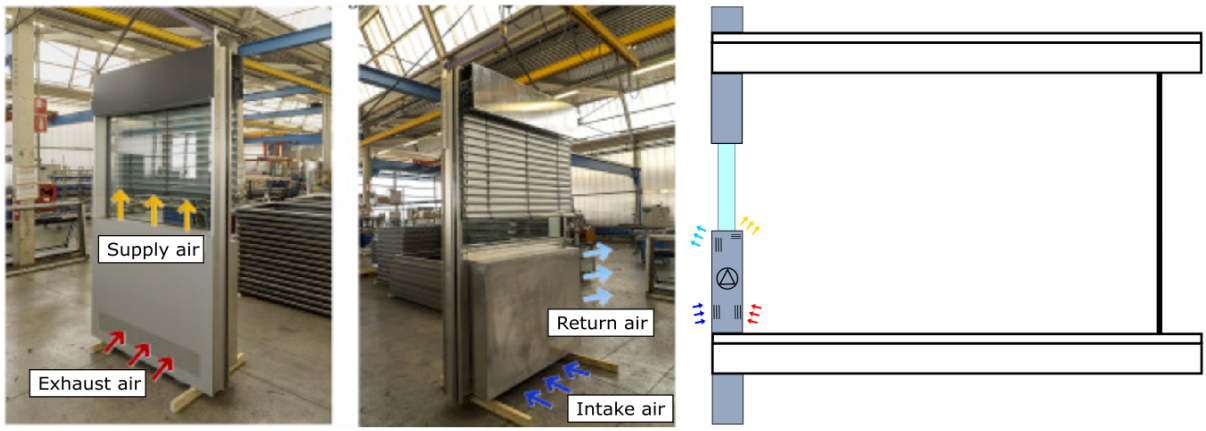

Figure 2.2: Façade integrated decentralized ventilation unit (Bonato et al., 2020)

Commercially façade integrated available units (see figure 2.2) are unknown, although the technology was shown to not lead to any significant energy or cost savings with the respective boundary conditions described (although it shows potential), where the highest cost savings was concluded to be with the ventilation control strategy of DCV using CO_2 concentration and temperature regulation (Bonato et al., 2020).

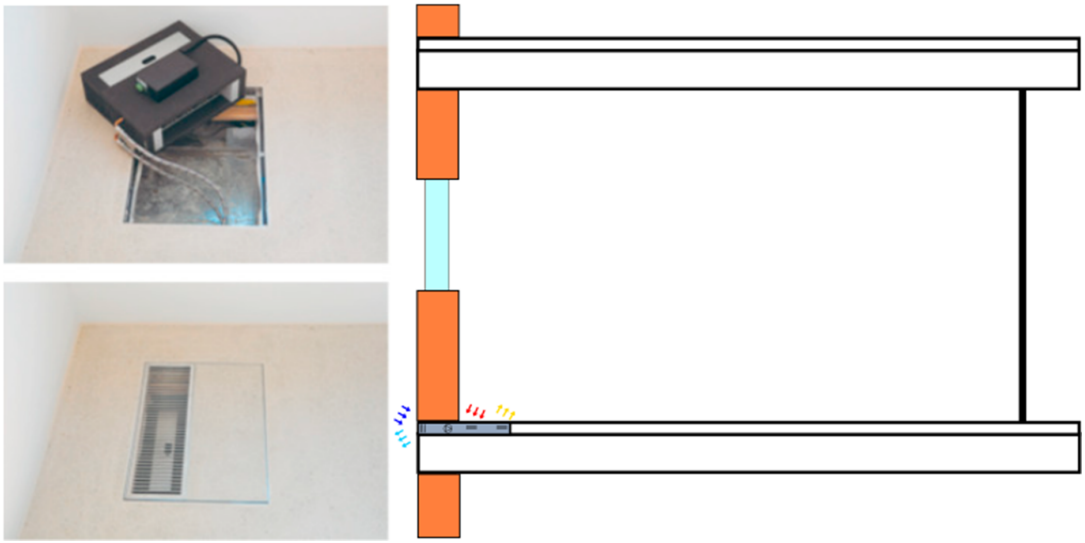

Figure 2.3: Floor type decentralized ventilation unit (Kim and Baldini, 2016)

Commercially floor type available units (see figure 2.3) include the TYPE FSL-U-ZAS from TROX.

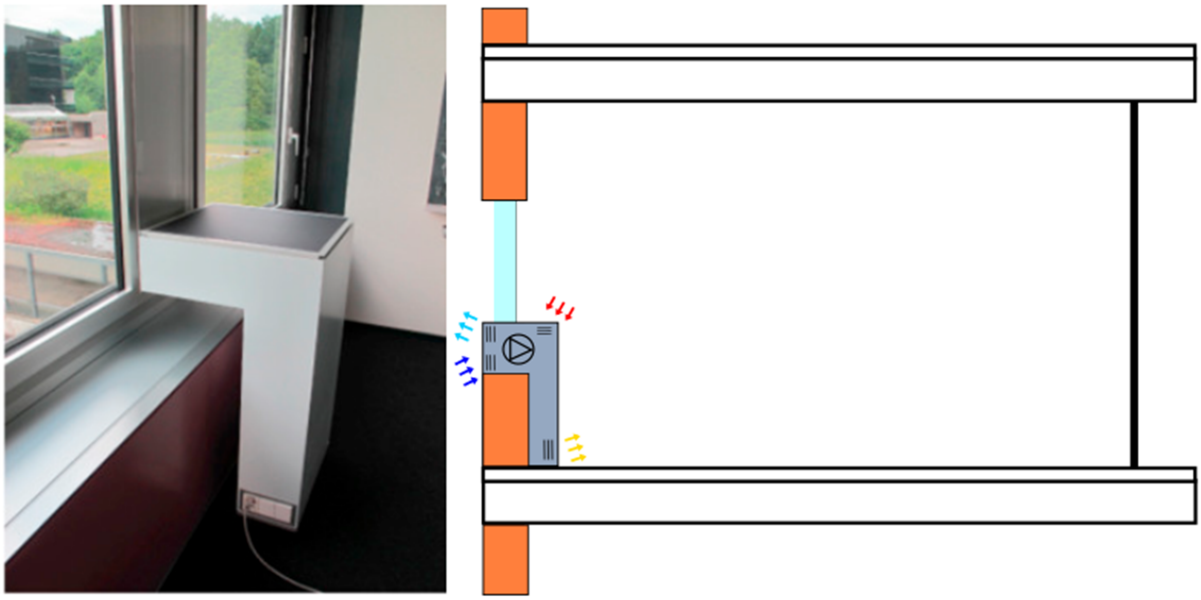

Figure 2.4: Floor-standing decentralized ventilation unit (Kim and Baldini, 2016)

Commercially floor-standing available units (see figure 2.4) include the AM 900 and AM 1200 from Airmaster.

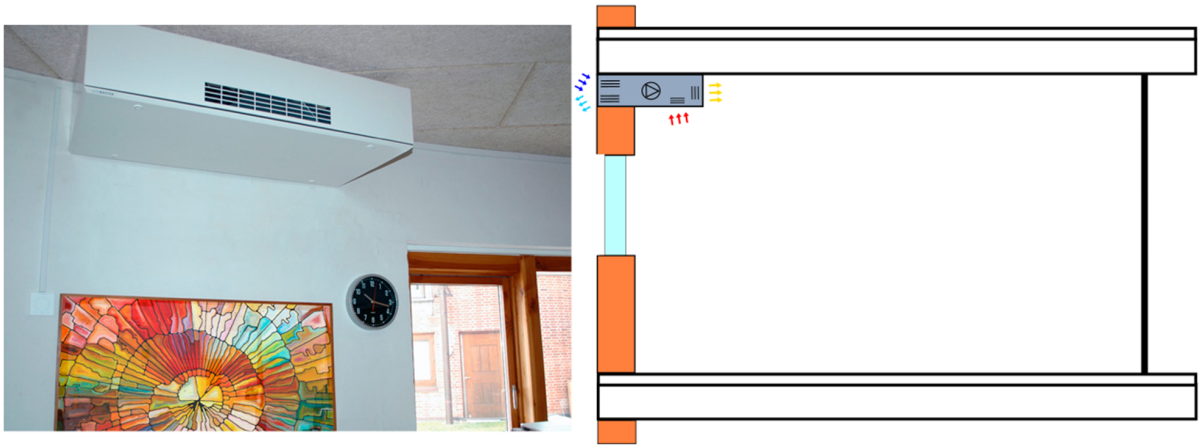

Figure 2.5: Wall-mounted decentralized ventilation unit (Airmaster, 2020a)

Commercially wall-mounted available units (see figure 2.5) include the AM 150, AM 300, AM 500, AM 800, AM 1000 and DV 1000 from Airmaster.

The wall-mounted unit is further investigated, as it is found in DV scientific literature and is the most relevant commercially for smaller rooms such as office cells, especially for fulfilling the demands of the Norwegian building code and relevant standards (Eivind Ernstsen, Sales manager at Airmaster).

2.1.2 Type of DV units

As aforementioned, the wall-mounted DV unit design (see figure 2.5) is further investigated, where there are two different types. These types are referred to as the recuperative type and the regenerative type (Merzkirch et al., 2016). Only the recuperative type is used when gathering scientific data to use in energy performance calculations, although a small explanation of the regenerative unit is given to better explain the differences in engineering design of the two DV units.

2.1.2.1 Regenerative HRU type

The regenerative type is designed as a bidirectional-flow thermal storage heat recovery unit which is controlled with periodic interval changes of supply air and exhaust air. These types of DV units can either be installed alone or as a pair to mimic a normal ventilation unit by supplying and exhausting air simultaneously. It is driven by an axial fan and is integrated with a thermal storage core that stores the relative heat or cooling energy which will transfer as the fan periodically changes from supply to exhaust, creating temperature differences and so heat transfer. The storage core comes in different types, such as ceramic or aluminum material (Merzkirch et al., 2016), or even phase change materials as latent heat storage (Gruner and Haase, 2012). The recuperative design is shown in figure 2.6:

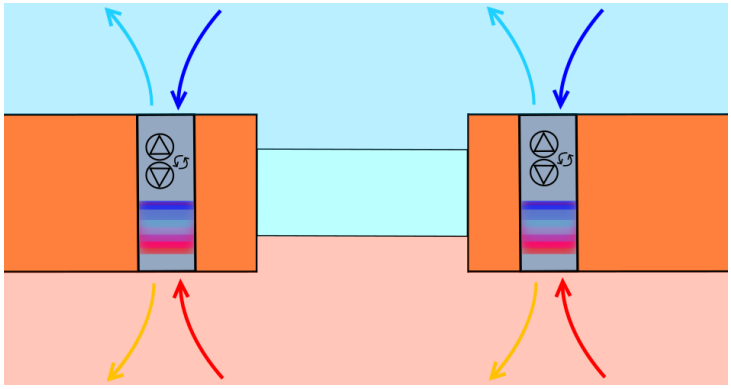

Figure 2.6: Two regenerative DV units installed in pair which are integrated in the facade

The regenerative type has been researched plentiful in scientific literature as well (Manz et al., 2000) (Merzkirch et al., 2016) (Coydon et al., 2015), but is not further looked into in the present work.

2.1.2.2 Recuperative HRU type

The recuperative design is described as a small centralized system since it provides supply air and extracts air simultaneously through separate flow paths using two radial or centrifugal fans depending on the product, with a recuperative heat recovery unit as a counter-flow air-to-air heat exchanger where the heat exchange happens directly and continuously through thin, high conductive plates (Merzkirch et al., 2016). The DV unit typically contains an air filter, drainer, damper, and a heating and/or cooling coil (also referred to as heating/cooling battery in Norway) (Kim and Baldini, 2016). Figure 2.7 shows a recuperative unit which is integrated with the façade:

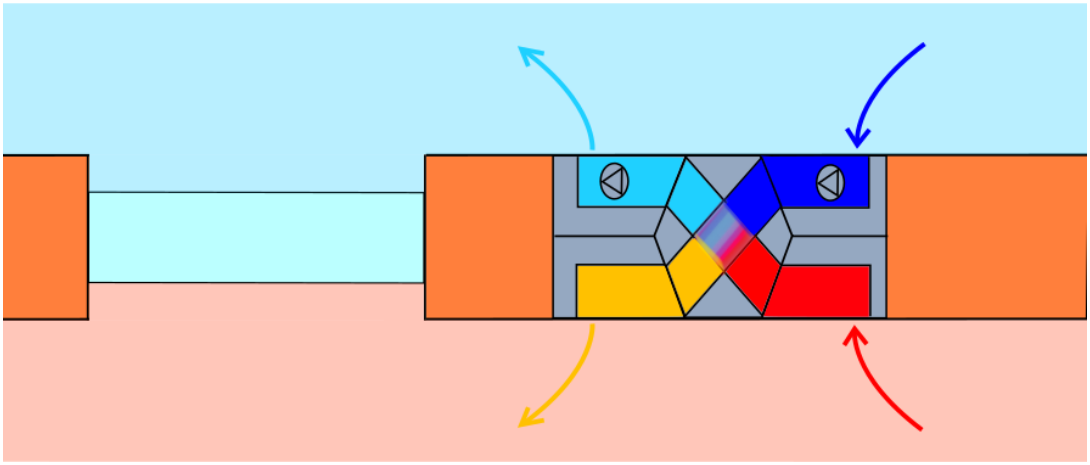

Figure 2.7: Recuperative DV unit integrated in façade

The recuperative DV unit design is utilized to mold a representative DV unit for monthly time-step energy calculations and building simulations upon the later discussed control strategies, and specifications are derived from field measurements mainly from FTDVS (Merzkirch et al., 2016). The derived field measurements used in the present work can be seen in chapter 3.2.

2.1.3 DV HRU frosting conditions

There are several strategies for dealing with frosting in the DV HRU, which are important to implement to avoid substandard HRU efficiencies and less cross-sectional area which contributes to increased pressure loss and consequently impaired SFP (Gendebien et al., 2019). Energy consumption for avoiding frost problems are excluded in the present work due to difficulty in determining accuracy, and it is assumed that the difference between the energy consumption for frost avoidance is insignificant between the control strategies, so that from a comparison perspective, including the additional energy consumption is not of value in the present work. A passive method of mixing indoor with outdoor air is also an option, which does not directly consume energy, although, with the strictness of indoor air quality demands in Norway, additional ventilation air rate would have to compensate for the mixture quality, so that additional energy consumption is the result either way, as well as decreased acoustic comfort concerning the DV unit due to increased ventilation load. In a scientific article on frosting conditions on DV units, the best strategy was concluded to be a defrost method, where the fresh air fan was shut off while keeping constant electric power on during the frosting phase (Gendebien et al., 2019).

The HRU efficiency is assumed to not be impacted as much so that the extracted DV unit specifications from field measurements such as FTDVS are assumed to be under sufficient accuracy even under frosting conditions. Even so, frost is noted to only appear below temperatures of -5.0 °C (Beattie et al., 2018), so that the number of hours of frost formation is limited in the south of Norway climate, although the number of hours increases when venturing further north, consequently lowering the potential of DV systems in northern climates, although to an unknown degree.

Further mentioning of frost conditions on the DV unit is excluded from the present work, although sufficient planning in building projects concerning frost condition strategies to maintain good HRU and SFP performance under Norwegian climate should be implemented for optimal energy performance.

2.2 Ventilation control strategies

2.2.1 Supply temperature regulation control strategies

The DV unit allows for more freedom on the condition of the fresh air, such as the temperature. A centralized system would typically only allow for a constant supply temperature due to being multi distributional to all zones if decentralized heating/cooling is not placed above the zone of interest, although personalized systems have been researched previously (Schiavon and Melikov, 2009). Supply air temperature regulation strategies (referred to as case) are inspired from the SvalVent project (SINTEF, 2021, 55:19), where it was tested if supply air temperature had any effect on thermal comfort in the room. From the SvalVent Webinar, it was concluded that the supply temperature had little effect on the thermal comfort, and also that the supply air velocity had a similar distribution, independent of the supply air temperature. With this insight in mind, some temperature regulation strategies which allow high supply air temperature are tested in terms of energy performance. Possible drawbacks include continuously decreased ventilation effectiveness (or contaminant removal effectiveness) with increased supply temperature concerning zone temperature when supply and exhaust vents are located near the ceiling (window ceiling placing not tested in referenced article) (Krajčík et al., 2012).

The strategies are simple regulation techniques that are possible to analyze in calculations and building simulations. Dynamic supply temperature regulation is therefore tested concerning energy performance, while the thermal comfort is evaluated and discussed utilizing Fanger's comfort criteria, which are extracted from the IDA ICE building simulation tool. The cases only apply to the summer season, as the boundary conditions of the winter season do not allow the case function to have any effects. The S-CO_2 + temperature control strategy is the used control strategy for visualizing the supply temperature regulation, as it is the most extreme case in terms of cooling of the zone. This can be seen in appendix I.

A visual representation of the supply temperature is given under each case, which is provided by IDA ICE building simulation during the hottest day, as it is the most extreme day in terms of cooling, and since it is best represented visually, see figures 2.8 - 2.10.

2.2.1.1 Case 1 - Constant supply temperature

Case 1 is the typical supply temperature distribution strategy in centralized systems (Thyholt et al., 2001), as changing the supply temperature dynamically based on signals is not typically done in individual rooms in centralized systems, and it already has great documentation on comfort and ventilation effectiveness (Krajčík et al., 2012), see figure 2.8:

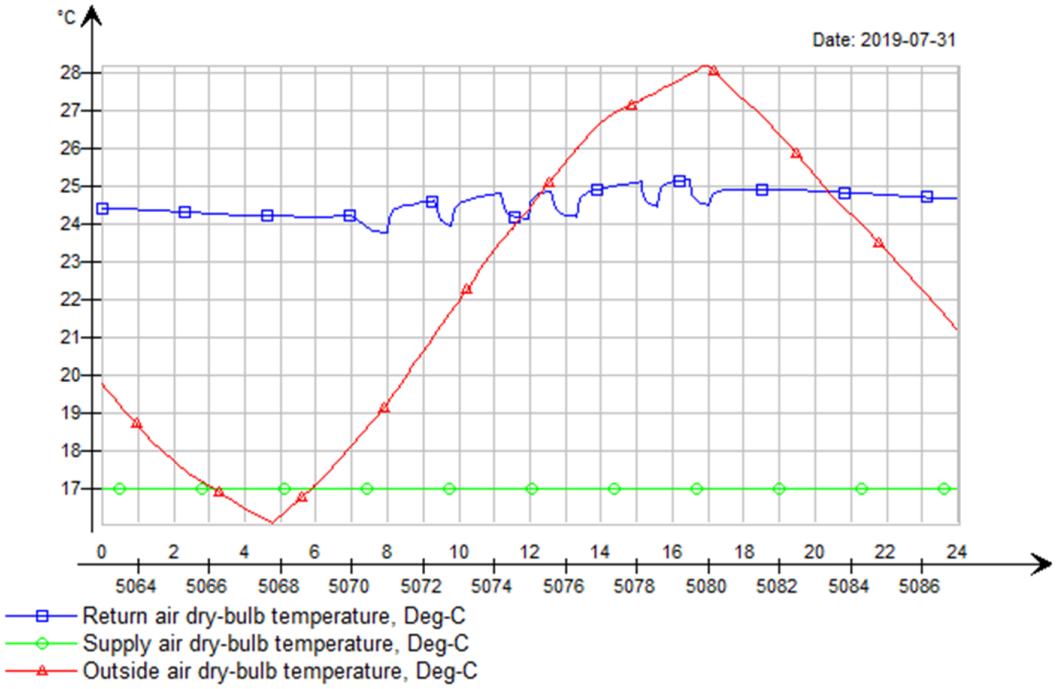

Figure 2.8: Case 1 supply temperature pattern on the hottest day using S-CO_2 + temperature control strategy

The exhaust temperature is kept at around 24.5 °C even during nighttime, which is thought to be due to high U-values in the building shell in combination with high outside dry-bulb air temperature.

2.2.1.2 Case 2 - Occupancy controlled supply temperature

Supply temperature during summer when occupancy is detected is 17 °C (which is achieved by bypassing the HRU), and while there is no occupancy detected during summer the HRU is utilized at no bypass, although an upper limit of the supply temperature is set to the lower limit of the zone temperature to avoid overheating, poor thermal comfort, impaired ventilation effectiveness (vacancy periods) and unwanted cooling loads. Case 2 is analyzed to better understand how much energy is saved or lost from leaving the HRU at full effect during vacancy intervals, which is thought to lower the heating demand of the zone as the supply air cools the zone less, which is thought to be energy efficient as there are no internal gains to neutralize the transmission and infiltration heat losses during vacancy intervals. The energy performance of this regulation strategy is also not immediately clear on the different ventilation control strategies, so further analysis is of interest. The case 2 supply temperature pattern is seen in figure 2.9:

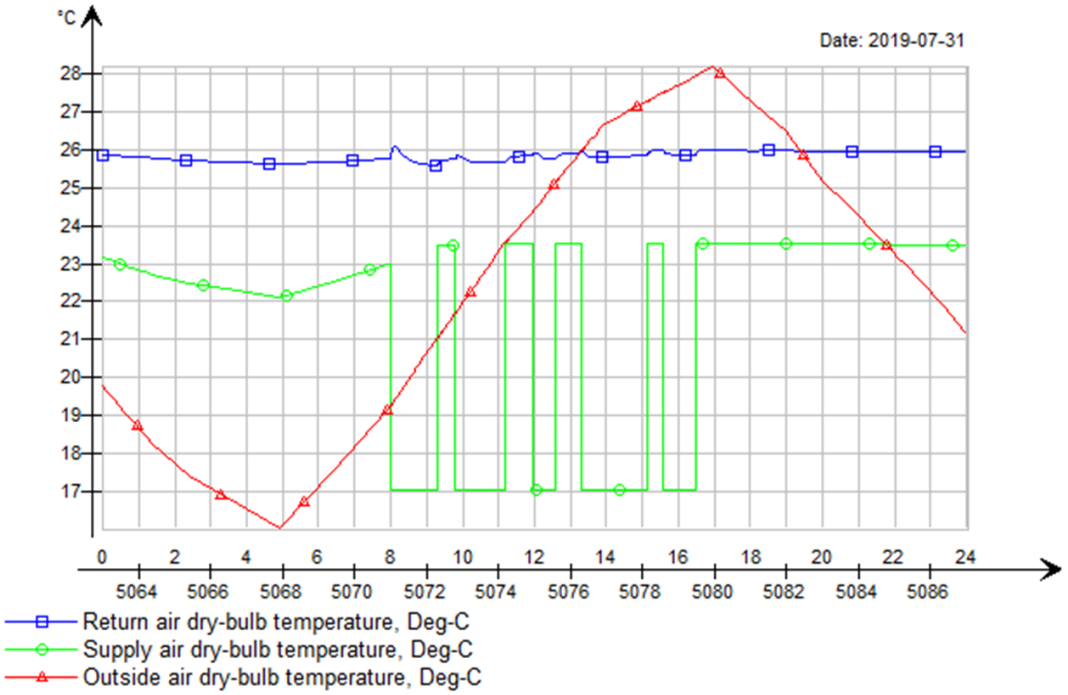

Figure 2.9: Case 2 supply temperature pattern on the hottest day using S-CO_2 + temperature control strategy

The exhaust temperature is kept constantly high due to the aforementioned reasons under case 1, although even less ventilation cooling is available under case 2 due to the increased supply temperature.

2.2.1.3 Case 3 - No bypass of HRU supply temperature

Supply temperature will never bypass the HRU during any time of the day, so an increased cooling demand is expected during occupancy periods, although less local zone heating is expected, and there is little need for AHU cooling. There are also different control strategies tested, so that the results may vary from strategy to strategy. Thermal comfort issues are expected, as this might induce too hot zones if not sufficient cooling is possible, as well as bad ventilation effectiveness as according to a research report from SINTEF (Mysen and Schild, 2014), mixing ventilation requires a supply air temperature of around 4 – 10 °C below the zone temperature for adequate ventilation effectiveness (centralized system). An upper limit of the supply temperature is set to the lower limit of the zone temperature similarly to case 2. The case 3 supply temperature pattern is seen in figure 2.10:

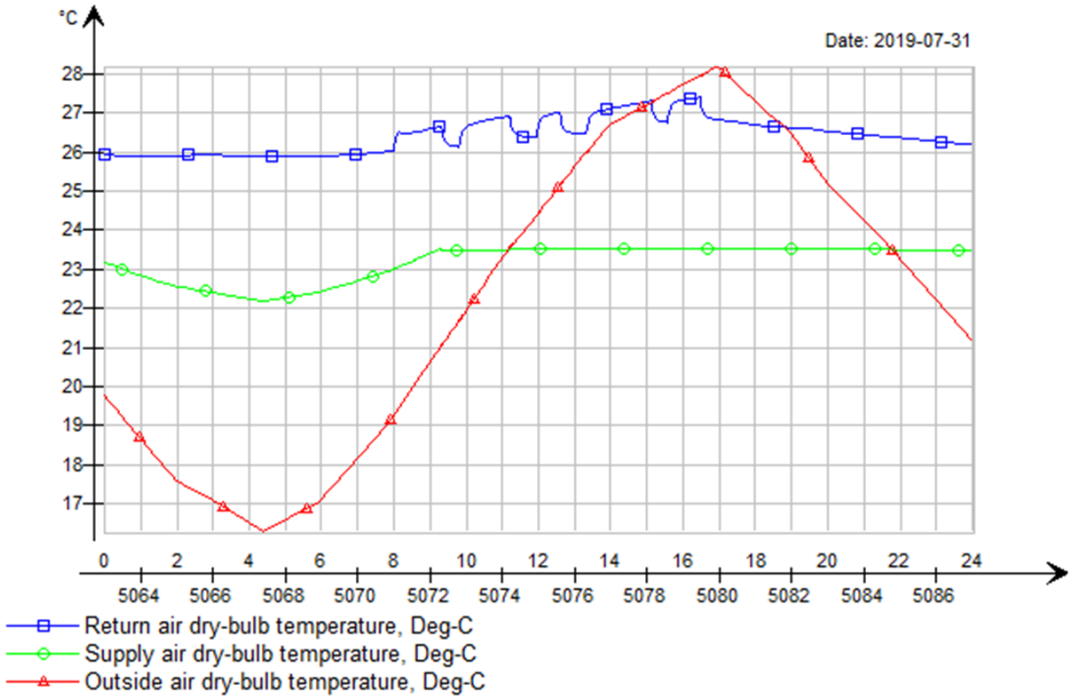

Figure 2.10: Case 3 supply temperature pattern on the hottest day using S-CO_2 + temperature control strategy

As observed in figure 2.10, the ventilation cooling required to achieve zone balance within zone temperature set-points within internal gains intervals is not possible with the ventilation cooling alone, producing poor thermal comfort for the occupants.

2.2.2 Air rate regulation control strategies

The air rate regulation control strategies are further referred to as DV control strategies, where there are five different control strategies tested. The control strategies are made up of three static operating control strategies (see figure 2.11 - 2.13), where there is a minimum air rate mode and a maximum air rate mode for single-person offices, and a discreet number of air rate modes for zones with higher occupancy (see figure J.4), so that these control strategies are not of dynamic nature. The last two control strategies are of dynamic nature, in which they are controlled constantly by zone signals (see figure 2.14 - 2.16).

The motivation behind analyzing different ventilation control strategies is that there are different commercial units available, with different availability of integrated sensors and equipment such as CO_2 sensors, PIR sensors, TVOC sensors, humidity sensors, and pressure sensors. A commercial DV unit with no available sensors and only static operation modes would possibly be economically more efficient under a DV CAV control strategy, which would be a cheap investment alternative, although likely less energy-efficient. A DV unit with a CO_2 sensor and no PIR sensor would possibly be better under case 1 than case 2, as case 2 needs a PIR sensor for accurately and quickly detecting occupancy. Products with less integrated sensors and equipment, and in general less elite in design will also generally be cheaper (Mysen et al., 2003), so analyzing the different control strategies are therefore of value for finding local minimums or maximums of optimized combined economic and energy-efficient operation of the building and/or single-person offices (not evaluated in the present work). Comfort evaluation is also a consideration, as sound generation might be a hinder for DV control strategies that utilize high air rates so that a low air rate control strategy might be the best consideration for following the Norwegian building code demands. Finding this optimized correlation of economy/comfort to energy performance is the main core objective of most ventilation projects when choosing the system, although there will be no economic analysis in the present work.

The ventilation patterns are given concerning the single-person reference zone for better visualizing of the unique ventilation pattern of each control strategy, see figures 2.11 - 2.15.

2.2.2.1 DV CAV control strategy

The decentralized ventilation constant air volume (DV CAV) control strategy operates under maximum load during weekdays in a defined interval of operating times, and in the remaining hours, it operates under minimum load. The defined operating time interval is from 07:00 – 17:00 which is typical for office cells (Halvarsson, 2012). A centralized CAV system would typically have around 12 hours (Mysen et al., 2003) – 24 hours (Mysen et al., 2005) of operating time, although the DV system is more flexible in that it only supplies air for one room, so an operating time more suited for a single-person office can be used. The 10 hour operating time is used as it is the most common for single-person offices (Wang et al., 2005).

The DV CAV control strategy would require no equipment other than an on/off button in practical circumstances, although this would not be completely reliable as forgetting to turn off the unit or turning on minimum air rate mode would be a problem. The strategy would therefore then at least require a clock or be connected to a type of fieldbus system which could be centrally controlled. Generally, the DV CAV control strategy is the cheapest strategy to implement economically, but the worst-performing in energy performance. The strategy requires a DV unit with only 2 steps minimum, a so-called min-max strategy, and dynamic control is therefore not necessary.

The control strategy is visualized in figure 2.11 (example pattern):

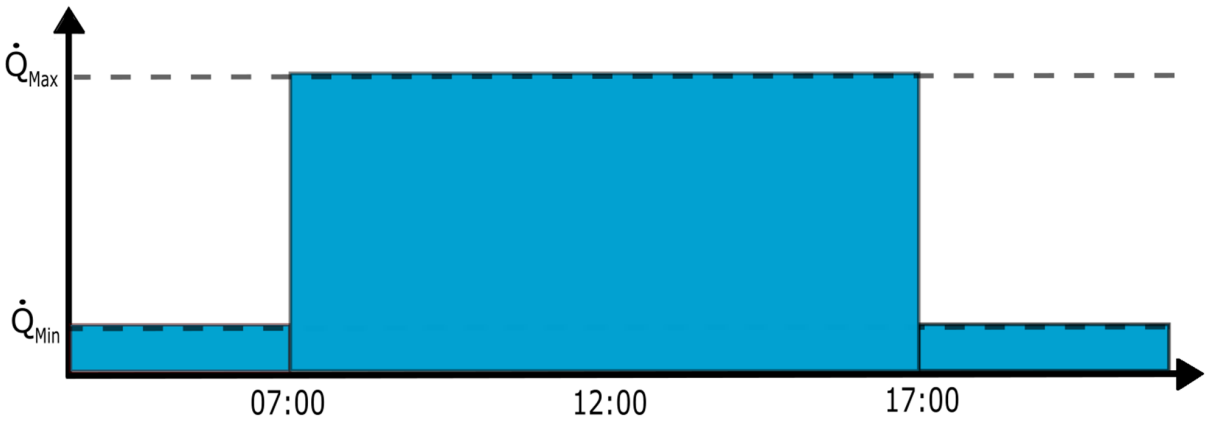

Figure 2.11: DV CAV control strategy ventilation pattern

2.2.2.2 DV PIR control strategy

The decentralized ventilation Passive InfraRed (DV PIR) control strategy supplies the maximum ventilation load whenever occupancy in the zone is detected so that the air rate intervals are entirely dependent on the occupancy schedule. The control strategy is described in other articles (Chenari et al., 2017), but in the present work, there is only one occupant for simplification. Although, if there would be more than one occupant, the fan would have to regulate accordingly to the number of occupants present (see figure J.4). In classrooms, it would generally only be necessary with a 2 step DV unit similar to a single-person office, as all the students are present as one lump (Mysen et al., 2005). The classroom used max ventilation load when occupancy was detected by the PIR sensor and minimum when the classroom was unoccupied so that the ventilation pattern would be similar to that of figure 2.12, although with class session intervals.

The DV PIR control strategy would require a PIR sensor (motion sensor) which detects infrared lights, installed separately or already integrated into the DV unit such as the AM 150 (Airmaster, 2020b). The motion sensor is not an absolute necessity, as the on/off button could also be used in this strategy, although leaving the responsibility to the user alone could worsen the IAQ by forgetting to use it, and so the PIR sensor might be necessary, or if accurate and fast enough algorithms can be used, a CO_2 sensor could suffice (Calì et al., 2015). The DV PIR control strategy also does not need to be of dynamic nature, only a discreet number of steps are required, or 2 steps for single-person offices or classrooms, and potentially other room types.

The control strategy is visualized in figure 2.12 (example pattern):

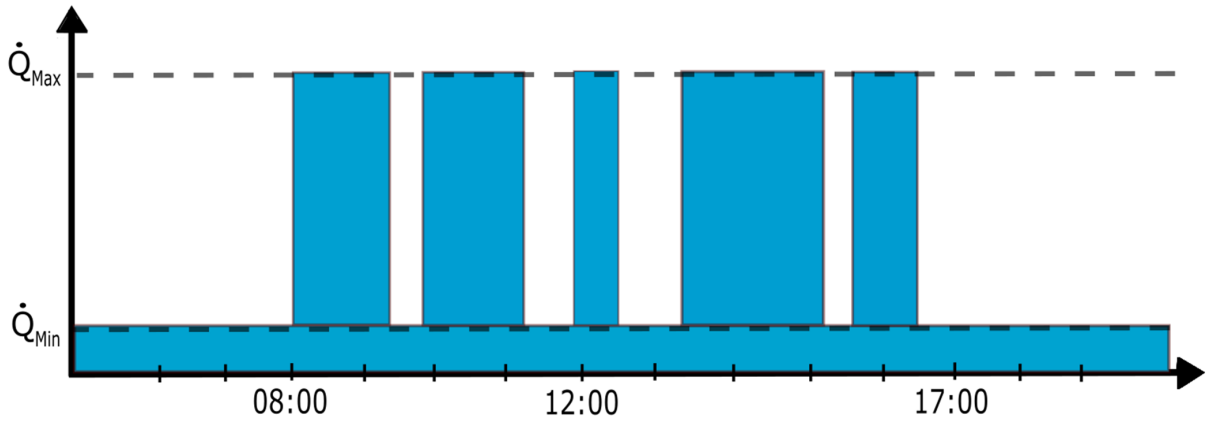

Figure 2.12: DV PIR control strategy ventilation pattern

2.2.2.3 DV S-CO_2 control strategy

The DV S-CO_2 (static-CO_2/N step-CO_2 regulation) control strategy supplies the maximum ventilation load whenever the zone CO_2 concentration is measured to surpass the set upper limit, which is only surpassed during occupancy hours, as occupants are the only source of CO_2 generation. This means that the S-CO_2 control strategy will have a similar pattern to the PIR control strategy, although the intervals of maximum loads are shorter due to the signal inertia. The strategy is presented in scientific articles as "CO_2 set point control of outdoor air (OA) damper to be at fully closed or fully opened positions" (Okochi and Yao, 2016) and "A maximum setpoint for indoor CO_2 concentration (1000 ppm) is defined. In this case, a CAV fan that operates only if the CO_2 concentration goes above the setpoint and stops, when it is below the setpoint" (Chenari et al., 2017). The control strategy is also presented with stricter control logic, where the maximum ventilation load is activated when the CO_2 concentration hits 900 ppm, and only changes to minimum load whenever the CO_2 concentration falls below 700 ppm, which means higher ventilation loads overall (Mysen et al., 2005). Here, the DV S-CO_2 control strategy would require a CO_2 sensor to notify the DV unit to turn on the required ventilation rate to neutralize the CO_2 balance in the zone at 1000 ppm, which is the recommended upper limit for achieving adequate ventilation (Arbeidstilsynet, 2016). Only a discreet number of steps are required for operation, as the air rate is not controlled dynamically by the CO_2 concentration, but rather by a signal of when to turn on the neutralizing ventilation air rate.

The control strategy is visualized in figure 2.13 (example pattern):

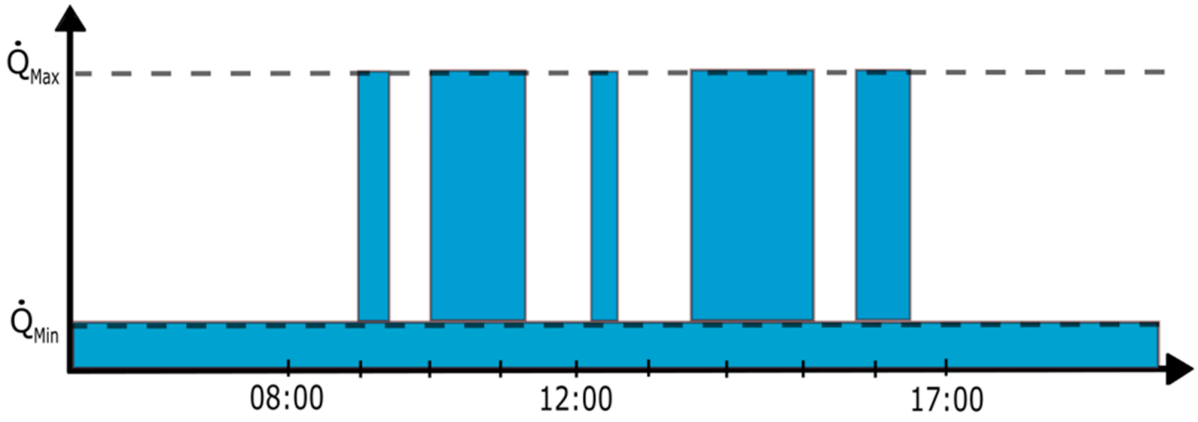

Figure 2.13: DV S-CO_2 control strategy ventilation pattern

2.2.2.4 DV D-CO_2 control strategy

The DV D-CO_2 (dynamic-CO_2) control strategy regulates the ventilation air rate dynamically after the CO_2 concentration level in the zone (Bonato et al., 2020). The ventilation air rate responds linearly to the CO_2 concentration increase, between the lower and upper limit of the CO_2 concentration with the lower and upper limit of the ventilation demands, which is set accordingly after TEK 17 § 14-3, rather than the S-CO_2 upper ventilation load (see figure 3.17), as it was found more energy efficient as it avoided zone cooling to a further extend (see appendix H.1.4) (S-CO_2 dynamic regulation not given). Typically this upper limit of ventilation demand is not reached since the CO_2 concentration function of the control strategy allows for neutralization of CO_2 generation below this upper limit of ventilation demand, which is reached linearly after a set amount of time of occupancy (see figure 3.17). The ventilation control strategy is described as: "The hygienic ventilation rate is adjusted comparing the measured CO_2 concentration with minimum and maximum thresholds" (Bonato et al., 2020).

Likewise to the DV S-CO_2 control strategy, the only sensor requirement would be the CO_2 sensor, although a dynamic DV unit is a necessity for allowing constant proportional control of the ventilation air rate of the D-CO_2 control strategy, unlike the S-CO_2 control strategy. This allows for safer control of the atmospheric climate, although higher ventilation loads are expected.

The control strategy is visualized in figure 2.14 (example pattern):

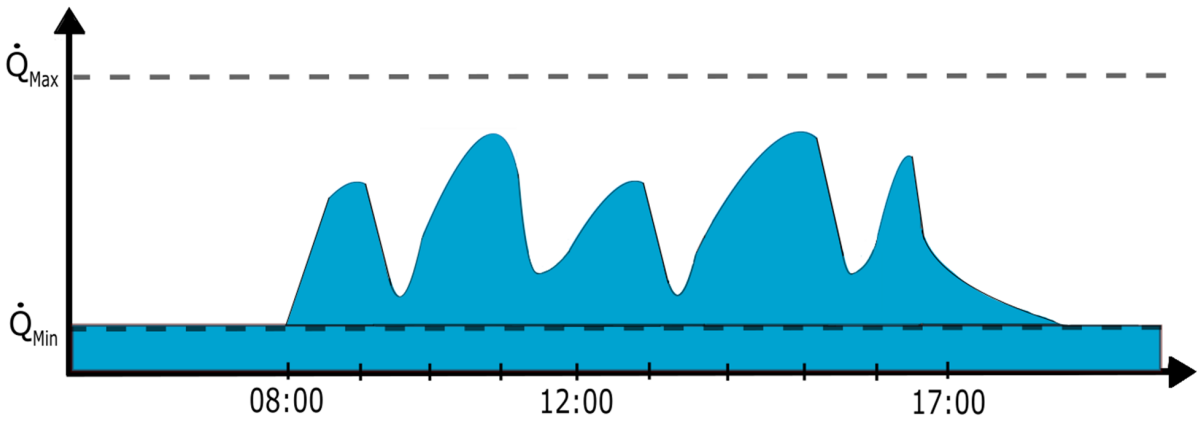

Figure 2.14: DV D-CO_2 control strategy ventilation pattern

2.2.2.5 DV S-CO_2 + temperature control strategy

The DV S-CO_2 + temperature control strategy is a combination of the DV S-CO_2 control strategy aforementioned in chapter 2.2.2.3, and a dynamically regulating control strategy which cools/heat (EQUA Simulation AB, 2013, p. 20) the zone by distributing fresh air accordingly to neutralize the thermal balance (Mysen and Schild, 2014, p. 17). The ventilation pattern produced from this control strategy varies on the zone temperature, and is therefore indirectly controlled by internal gains, outside temperature, supply air temperature, transmission, infiltration, and solar radiation.

The DV S-CO_2 + temperature control strategy would require the CO_2 sensor and a thermostat in the room, or a combined CO_2- and temperature sensor. An investment for a dynamic DV unit would be required for this control strategy, and the DV unit also needs to be able to supplement air at high enough loads to cool the zone effectively, which can act as a barrier with DV units as there are strict demands for noise pollution from TEK 17 § 13-6, as noise has been reported to be disturbing when using a DV system (see figure 2.20).

The control strategy is visualized in figure 2.15 (example pattern):

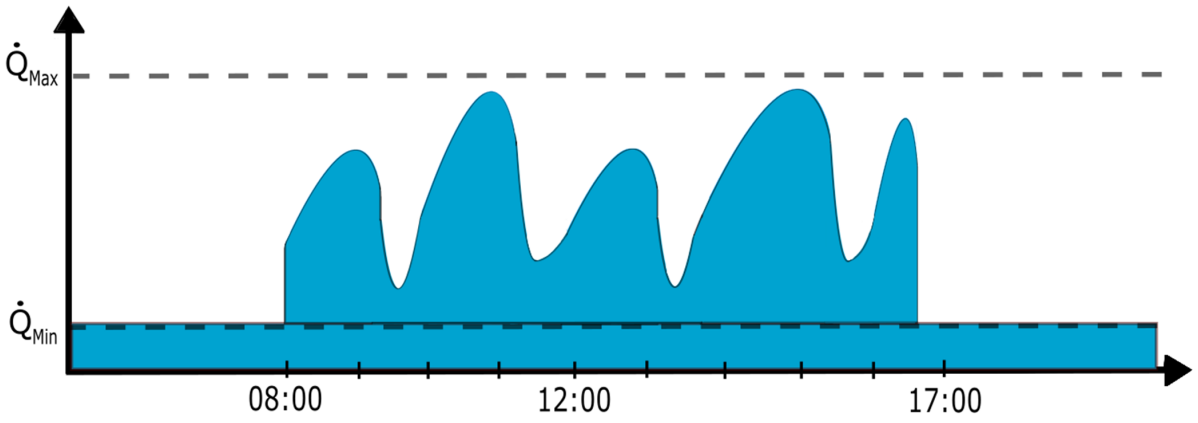

Figure 2.15: DV S-CO_2 + temperature control strategy ventilation pattern

2.3 Comfort criteria

The DV units need to be able to deliver fresh air into the building while simultaneously keeping the comfort within acceptable levels. The relevant comfort criteria are temperature, relative humidity, indoor air quality, odors, draught, and noise (Mahler and Himmler, 2008). Different control strategies with case 1 condition are used for visualizing the comfort criteria graphs from IDA ICE, depending on their respective criticality of each comfort criteria, although these results are only for a simplified model of the DV system (boundary conditions see chapter 3.1 and 3.2).

2.3.1 Operative temperature

Studies on personalized ventilation in cold climates has shown that having a higher permissible operative temperature set-point will improve the energy performance, as less local zone cooling is the result so that the choice of control strategy will also heavily rely on the thermal demands of the zone (Schiavon and Melikov, 2009). It is concluded by NS-EN 15251:2007+NA:2014 (replaced by NS-EN 16798-1:2019) that the additional expense from poor inner climate exceeds the saved expenses from the energy reduction costs gained from acceptance of lesser inner climate comfort category. Following the strictest demands is therefore always of interest, as long as practicality and economy of the project allow it, although, with personalized ventilation, the general demands are of lower importance as the occupants "personal" inner climate category A can be of much higher operative set-point so that both good energy performance and good comfort is a potential result.

The Norwegian building code TEK 17 § 13-4 recommends an operative temperature between 19 – 26 °C in activity groups of light work (such as office work). This recommendation can be exceeded in hot summer periods when the outdoor air temperature is above the upper limit for 50 hours during a normal year. NS-EN ISO 7730:2005 offers stricter design criteria's for light work, which is presented as an activity of 70 $\frac{W}{m^2}$ or 1.2 MET, in which there are three different categories A to C of strictness, where A is the strictest. In office cells, following category A, the operative temperature is 24.5 ± 1.0 °C in the summer and 22.0 ± 1.0 °C in the winter, with a clothing factor (clo) of 0.5 and 1.0, respectively.

The maximum required AHU cooling and heating coil power is given (see figure 2.16 - 2.17), which is the required power to either cool the supply air to 17 °C or heat the supply air to 20 °C. The cooling coil power is at a maximum of around 500 watts during the hottest day of the year (highest of all control strategies). The heating coil power is at a maximum of around 250 watts on the coldest day of the year (highest of all control strategies). Both of these upper values of coil power are below the given coil power of the AM 150 combined with the CC 150 (cooling coil) (Airmaster, 2020a), which is designed for Norwegian dimensioning conditions (Eivind Ernstsen, Sales manager at Airmaster). Further comparison evaluation concerning coil power is not included, as it is assumed sufficient for all control strategies. See appendix I for the hottest and coldest week operative temperature patterns for all control strategy and case combinations.

The zone temperatures with their respective AHU cooling coil power (figure 2.16):

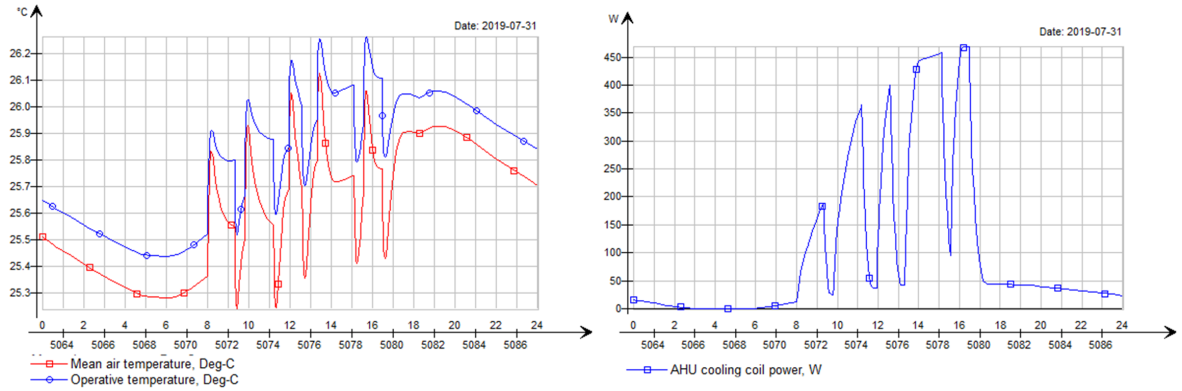

Figure 2.16: Operative temperature and cooling coil power on the hottest day of the year (DV S-CO_2 + temperature control strategy case 1)

The zone temperatures with their respective AHU heating coil power (figure 2.17):

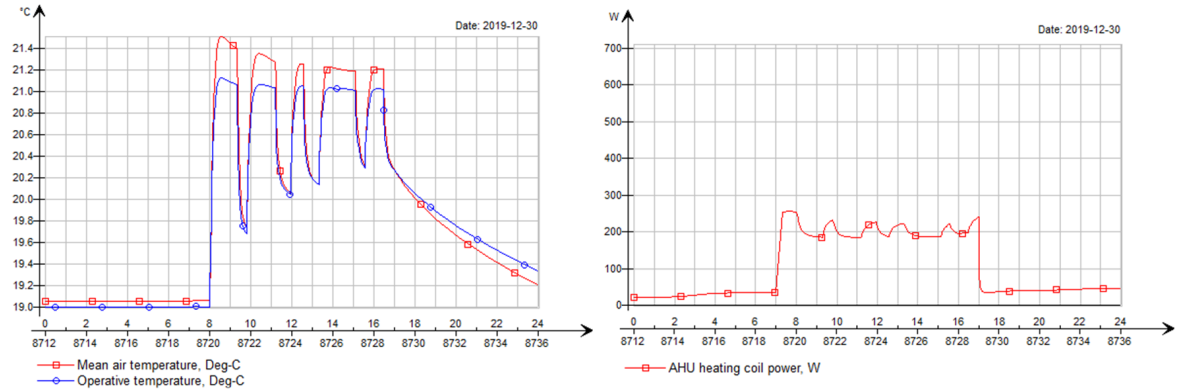

Figure 2.17: Operative temperature and the heating coil power on the coldest day of the year (DV CAV control strategy case 1)

2.3.2 Relative humidity

The biggest problems for relative humidity in the Norwegian climate are too dry air inside during winter months, and it would be desirable to humidify the air to achieve optimal comfort, although the Norwegian building code does not demand criteria for relative humidity. It is stated in DeAL; "the effort to design a decentralized ventilation with humidifying action is substantial and should only be considered for special occasions" (Mahler and Himmler, 2008).

Commercial products available such as the AM 150 from Airmaster, is stated to be available with an enthalpy exchanger for moisture exchange (Eivind Ernstsen, Sales manager at Airmaster), although the humidity transferability of the enthalpy exchanger cannot be evaluated in the present work, so further mentioning is excluded.

Figure 2.18 shows the relative humidity on the coldest day:

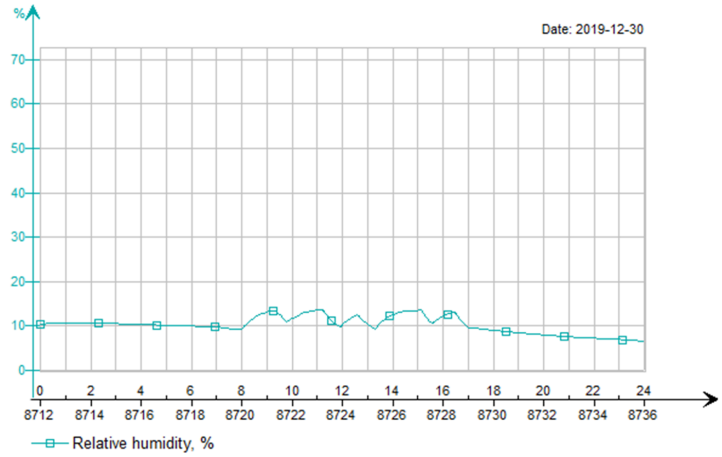

Figure 2.18: Relative humidity on the coldest day of the year (DV CAV control strategy case 1)

The average relative humidity is around 12 % during occupancy hours with an inside dry-bulb temperature of around 21.4 °C, resulting in an absolute humidity of around 2.3 g/kg which are similar to other simulated results using DV units (Gruner and Haase, 2012). Control strategies based on CO_2 had around 18 % (2.8 g/kg). Experiments have shown that an RH between 20 – 70 % does not have any notable influence on the comfort (Ingebrigtsen, 2017, p. 117), so that a CO_2 based control strategy is thought to be better during winter concerning RH (lower air rates).

2.3.3 Indoor air quality

Indoor air quality (IAQ) is referred to as the pollution in the air, which is a factor of the pollution generation and the air recirculation of the zone. The major emissions sources vary on the location, but in office cells, the most typical ones are pollutants from the outside air, organic substances from building materials, people, and processes from cleaning (Jones, 1999) (Arbeidstilsynet, 2016). These pollutants must be deconcentrated by adequate air change with the ambient air, in combination with a sufficient filter. The filter category required depends on the pollution concentration of the outside air, in which cities with high traffic and industry are ranked highest. ISO 16890:2016 recommends at least the ePM1 filter for lasting residence such as office cells, which is traditionally known as an F9 filter at $>$ 75 % elimination from NS-EN 13779:2007 (replaced by NS-EN 16798-1:2019). TEK 17 § 13-1 require filter choice to be made based on the zone of outside air quality from a communal air zone map, which is categorized as the green, yellow, and red zone, although the filter choice is not thought to be a significant factor in control strategy determination. The AM 150 is available with an ePM1 80 % filter if requested (Eivind Ernstsen, Sales manager at Airmaster).

Ventilation demands are described in TEK 17 § 13-3, where the demand is 26 $\frac{m^3}{h}$ per person present in the room, 2.5 $\frac{m^3}{hm^2}$ floor area when the room is occupied, and 0.7 $\frac{m^3}{hm^2}$ floor area when the room is not occupied. The demands are solely based on light activity, which is the present framework. The demand is used when there is sufficient documentation that the building materials in the room are classified as low-emitting, which is the typical case around office cells.

Adequate ventilation should maintain the CO_2 concentration below the recommended norm of 1000 parts per million (ppm), meaning that CO_2 can be used as a measurement of IAQ (Arbeidstilsynet, 2016). Certain ventilation control strategies will therefore regulate the ventilation demand based on the CO_2 concentration, or just activate the required ventilation rate to keep the CO_2 concentration always under 1000 ppm. DCV strategies can also be controlled by temperature, in which ventilation is used for cooling/heating the inside air, although this must be combined with CO_2 control logic as the ‘’adequate ventilation” criteria is only fulfilled when the CO_2 concentration is below 1000 ppm (Arbeidstilsynet, 2016), see chapter 2.2.2.3 – 2.2.2.5.

This reduces the ventilation demand and therefore typically the energy consumption of the system, although this is not always the result (Schiavon and Melikov, 2009). The trade-off when comparing energy reduction of the DCV control strategy contra the price investment of the required sensors and equipment for centralized systems have only proven profitable as the zone area and occupancy load increases, and as the occupancy schedule accumulation decreases as the gap of energy consumption increases of this (Merema et al., 2018). A study on DCV on office cells found that the reduced energy costs could cover an extra investment cost of around 300 EURO per office cell, although this study was performed on a centralized system (Mysen et al., 2003). In the case of a project which has specifically determined to use DV systems, the choice of control strategy might be of higher ambiguity.

The CO_2 concentration is shown during the hottest and coldest day of the year, see figure 2.19:

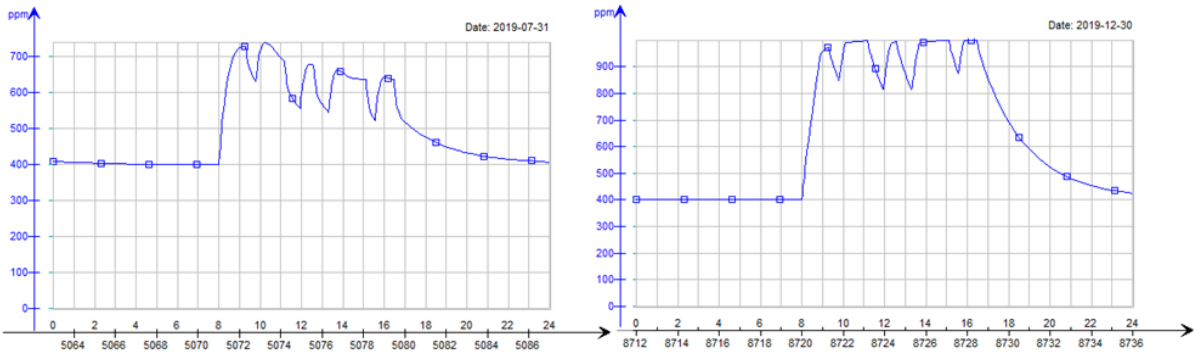

Figure 2.19: CO_2 concentration pattern on the hottest day of the year (left) and the coldest day of the year (right) (DV S-CO_2 + temperature case control strategy 1)

The ventilation control strategies which are not controlled by CO_2 concentration, which are the DV CAV and DV PIR control strategy (see chapter 2.2.2.1 – 2.2.2.2), will also not surpass the upper limit of 1000 ppm, as the ventilation load during occupancy is higher than the neutralizing ventilation load and the intervals are longer.

2.3.4 Odors

Building materials and moisture can still produce foul odors when the recommended values of the emission source are maintained. High moisture content can initiate moisture damages in which increased odor generation is the consequence. Concerning the filters of the ventilation units, certain pollutants may get caught by the filter or get caught in the DV unit walls, and with the combination of moisture, another odor generation source is potentially produced (Arbeidstilsynet, 2016). The odors and waste gases from neighbors, city street activities and/or cars, etc. are more easily taken in by a DV system on the façade of the building, rather than the typically more strategic placing of the centralized ventilation system (Kim and Baldini, 2016). Foul odors will decrease the indoor climate quality if not dealt with, so the evaluation of odor problems surrounding DV units is of vital importance (Arbeidstilsynet, 2016), although concerning control strategy comparison, the odors are thought to be of little impact, and therefore further excluded.

2.3.5 Draught

Draught is recommended to not exceed an air velocity of 0.15 $\frac{m}{s}$ in a workplace with light activity level, such as an office room (Arbeidstilsynet, 2016), although recent studies such as SvalVent has shown that higher velocities could also be used for comfort in combination with higher zone and supply temperatures (SINTEF, 2021, 55:19), which is an important insight for the supply temperature regulation strategies. The draught depends on location, air rate, geometric properties of the air diffusers of the DV unit, and the occupant's placing in the room. Mixing ventilation, which is when the DV unit is installed near the ceiling, will take advantage of the Coandă effect, where the air jet stays attached to the ceiling and slows down to acceptable air velocities when reaching the residence zone. Displacement ventilation, which is when the DV unit is installed near the floor, will be supplied at lower air velocities and will increase in speed due to the buoyancy force and then create a thermal plume when heated to a lower air density.

The AM 150 takes advantage of the mixing principle, as it is installed near the ceiling at the façade while spewing air horizontally along with the ceiling. There are supply diffusers with slats to control the supply air discharge range (Airmaster, 2020a), which could be used to compensate for higher supply temperatures (SINTEF, 2021, 55:19).

2.3.6 Noise

The Norwegian building code TEK 17 § 13-6 sets the demand to satisfy at least the sound class C in NS 8175:2012, where the sound level should not exceed $L_{p,AF,max} = 40$ dB(A) in offices from technical installations, where the DV unit would fall under the category as a technical specification. Byggforsk 421.421 recommends the sound level to not exceed $L_{p,AF,max} = 30$ - 35 dB(A), and the total sound level to not exceed $L_{p,Aeq} = 35$ dB(A). The purpose of these demands and recommendations are to optimize the productivity, concentration, and relaxation abilities of the occupant, as it is stated in Byggforsk 421.421. Noise pollution such as high noises, irregularities in the noise pattern, or specific bothersome noises will add to a worse indoor climate. As the DV unit is installed inside the room with the occupant, the risk of noise pollution is increased as the source is in near proximity. The DV unit will have a specific upper air rate limit which is determined by the noise pollution and control strategy, where static operation must be upheld according to the Norwegian building code or CO_2 neutralization air rate without compromising acoustic comfort, such as simpler VAV strategies or CAV, and demand operation mode, which is decided based on noise emission only. This is to ensure optimized ventilation control strategies, as the noise pollution can act as a barrier for certain strategies, where the example of temperature regulation might be a problem, in that sufficient cooling is hindered as higher air rates are not possible due to noise pollution demands, especially for case 3 conditions. The AM 150 DV unit has documentation on the sound levels, where the strictest filter demand has a sound level of $L_{p,Aeq} = 35$ dB(A) at around 115 $\frac{m^3}{h}$ (with referenced specific test conditions) (Airmaster, 2020a), although field measurements from DeAL is used for the representative DV unit schematic. Another important consideration is the noise pollution from the streets and surroundings, such as street activities and extreme weather, which needs to be muzzled with a well-designed damper inside the DV unit, which also simultaneously reduces the air fan noise (Kim and Baldini, 2016).

2.4 Results from DeAL on comfort criteria's of DV units

DeAL carried out user surveys in 4 buildings referred to as 201, 202, 203, and 204 (out of the total 10 investigated buildings). Here 10 – 20 standardized and anonymous questionnaires per building were distributed (daylight and shading are excluded from the poll). The DV units of the survey are not described, so further conclusions than the average results from each building cannot be given (Mahler and Himmler, 2008). A translation of the survey is previously given (Gruner and Haase, 2012), although the information given does not fully correlate to the DeAL reference in the present work, so an additional translation is given to ensure clarity.

The original poll can be found at the reference (Mahler and Himmler, 2008). Here, a translation to English is given in figure 2.20:

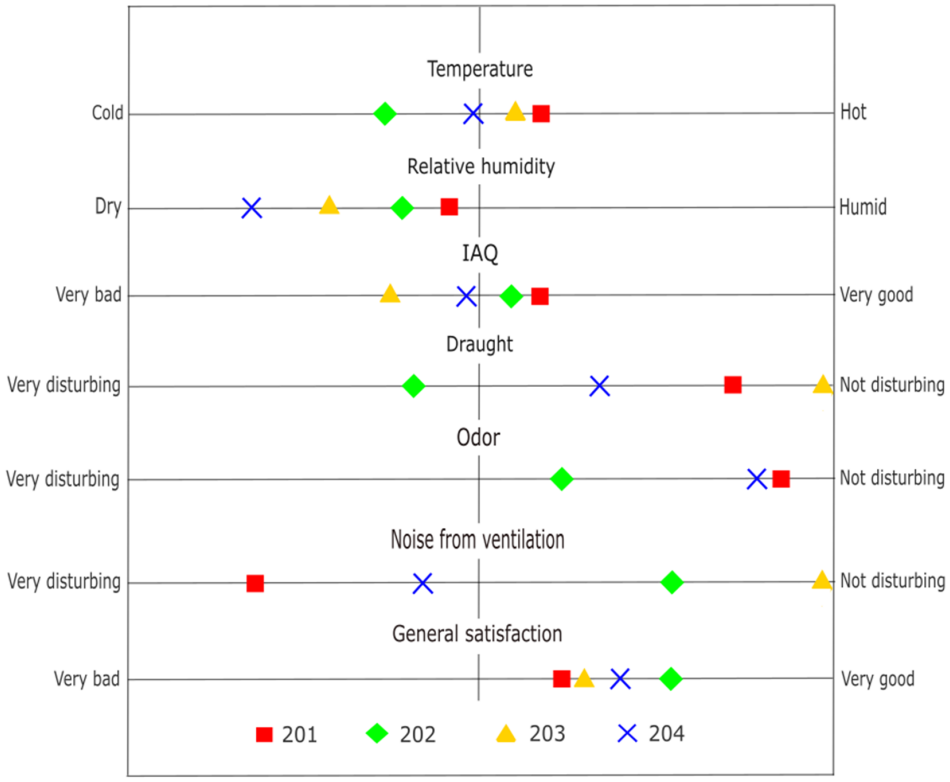

Figure 2.20: Comfort criteria survey from DeAL (Mahler and Himmler, 2008)

Overall, the survey shows satisfaction with the indoor environment. The biggest standouts are building 201 which has high noise production and building 203 and 204 which have too dry air. The other results are either more neutral or placed on the right side.

A feedback poll of 16 operators was also included in the study. The satisfaction was mostly positive as 13 of the operators were satisfied with the DV system, while 3 operators had problems or meant that the DV system was the wrong decision. The main negative feedback regards were too much noise and too hot/cold temperature, although it is stated that there was little or no feedback from the office users. There is also no saying of which feedback are to which buildings (Mahler and Himmler, 2008).

A noise emission graph is given, although the interpretation of the graph is not fully understandable, see figure 2.21 (the graph is extracted directly from DeAL):

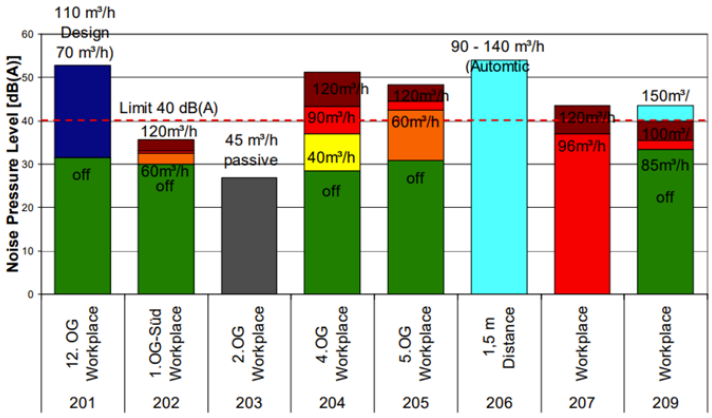

Figure 2.21: Noise measurements from each building from DeAL (Mahler and Himmler, 2008)

Most of the DV systems exceed the minimum requirement of 40 dB(A) according to TEK 17 § 13-6, although their respective air rate of surpassing the requirement varies on the system. TEK 17 § 13-3 minimum demands for air rates do not surpass the 40 dB(A) mark for most DV systems in the given graph. The study DeAL is from 2008, so the technology might have improved sufficiently over the years, such as the AM 150 unit which is specifically designed to satisfy the Norwegian building code. A newer study should therefore be conducted for a better conclusion on the noise pollution risk in Norway.

3 Methodology

3.1 System and zone description

The following description of the system is valid for both the monthly time-step energy analysis and the building simulation, so its foundation is laid out first.

The minimum demands according to the Norwegian building code TEK 17 and NS 3701:2012 are guidelines for energy-related demands, while NS-EN ISO 7730:2005 and TEK 17 are guidelines for comfort-related recommendations and demands. NS-EN 15193-1:2017 is applied for verification of typical occupancy behavior in office rooms, scientific articles are used for typical internal gains, and the occupancy schedule utilized (see figure 3.1), is in appendix B described in detail. The remaining boundary conditions are made from typical values applied in Norway, and discussed with the external supervisor (Ørnulf Kristiansen, project leader at Multiconsult), as a comprehensive description of the system is essential for the interpretation of how the results are produced and what they represent. Tables of the relevant descriptions are given in appendix A.

The reference zone (single-person office room) has a net floor area of 10 m^2, and a height of 2.7 m from floor to ceiling, which yields a room volume of 27 m^3. With these geometric values, the minimum demands according to TEK 17 § 13-3 for the ventilation load is given at $\dot{Q}_{min}$ equal to 7.0 $\frac{m^3}{h}$, which is simplified to 8.0 $\frac{m^3}{h}$ due to compensation of external short circuit problems (13 %) (Merzkirch et al., 2016), while the maximum ventilation load is given at $\dot{Q}_{max}$ equal to 51.0 $\frac{m^3}{h}$, which is simplified to 58.0 $\frac{m^3}{h}$ due to compensation of external short circuit problems similar to $\dot{Q}_{min}$, although this maximum ventilation load is only utilized in the DV CAV and DV PIR ventilation control strategies, as the CO_2 control strategies do not follow the ventilation demands of TEK 17, but are controlled by signals from zone sensors. The minimum demand $\dot{Q}_{min}$ must be followed during all ventilation control strategies to ventilate material emissions. The minimum demands of the U-values used for the external wall is 0.22 $\frac{W}{m^2K}$ according to TEK 17 § 14-3, and 0.80 $\frac{W}{m^2K}$ for the external window according to NS 3701:2012, where the solar transmittance of the window is set to 0.7 and the window area to 1.5 m^2 according to the equation $A_g \geq 0.07 * A_{floor}$ / LT from TEK 17 § 13-7.

The chosen infiltration rate, given by the air change per hour (ACH), is set to constant 0.1 h^{-1}, which is a typical value used in scientific literature when analyzing office cells concerning decentralized ventilation (Cui et al., 2017) (Kim et al., 2014), which also is within the minimum demand of TEK 17 § 14-3 (assuming typical pressure differences).

A major boundary condition used in this thesis, is that there is only one occupant present in the reference zone, which is important to consider when analyzing the results, as the ventilation control strategy energy comparison results rely heavily on the occupancy pattern of the analyzed room, where a bigger room with an unpredicting occupancy pattern will yield more energy savings during DCV strategies compared to simple control strategies such as CAV, which has been confirmed with plentiful of scientific documentation in centralized systems previously (Merema et al., 2018) (Mysen et al., 2003) (Mysen et al., 2005). The reason behind the one-person reference zone is the simplified calculations and simplified occupancy pattern, and the fact that one-person office rooms also need to be ventilated if the building chooses a system of DV units over a centralized system. The ventilation control strategy and DV unit design to implement in single-person rooms is also important to choose beforehand, as these two things are essential to synergize for cost efficiency. Even so, as aforementioned, it is already heavy documentation on the cost efficiency of DCV control strategies on unpredicting occupant patterns in larger rooms, so that the decision there is of less ambiguity and uncertainty, making the results from single-person rooms on DV system control strategies of more interest.

The utilization rate (UR) is described as the fraction of time that a room is occupied, within a specific time period (Halvarsson, 2012), so that in a single-person office at a specific point in time the UR is either 0 or 1, and over a working day it is set to a mean value of 0.60 during the typical office hours of 07:00 – 17:00 according to NS-EN 15193-1:2017, which is also the UR found from the occupancy schedule described in appendix B, and figure 3.1. An occupancy schedule for single-person offices could not be found, so one is derived from the scientific peer-reviewed article; «Modeling occupancy in single person offices» (Wang et al., 2005) (see appendix B), where a statistical analysis was performed using field data of 35 single-person offices over a one year period. The occupancy schedule is important as it is used for predicting periods of internal gains and maximum ventilation loads, which are essential to all ventilation control strategies.

The following occupancy schedule in figure 3.1 is the derived results, and the full derivation is given in appendix B:

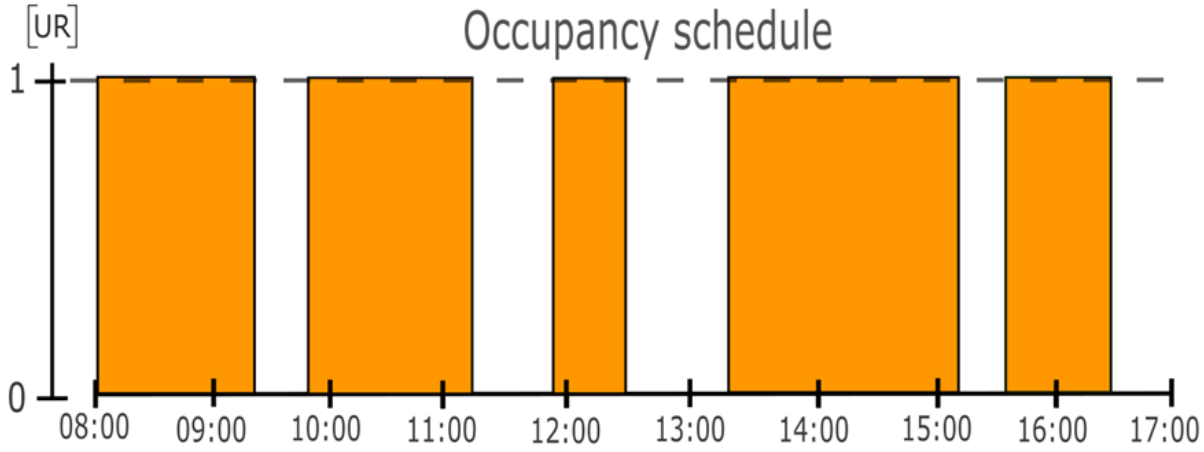

Figure 3.1: Occupancy schedule derived from occupancy model (Wang et al., 2005), see table A.2 for specific occupancy intervals

As the derived occupancy schedule corresponds to the UR from NS-EN 15193-1:2017, the occupancy schedule is assumed to be of sufficient accuracy, although the conclusions drawn from using the occupancy schedule must be treated by how it was derived.

Operative temperature set-points in the reference zone are decided through NS-EN ISO 7730:2005 and TEK 17 § 13-4, where the operative temperature stays within 19.0 °C – 26.0 °C according to TEK 17 § 13-4 with an office metabolism of 1.2 MET at vacancy intervals, although while occupancy is detected, the operative temperature is set to a stricter demand of 24.5 ± 1.0 °C with a clo value of 0.5 during summer periods, and 22.0 ± 1.0 °C with a clo value of 1.0 during winter periods according to NS-EN ISO 7730:2005. These are set-points that follow category A, which is the strictest comfort category in NS-EN ISO 7730:2005. This alternation of set-points creates more freedom of operative temperature fluctuations during vacancy intervals, although the zone is still always within minimum demands and ready to acquire occupancy. The ventilation supply temperature is set to 17.0 °C during summer periods, and 20.0 °C during winter periods for case 1 condition, which is the typical supply temperature regulation strategy, where the supply temperature regulation strategies case 2 and case 3 were previously explained under chapter 2.2.1.

Local cooling and heating units are set to 1000 watts power in IDA ICE, which is somewhat high for small offices (Ørnulf Kristiansen, project leader at Multiconsult), although the main purpose of the present work is to compare the primary energy consumption of the different control strategies and case conditions combinations.

The internal gains are extracted from a scientific article on internal heat gains in office buildings, where the weighted mean values of power consumption by lighting (assumes LED) after 2015 was 17 watt (assumes 2 lights in office), and the weighted mean values of power consumption by equipment (assumes desktop and an extra monitor) after 2015 was 53 watt + 32 watt respectively, which equals 85 watts (assumes power consumption = heat gain) (Kim et al., 2018). The internal load from the occupant is chosen to be 120 watts (126 watts in IDA ICE simulations) with the metabolism of 1.2 MET (Ingebrigtsen, 2017, p. 346). All internal gains are controlled by the occupancy schedule (see figure 3.1), and the assumption of zero power consumption of lighting and equipment is utilized during vacancy intervals, rendering the reference zone with no internal gains when empty.

A visualization of the zone energy balance in the reference zone is provided in figure 3.2:

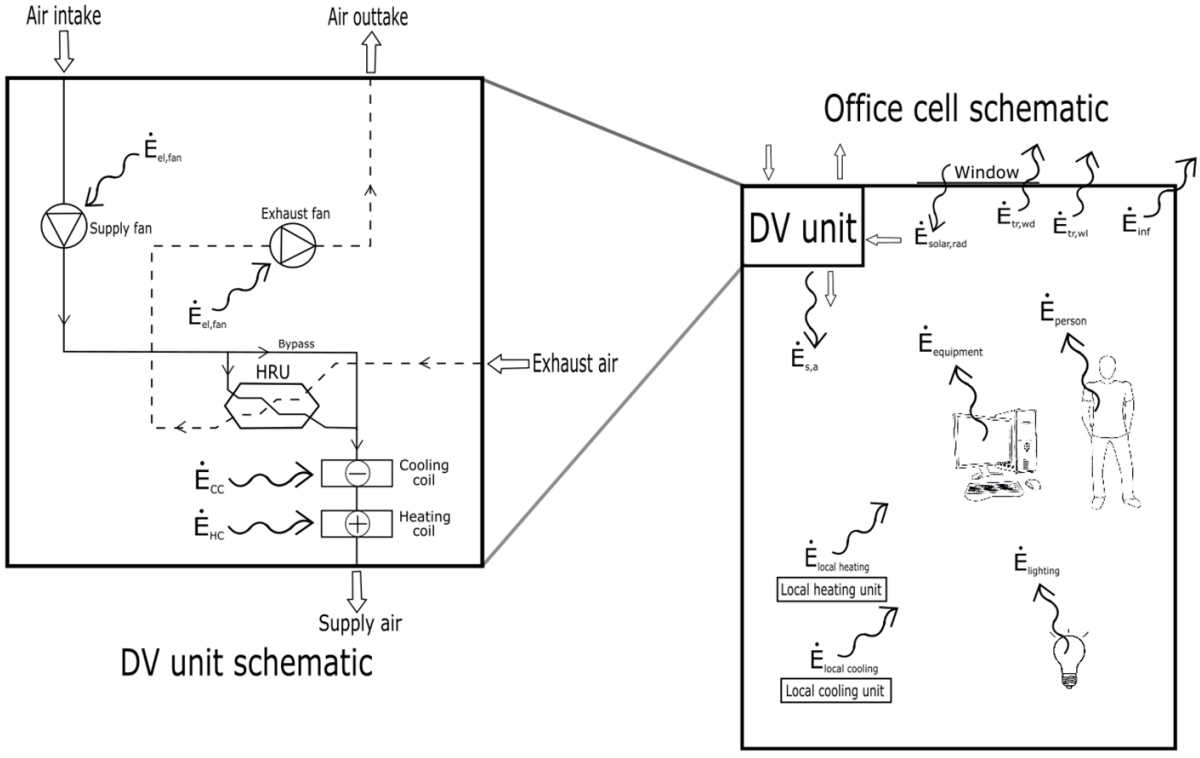

Figure 3.2: Office zone and DV unit energy balance schematic, see appendix D

3.2 Representative DV unit from field measurements

With DV systems, specific challenges arise which have to be dealt with accordingly. These problems are volume flow unbalances, unwanted recirculation/short-circuiting, and sensitivity to wind pressure. From NS-EN 13141-8:2014 it is recommended that the deviation of supply and exhaust air rate should not exceed 10 % of the respective higher air rate with a pressure difference of ± 20 Pa. The Norwegian building code only allows for recirculation of air if properly documented, however, application of this is unlikely.

Field measurements from FTDVS cover all these particular challenges, including SFP values and HRU efficiencies, which are further transformed to an intelligible table for a better overview. Only the recuperative DV units (unit C and D from the referenced article) are included in the present work, as the regenerative units are not of interest. All values are directly extracted from FTDVS (Merzkirch et al., 2016), and can be seen in figure 3.3:

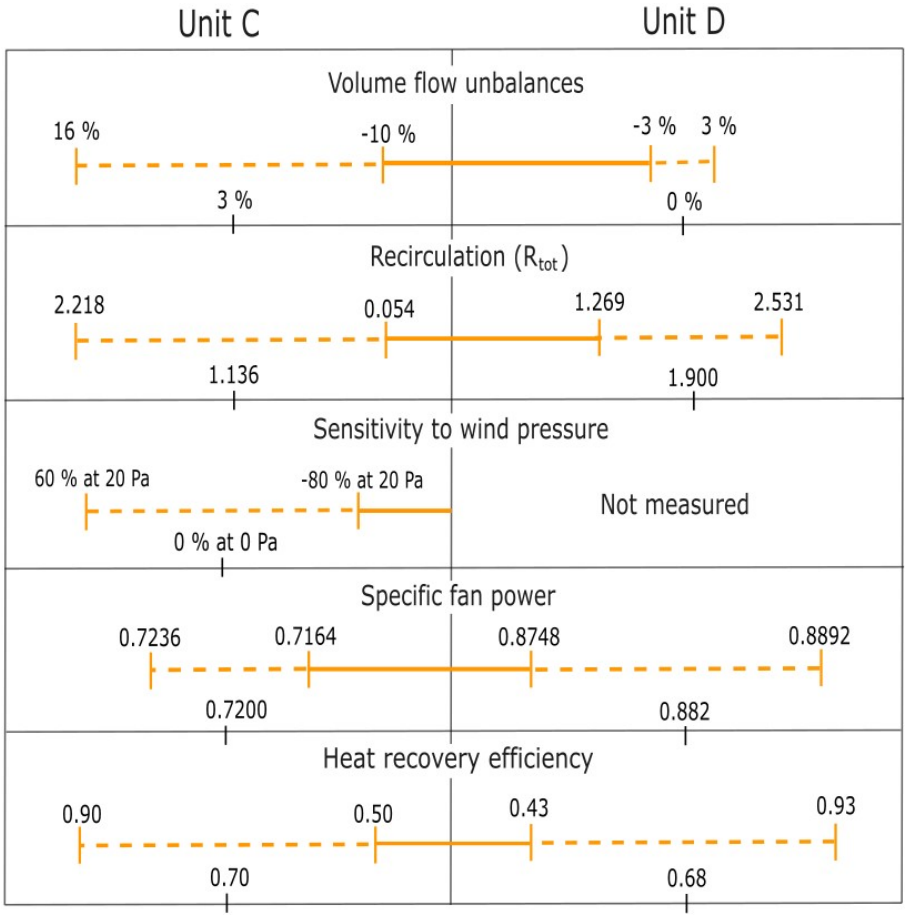

Figure 3.3: FTDVS field measurements of the recuperative type DV units (Merzkirch et al., 2016). Mean values and outer limits shown

Unit C was tested with an air rate of 31.7 ± 1.7 $\frac{m^3}{h}$ (n = 5), and unit D was tested with 35.0 ± 2.0 $\frac{m^3}{h}$ (n = 5) (Merzkirch et al., 2016). The mean value is shown in the middle of the stripped line, with the outer limits as the minimum and maximum values.

Volume flow unbalances were only snapshots in operation times which were dependent on the differential pressure caused by wind and stack effects, which activates the possibility of assuming exclusion of these unbalances into consideration when doing energy analyses, which is a typical simplification (Bonato et al., 2020). The measurements were performed in an urban surrounding with low wind exposure so that DV units should be further evaluated at open areas where the differential pressures vary more.

Measurements of the DV units showed a recirculation of around 13 %, which was a consequence of external mixing due to the close placements of inlet and outlets. Wind intensity and direction significantly influenced the amount of recirculation (Merzkirch et al., 2016). These measurements arguments for higher air rates than the Norwegian building code demands, as it typically does not allow for recirculation, and therefore compensation is required for typical ventilation control strategies that follow TEK 17 § 13-3 demands. DCV strategies will self-regulate based on temperature and the CO_2 concentration, so that as long as the upper limit of ventilation air rates is sufficient, the system will compensate appropriately.

The recirculation ratio is calculated by using the constant emission tracer gas method using the equation:

$$R_{tot} = R_{ext} + R_{int} = \frac{C_{outside} - C_{ambient}}{C_{exhaust} - C_{ambient}} = \frac{C_{supply} - C_{outside}}{C_{exhaust} - C_{outside}}$$

The sensitivity to wind pressure shows deviation from nominal air rate with supply air as the maximum value and exhaust air as the minimum value, where the transition from 0 to 20 Pa is approximately linear so that 10 Pa gives around 30 % deviation from the nominal value of supply air. The field measurements of sensitivity to differential pressure of unit C was shown to exceed the recommendation of NS-EN 13141-8:2014, which during cold winter days, a possibility of draught and decreased HRU efficiency could be a consequence (Merzkirch et al., 2016).

The specific fan power is the sum of the nominal air rate SFP and the added air rate to compensate for the recirculation percentage measured, in accordance to the equation:

$$SFP_{fan} = \frac{P_{elec}}{\dot{Q}_{min}(1 - R_{tot})} = \frac{U * I * cos(\varphi)}{\dot{Q}_{min}(1 - R_{tot})}$$

Where the consumed electricity, current, voltage, and phase shift angle are measured with a wattmeter. The relatively small SFP values compared to centralized systems is a product of the non-existent ductwork and fewer installation mistakes (Merzkirch et al., 2016). Looking at the measurements of SFP values by unit C and D, a mean value of 0.800 $\frac{kWs}{m^3}$ is found (ignoring standard deviation). In another scientific article, field measurements have measured the recuperative SFP to be 0.698 $\frac{kWs}{m^3}$ at 50 $\frac{m^3}{h}$ according to NS-EN 13779:2007 (replaced by NS-EN 16798-1:2019), although there was only tested one unit, and no standard deviation was found (Coydon et al., 2015). Even so, this result can help support the FTDVS measurements of the recuperative DV unit, so that the mean value of 0.800 $\frac{kWs}{m^3}$ is further defended to not be optimistically exaggerated.

The HRU efficiency is measured with consideration to leakage by R_{int}, which activates the possibility of difference between $\dot{m}_{extract}$ and $\dot{m}_{exhaust}$, and only considers the sensible heat, and is calculated with the equation:

$$\eta_{HRU} = \frac{T_{extract} * \dot{m}_{extract} - T_{exhaust} * \dot{m}_{exhaust}}{T_{extract} * \dot{m}_{extract} - T_{ambient} * \dot{m}_{exhaust}} = \frac{T_{extract} * \dot{m}_{extract} - T_{exhaust} * \dot{m}_{extract}(1 - R_{int})}{T_{extract} * \dot{m}_{extract} - T_{ambient} * \dot{m}_{extract}(1 - R_{int})}$$

The measured mean heat recovery efficiencies of the DV units mostly lied within the range of 0.68 – 0.76 (including regenerative type), where smaller values were due to mistakes during installation. Higher values were not commented upon. In discussion, the mean heat recovery of 0.70 with a standard deviation of 0.17 is stated (Merzkirch et al., 2016). In another scientific article, field measurements have measured the recuperative HRU to achieve efficiencies of 64.6 % - 70.0 % using measurement methods according to EN 308, EN 13053, PHI method, and exhaust side calculation, while an efficiency between 69.1 % - 79.3 % was found using three separate calorimetric measurement methods (Coydon et al., 2015). These findings correlate and are not too far away from the average HRU efficiency of 0.70 so that this simplified HRU efficiency can be further used as the foundation.

The SFP and HRU efficiency values derived from FTDVS must be treated as a simplification to the more advanced reality of the variation of efficiencies that will occur during a year, and the accuracy of the results produced from these simplifications are difficult to determine, although the results are still assumed sufficiently accurate for the comparison analysis.

Furthermore, volume flow unbalances and sensitivity to wind pressure factors are further ignored, as this complicates the calculations due to the uncertainty and variety of the external conditions that alter these parameters. Even so, it is stated that these are mere snapshots of the big picture of operation (Merzkirch et al., 2016). Discussion with the sales manager of Airmaster and their engineering team has been done to further discuss these DV unit-specific problems, where it was stated that pressure imbalances caused by wind and the volume flow imbalances was rare and taken into consideration in the design of the DV unit, although this can only be said for their respective DV units, and not in general. Recirculation is more easily handled by adding the extra air rates to compensate for the recirculation, which is done to ensure that the stricter rules of recirculation according to the Norwegian building code are maintained (Eivind Ernstsen, Sales manager at Airmaster), which has been implemented in the present work. These complications have also been further ignored in scientific literature as aforementioned (Bonato et al., 2020).

3.3 Monthly time-step energy analysis

The monthly time-step energy analysis's main purpose is having further comparison data, which is investigated under the static control strategies and climate situations purely by hand calculations, as this helps better understand how and why different control strategy combinations differ in energy performance, which could be harder to decipher in simulations. The results are to be discussed solely by comparison to each other, where a total of 27 different calculations are conducted. The results are not meant for accurate prediction of real-life scenarios. Only primary energy consumption accumulated under operating times are included for comparison of control strategies under the monthly time-step energy analysis, see appendix D.

3.3.1 Boundary conditions, zone energy balance and weather data

A scientific article on the VAV technology (Okochi and Yao, 2016) explains some conditions for simplifications so that the following assumptions are made:

- Uniform distribution of zone temperature due to proper mixing of air. This enables the dynamics of the conditioned space to be expressed as a lumped parameter model
- Mean values of set-points temperatures are utilized in zone energy balance equations so that the zone temperature is set to constant at 24.5 °C during summer and 22.0 °C during winter
- Constant specific heat capacity of air $C_{p,a} = 1006\ \frac{J}{kgK}$. Assumed constant as it varies little with outdoor temperature
- Constant air density $\rho_{s,a} = 1.263\ \frac{kg}{m^3}$. In the standard reference year, the yearly average outdoor air temperature was 6.3 °C (based on monthly mean averages)
- The exhaust air is assumed to be ideally controlled to match the supply air rate and maintain a constant room pressure (Baldini et al., 2008)
- Temperature rise over fan is assumed to be 0 K. Based on $\Delta T_{fan,\ rise} = 0.0011{*}\Delta p$ (Ingebrigtsen, 2017, p. 343), where Δp is small (typically $<$ 100 Pa) (Merzkirch et al., 2016) in DV units

The weather data which is used in monthly calculations are the standard reference year according to NS 3031:2014 (withdrawn) (see figure 3.4), which must be used for monthly calculations following the Norwegian building code. For a wider investigation, Fornebu weather data from February 2020 to January 2021 is also used which is extracted from YR, where the hottest days are picked from each month to represent that specific month, so that the year is further described as an "extreme hot year", similarly, this is done to produce an "extreme cold year" (see figure 3.4). January 2021 is used instead of 2020, since January 2021 is colder and therefore more interesting to analyze. The extreme hot and cold years do not represent any real typical climates but are only investigated based on their extremity to better understand the climate's impact on energy consumption on the different control strategies. The graph of each year can be seen in figure 3.4:

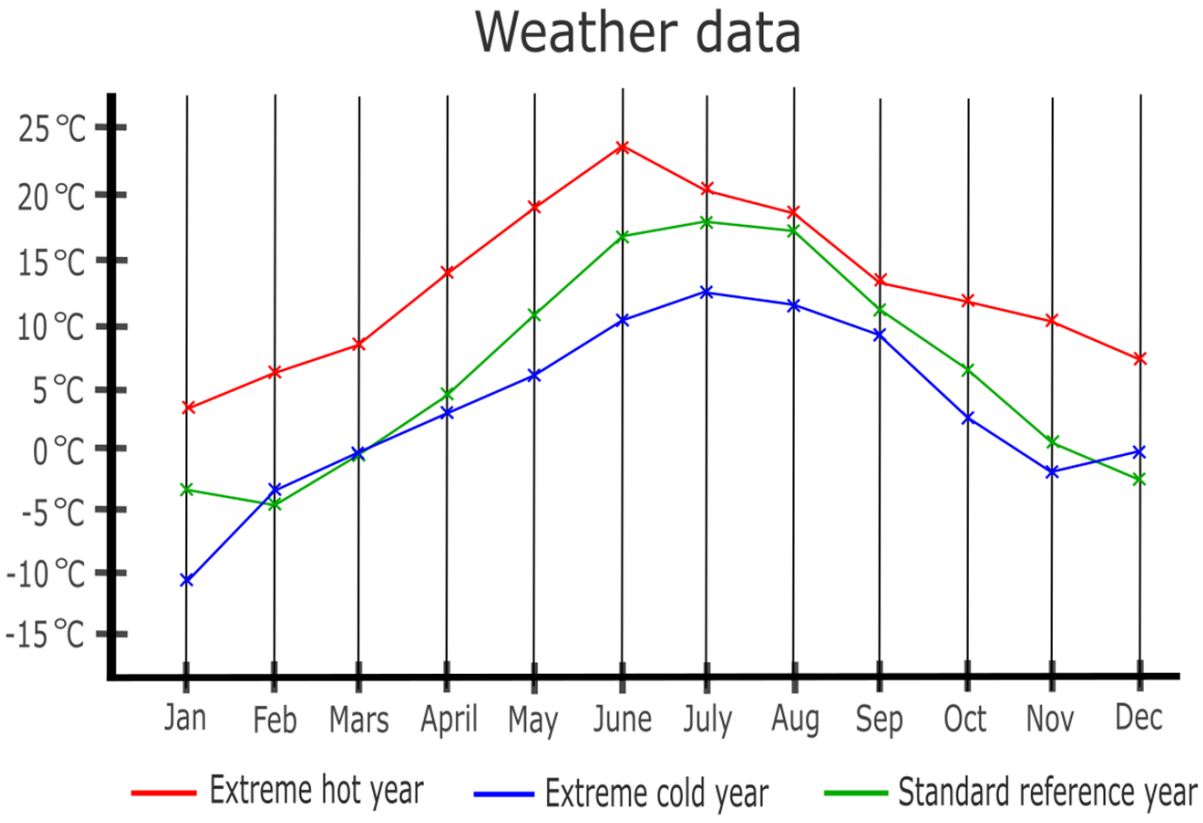

Figure 3.4: All weather data used for monthly calculations

The chosen DV unit specifications in monthly time-step energy analysis are extracted from FTDVS (Merzkirch et al., 2016), in combination with other scientific articles which includes wind loading (Baldini et al., 2008) (Baldini and Meggers, 2008) (Mikola et al., 2019). Conclusions based on these results in themselves are not given due to difficulty in determining accuracy, although the comparison between the examined relationships is discussed.

The wind load is determined from (Mikola et al., 2019):

$$P_{wind} = \frac{C_{p,wind} * \rho_a * U_{wind}^2}{2}$$

The specific fan power with wind loading is determined from (Schild and Mysen, 2009):

$$SFP_{wind} = \frac{\Delta P_{tot,wind}}{\eta_{fan}}$$

The assumed SFP value is given without and with wind loading respectively:

$$SFP_{no,wind} = 0.800 \, \frac{kWs}{m^3} \rightarrow SFP_{wind} = 0.732 \, \frac{kWs}{m^3}$$

The SFP value is calculated with the constant addition of 11 Pa $\left(6.5 \, \frac{m}{s}\right)$ from wind, which is an optimistic estimation of the actual effect on wind loading, although other scientific articles have been more optimistic when determining wind loading effects on DV units (Baldini et al., 2008) (Lu and Ip, 2009) (Baldini and Meggers, 2008). In reality, the wind speed varies a lot, and so does the direction, meaning that the pressure coefficient $C_{p,wind}$ (0.4 is used in the present work) will change between being both negative and positive, and with different values. The stack effect which also contributes to differential pressures (Mikola et al., 2019) is not included in the present work.

The wind loading is not meant to produce any accurate results, but rather to compare and see how the different control strategies utilize the lowered SFP, so that wind loading could potentially create superior control strategies in that regard.

The constant HRU efficiency is set at 0.7.

3.3.2 Ventilation control strategies (monthly calculations)

The calculation methodology and assumptions of the static control strategies for the monthly time-step energy analysis are described in the following subsections. The equations used for energy calculations in each control strategy can be seen in appendix D.

It is assumed that the transition between internal gains and no internal gains with respect to the occupancy schedule are instantaneous. Heating losses to infiltration and transmission, $\dot{E}_{inf} + \dot{E}_{tr,wl} + \dot{E}_{tr,wd}$ work independently of time, and are constant. The internal loads $\dot{E}_{internal}$ all follow the same occupancy schedule (figure 3.1)

3.3.2.1 DV CAV control strategy

Regular CAV, 10 hours (07:00 – 17:00) operating time (Halvarsson, 2012) (min-max air rate strategy). Operating time 10 hours a day, 5 days a week, 50 weeks a year. That is 2500 hours used for maximum air rates ($t_{max,CAV}$). The hours outside of the operating time 8760 – 2500 = 6260 hours used for minimum air rates ($t_{min,CAV}$). There are three different stationary scenarios (S1, S2 and S3, where scenario 3 is excluded from results) of energy balance equations which must be calculated to see when and how much cooling/heating is necessary to achieve the chosen zone temperature balance, see figure 3.5:

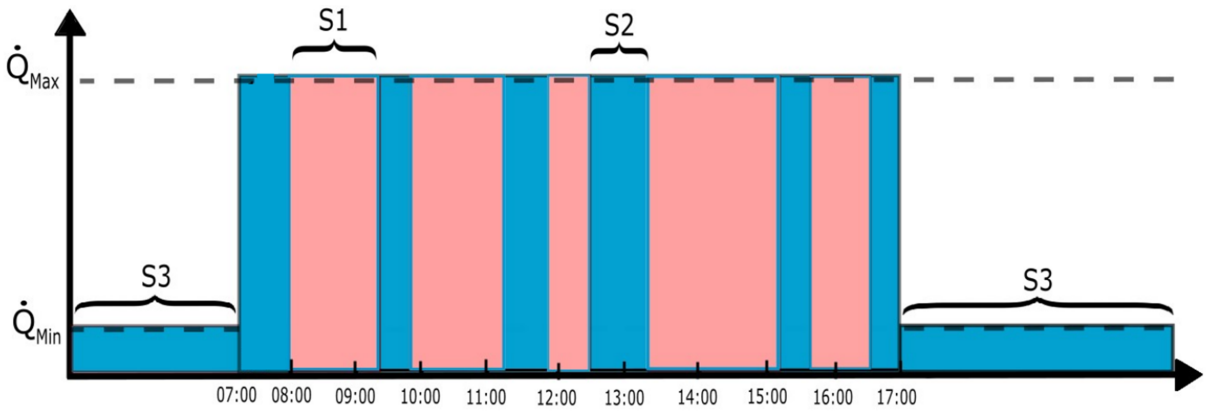

Figure 3.5: DV CAV control strategy ventilation pattern, occupancy schedule and the different scenarios

Here all the tall pink blocks (occupancy pattern) are intervals of scenario 1 (S1, occupancy and max ventilation load), all the tall blue blocks are intervals of scenario 2 (S2, vacancy and max ventilation load), and the small blue blocks are intervals of scenario 3 (S3, vacancy and minimum ventilation load, excluded from results).

3.3.2.2 DV PIR control strategy

Operating time 10 hours a day (07:00 – 17:00) (Halvarsson, 2012), 5 days a week, 50 weeks a year. That is 2500 hours ($t_{max,CAV}$). The room only needs max air rate 60 % of the time during the 10 hour interval (see figure 3.1), which is the same as having the operating time at 1500 hours ($t_{max,PIR}$) for ventilation of $\dot{Q}_{max}$. There are two different stationary scenarios (S1 and S2, where S2 outside operating time is excluded from results) of energy balances which must be calculated to see when and how much cooling/heating is necessary to achieve the chosen zone temperature balance, see figure 3.6:

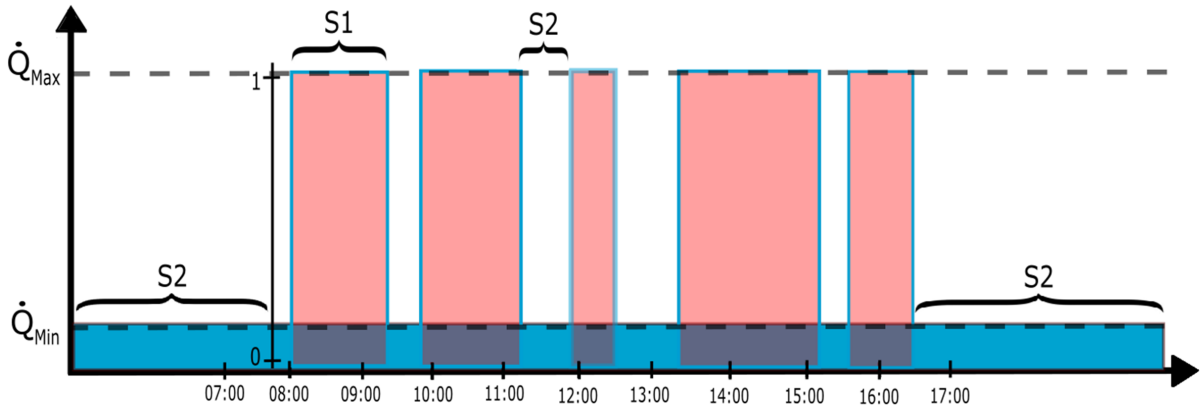

Figure 3.6: DV PIR control strategy ventilation pattern, occupancy schedule and the different scenarios

Here all the tall pink blocks (occupancy schedule) are intervals of scenario 1 (S1, occupancy and max ventilation load), and the small blue blocks are intervals of scenario 2 (S2, vacancy and minimum ventilation load, where the interval of 17:00 - 07:00 is excluded from results).

3.3.2.3 DV S-CO_2 control strategy

The full derivation of the DV S-CO_2 control strategy can be seen in appendix C. The complete CO_2 concentration timeline is visualized in figure 3.7:

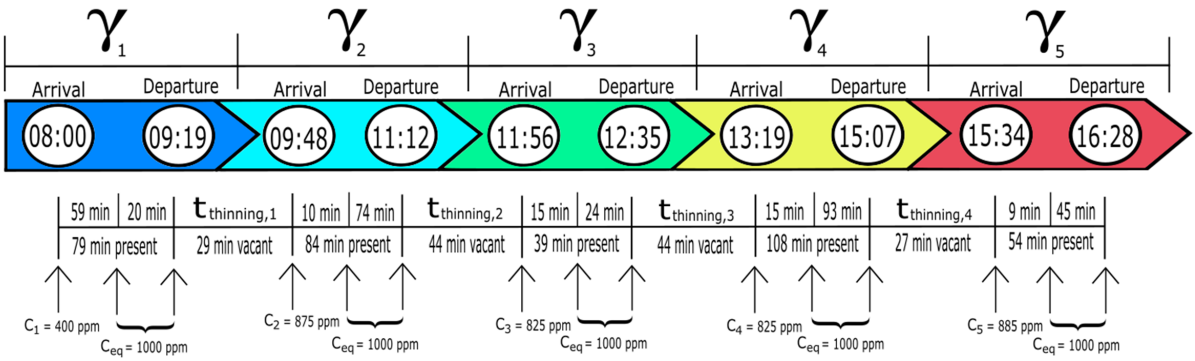

Figure 3.7: Complete CO_2 concentration timeline

There are three different stationary scenarios (S1, S2 and S3, where S3 outside operating time is excluded from results) of energy balances which must be calculated to see when and how much cooling/heating is necessary to achieve the chosen zone temperature balance, see figure 3.8:

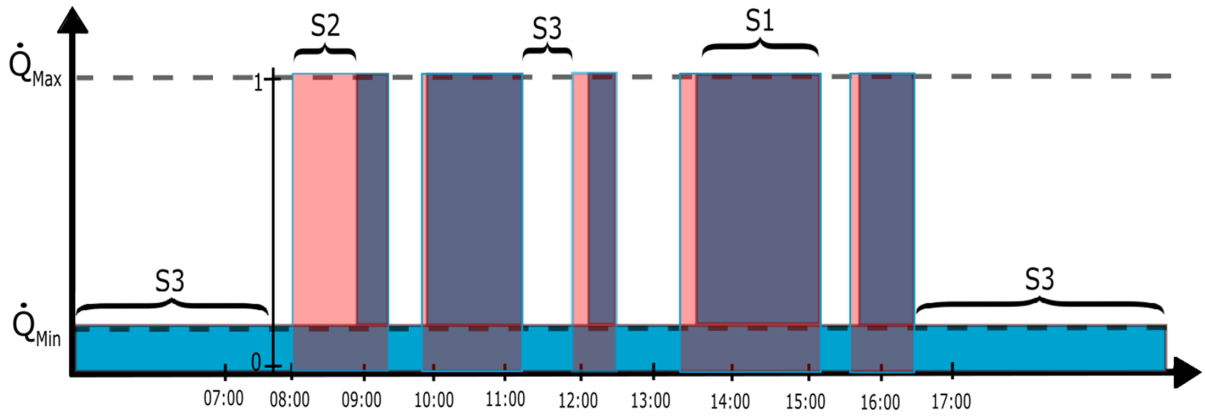

Figure 3.8: DV S-CO_2 control strategy ventilation pattern, occupancy schedule and the different scenarios

Here all the tall dark blue blocks are intervals of scenario 1 (S1, occupancy and max ventilation load), the tall pink blocks are intervals of scenario 2 (S2, occupancy and minimum ventilation load), and the small blue blocks are intervals of scenario 3 (S3, vacancy and minimum ventilation load, where the interval of 17:00 - 07:00 is excluded from results).

3.4 Building simulation

The building simulation is done through IDA ICE version 4.8, and is conducted for a more accurate representation of the primary energy consumption of each control strategy, for a stronger conclusive power when comparing the control strategies to each other. The accuracy of the produced results are limited to the accuracy of the building simulation program itself, and the boundary conditions, assumptions and input combinations utilized when running the simulations, which is further explained in detail for a full overview.

3.4.1 Boundary conditions

Firstly, the zone model is described, with the general specifications that are equal for all the ventilation control strategies and cases. The constructed office zone model can be seen in figure 3.9, and the full set of input parameters can be seen in appendix E.

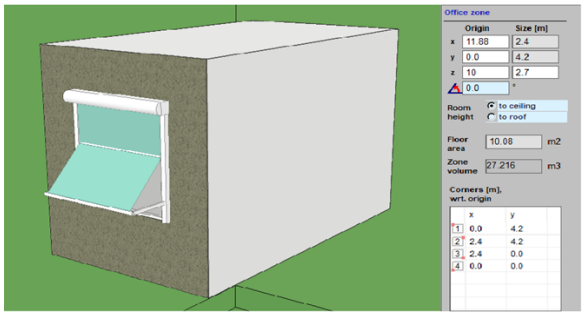

Figure 3.9: Office zone model and its geometric values in IDA ICE

Simulations are run separately divided into summer and winter, into subcategories of case 1, case 2, and case 3. The weather data utilized is the Oslo/Fornebu_ASHRAE weather file, in the period 01.04.19 – 31.03.20, see figure 3.10:

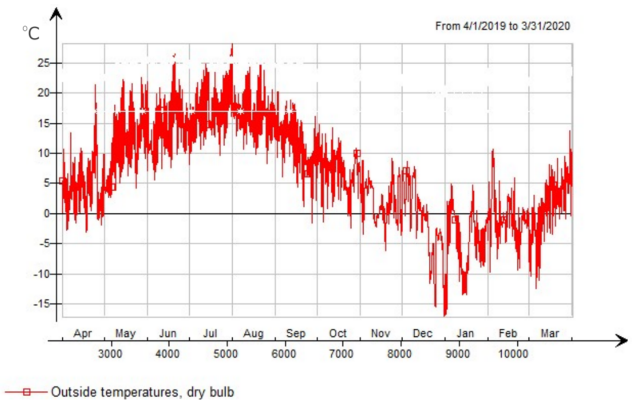

Figure 3.10: Oslo/Fornebu_ASHRAE weather data, 01.04.19 – 31.03.20

3.4.2 Ventilation control strategies (IDA ICE)

Instead of describing how calculations are done, the inputs of how to make the program simulate each control strategy and case are described.

The supply set-point temperature in cases 2 and 3 is regulated by calculating the maximum supply of air which can be achieved through only utilizing the HRU, which is a function of the exhaust air temperature, ambient dry-bulb temperature, and HRU efficiency. During winter months, case 2 and 3 are rendered with no effect, as the exhaust temperature and the outdoor temperature are lower, so that the energy consumption during winter months are not altered from case to case, which is similar to other findings, where fan-assisted natural ventilation was only partly available during October with Copenhagen weather data (Kim and Baldini, 2016).

The cases and their supply temperature pattern was presented under chapter 2.2.1, and the IDA ICE regulation control of the three cases are presented in appendix F.1, figure F.1 - F.4, which are manipulated inside the AHU control panel. Since supply temperatures during case 2 and 3 are not automatically calculated by the software, there will be some error in results in the shape of additional AHU heating energy to satisfy the supply temperature input, although in practical situations this will not happen, so this extra AHU heating is further removed from the results.

The AHU acts as the decentralized unit here, where the SFP and HRU efficiency is regulated to the values found in FTDVS. The AHU simplification to act as a DV unit is defended by how the recuperative DV unit acts as a small, centralized unit inside the room, as the fans are of the radial or centrifugal type, and the HRU is of counter-flow type.

3.4.2.1 DV CAV control strategy

The DV CAV control strategy is in practical circumstances a VAV schedule strategy in IDA ICE, which follows the timeline of 07:00 – 17:00 as the typical operation time within single-person offices (Halvarsson, 2012). The schedule followed is shown in figure 3.11:

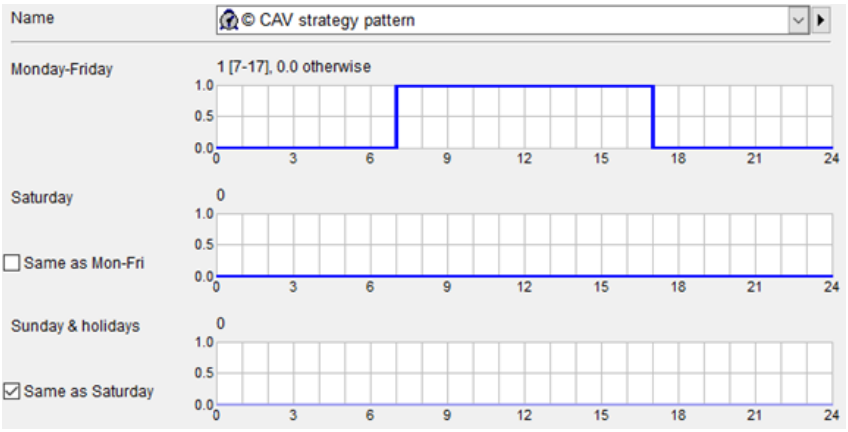

Figure 3.11: DV CAV control strategy schedule in IDA ICE

When the blue line is equal to y = 1.0, the ventilation air rate is set to max, which is the ventilation demand of 58 $\frac{m^3}{h}$ (16.11 $\frac{l}{s}$), and while it is equal to y = 0.0, the ventilation air rate is set to the minimum ventilation demand of 8 $\frac{m^3}{h}$ (2.22 $\frac{l}{s}$). This ensures that the Norwegian building code is always upheld year around. The ventilation pattern is shown under figure 3.12:

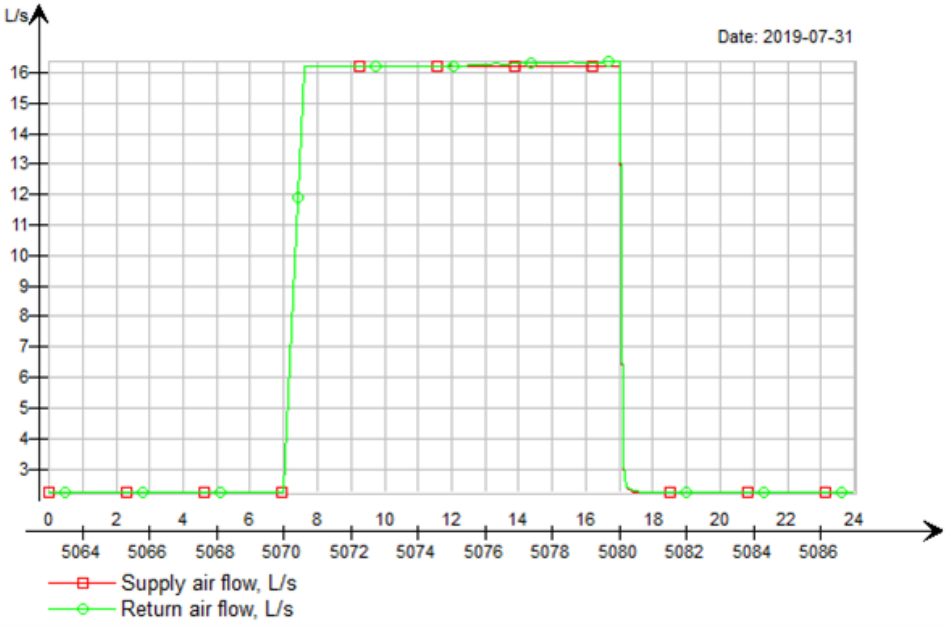

Figure 3.12: DV CAV control strategy ventilation pattern

3.4.2.2 DV PIR control strategy

The DV PIR control strategy is in the simulation software also a VAV schedule control strategy, although here, the timeline matches that of the occupancy schedule (see figure 3.1), which under practical circumstances will replicate a PIR sensor control strategy, since the max air rate is activated whenever the occupancy is detected. The schedule followed is shown in figure 3.13:

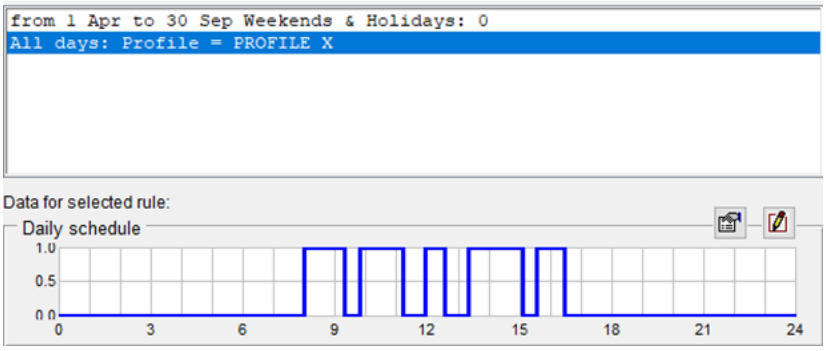

Figure 3.13: DV PIR control strategy schedule in IDA ICE

When the blue line is equal to y = 1.0, the ventilation air rate is set to max, which is the ventilation demand of 58 $\frac{m^3}{h}$ (16.11 $\frac{l}{s}$), and while it is equal to y = 0.0, the ventilation air rate is set to the minimum ventilation demand of 8 $\frac{m^3}{h}$ (2.22 $\frac{l}{s}$). This ensures that the Norwegian building code is always upheld year around. The ventilation pattern is shown under figure 3.14:

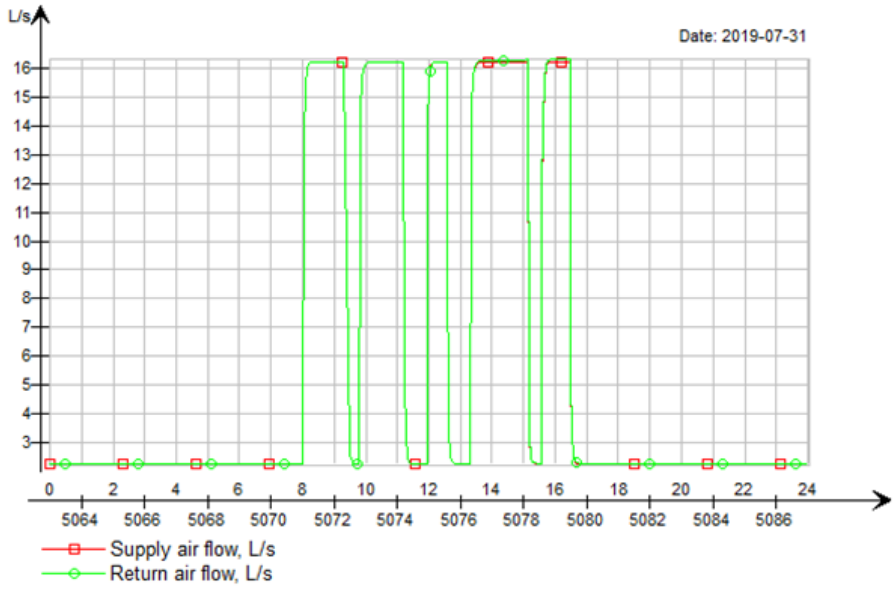

Figure 3.14: DV PIR control strategy ventilation pattern

3.4.2.3 DV S-CO_2 control strategy

The DV S-CO_2 control strategy requires a custom control, which is done by measuring the zone CO_2 concentration and implementing the CO_2 max set-point = 1000 ppm into a proportional controller. This ensures the max air rate to be activated whenever the CO_2 concentration exceeds 1000 ppm, which only happens during occupancy. The custom controller is shown in figure 3.15:

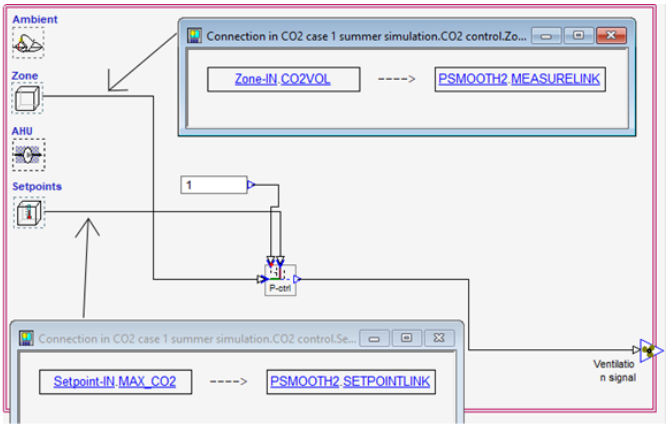

Figure 3.15: DV S-CO_2 custom control for two step CO_2 control strategy

When the CO_2 concentration is measured to be a 1000 ppm, the ventilation air rate is set to max, which is the required air rate for maintaining the CO_2 concentration at exactly 1000 ppm, which in accordance to the IDA ICE simulation inputs, is equal to 32 $\frac{m^3}{h}$ (8.89 $\frac{l}{s}$) per person (IDA ICE pre-defined CO_2 generation rate using 1.2 MET), and while the CO_2 concentration is below 1000 ppm, the minimum ventilation demand of 8 $\frac{m^3}{h}$ (2.22 $\frac{l}{s}$) is used. The ventilation and CO_2 concentration pattern are as shown under figure 3.16:

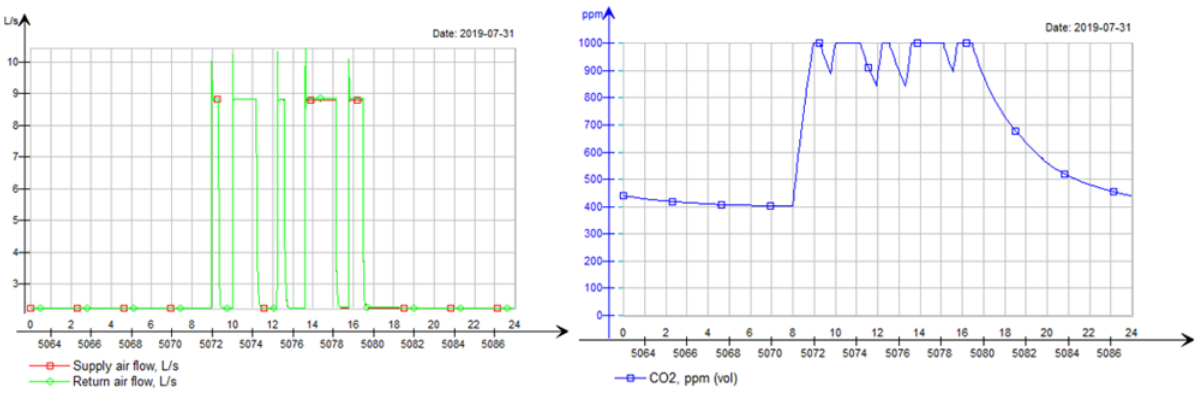

Figure 3.16: DV S-CO_2 control strategy ventilation pattern (left), and CO_2 concentration pattern (right)

3.4.2.4 DV D-CO_2 control strategy

The pre-defined D-CO_2 control strategy custom control could not be extracted from IDA ICE, as it was not visually available. The dynamic proportional control (red line) is rather visualized as compensation for the lacking IDA ICE control scheme, see figure 3.17:

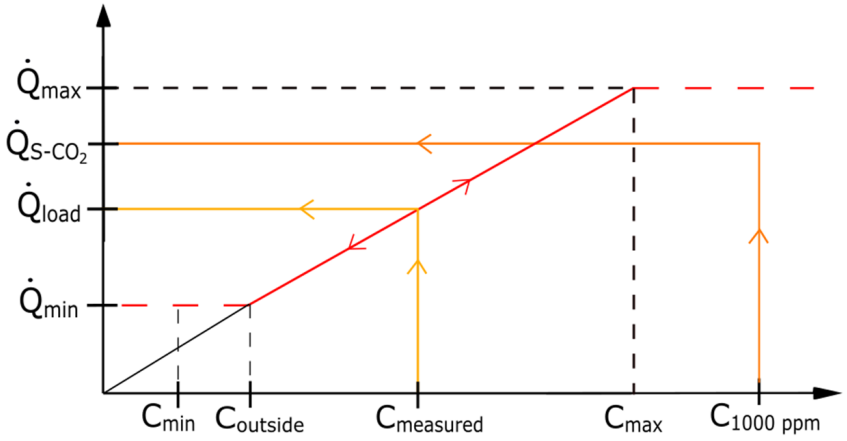

Figure 3.17: Dynamic proportional control principle of the DV D-CO_2 control strategy (Bonato et al., 2020)

The red line is the ventilation pattern, where $\dot{Q}_{min}$ is the lower limit ventilation demand when the room is not in use, while $\dot{Q}_{max}$ is the maximum load ventilation demand during occupancy intervals according to the Norwegian building code TEK 17 § 13-3. The ventilation control strategy does not take into consideration these demands directly but rather ventilates proportionally to whatever the CO_2 concentration meets on the red line (figure 3.17), which decides the ventilation load between the lower and upper ventilation demand (Bonato et al., 2020) (Airmaster, 2020b). The ventilation and CO_2 concentration pattern are as shown under figure 3.18:

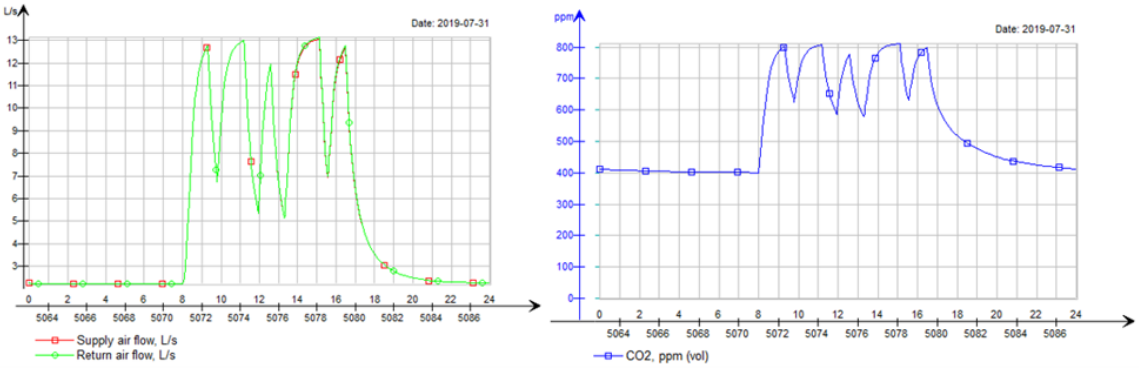

Figure 3.18: DV D-CO_2 control strategy ventilation pattern (left), and CO_2 concentration pattern (right)

3.4.2.5 DV S-CO_2 + temperature control strategy

The DV S-CO_2 + temperature control strategy requires a custom control, which is already pre-defined in the simulation software. Similar to the S-CO_2 control strategy, the strategy forces a neutralizing air rate to keep the CO_2 concentration below 1000 ppm at all times, while simultaneously using a PI controller to cool the zone using the interval of the upper and lower ventilation set-points, concerning the heating and cooling set-points. A local zone cooling unit is not utilized during this control strategy, as the ventilation cooling is assumed sufficient, even so, the software does not allow for cooling units regardless during this control strategy combined with heating and cooling set-points controlled by schedule. The maximum air rate is limited by the DV unit capacity and the noise demands which must be followed in accordance to TEK 17 § 13-6. The total sound level is determined to not exceed $L_{p,Aeq} = 35$ dB(A), which is the recommendation by Byggforsk 421.421. FTDVS noted that units C and D could deliver an air rate of 30 $\frac{m^3}{h}$ at around 25 dB(A). DeAL showed deviations from building to building, where noise emissions did not have a clear pattern of air rate to noise correlation. Under building 202, 207 and 209, an air rate of 85 $\frac{m^3}{h}$ could keep the noise under 35 dB(A) (see figure 2.21). With these considerations, a max air rate of 85 $\frac{m^3}{h}$ is chosen in simulations for regulating cooling loads (varies with DV system).

The pre-defined custom control is shown under figure 3.19:

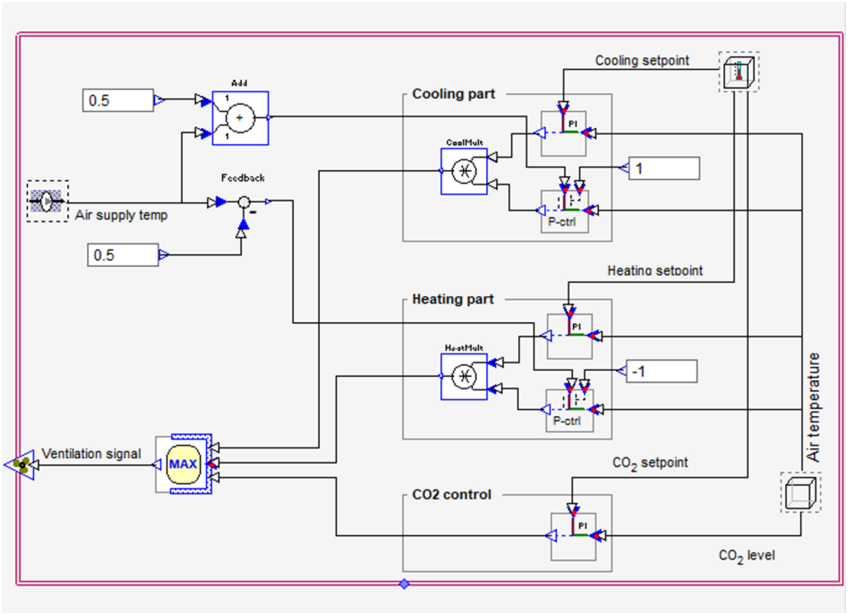

Figure 3.19: Pre-defined S-CO_2 + temperature custom control in IDA ICE

The ventilation pattern during summer is shown under figure 3.20:

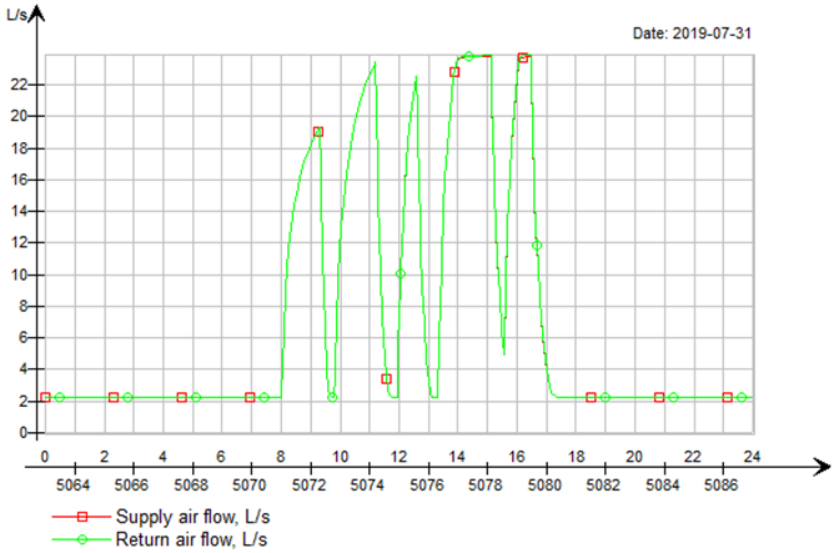

Figure 3.20: DV S-CO_2 + temperature control strategy ventilation pattern, case 1

The ventilation pattern during winter is almost identical to that of figure 3.16, as it is purely controlled by the S-CO_2 strategy whenever the zone does not require cooling.

The CO_2 concentration control is mostly not necessary during the summer season as the cooling load requires such high ventilation rates that the CO_2 concentration never reaches 1000 ppm anyways, this leads to better indoor air quality than the pure S-CO_2 control strategy in that regard. During the winter season, the reason behind the CO_2 control becomes much clearer, see figure 3.21:

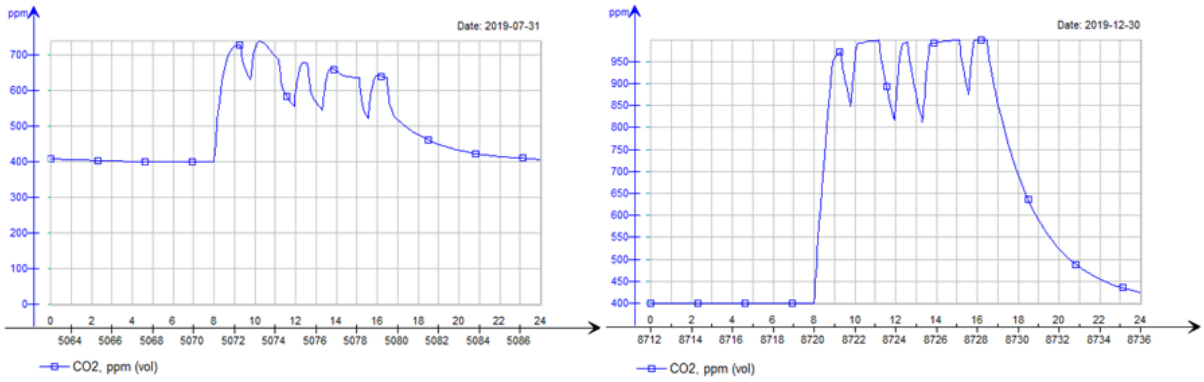

Figure 3.21: CO_2 concentration pattern on the hottest day (left) and coldest day (right) of the year, case 1

3.4.3 Centralized CAV system for energy comparison

A centralized system with a CAV control strategy is used as the frame of reference for energy savings comparison. Primary energy consumption is referred to as CV CAV S, CV CAV W, and CV CAV A for summer, winter, and annually respectively. Typically, a whole building is used for the frame of reference, although the relevant zone is only a single-person office room, so some simplifications are necessary.

The full description and results of the centralized CAV system primary energy consumption can be seen in appendix K.

3.4.4 Comparison of energy performance to three-person office

A comparison of the single-person office room results is compared to a three-person office room as the different control strategies might react differently to different boundary conditions. These boundary conditions are increased floor area, increased occupancy load, different occupancy schedule, and different demands of the room. Specific boundary conditions are extracted from a peer-reviewed article, which did an energy analysis of a façade integrated ventilation system on a three-person zone (Bonato et al., 2020). The boundary conditions extracted are the occupancy load and schedule, with some of the geometric values of the reference zone. The window is changed to fit the window to floor area relationship of the single-person office zone so that the energy comparison is more reliable. This comparison analysis is conducted because of the important insight to be gained from which control strategy fits best in different room sizes and occupancy loads/schedules.

The extraction description and specific results are given in appendix J. The comparison results can be seen under chapter **??**.

3.4.5 HRU absence and efficiency variations on energy presence

The HRU's purpose is to save energy by utilizing the thermal energy of the exhaust air and transferring this energy to the supply air. The HRU, therefore, has the greatest effect during larger temperature differences, so that colder climates will rely more on heat recovery units, and more neutral weather conditions such as Rome, do not need the heat recovery unit to the same extent (Kim and Baldini, 2016). An important question, therefore, arises on when the HRU is actually needed, and when it would become a poor choice in terms of energy performance to economy optimization. Firstly, if a much cheaper product without an HRU is possible, the energy savings in a neutral climate might not surpass the investment cost, making it economically a bad choice. Secondly, the additional pressure which the supply air must overcome in the HRU path for efficient heat exchange is a major source of increased fan power energy consumption (Gendebien et al., 2012). The question of interest is then how much energy consumption is saved or lost in the local Norway climate by not integrating the HRU, or buying a DV unit without an HRU. This question is firstly checked seasonally by summer and winter, and then annually so that a decision based upon seasonal energy consumption can be a factor of choice of DV unit.

The relevant HRU is the recuperative counter flow air-to-air heat exchanger, which is the most commonly used HRU in the relevant DV unit (recuperative unit). This HRU is found in the AM 150 DV unit as well (Airmaster, 2020a), although the pressure loss relationship of pathing through the HRU, contra the bypass is not known for this specific DV unit, so a more general approach of deciding the pressure relationship must be employed.

The pressure subtraction description by removing the HRU from the DV unit is given in appendix L, while the specific results can be viewed in appendix H.2. The comparison results can be seen under chapter 4.2.3.

3.4.6 AM 150 with manufacturer datasheet specifications

The AM 150 is a commercial DV unit from Airmaster which is specifically designed for smaller spaces such as office cells, small meeting rooms and group rooms (Airmaster, 2020a). This DV unit is used as the inspirational design for the representative DV unit present in this work, which is the recuperative DV unit design aforementioned. It is designed for Nordic climates and is stated to comply with the Norwegian building code and Norwegian Labor Inspection Authority (Eivind Ernstsen, Sales manager at Airmaster). The unit comes with a PIR sensor and CO_2 sensor, which makes all the relevant control strategies possible without having to further invest in the necessary equipment (Airmaster, 2020b). It can be combined with the CC 150 which acts as the cooling coil. The specifics such as SFP and HRU efficiencies are given in the datasheets (Airmaster, 2020a).

The DV unit uses a mixing ventilation principle, which is supplied through diffusers as shown in figure 3.22 (the figure is extracted directly from an Airmaster presentation (Airmaster, 2018)):

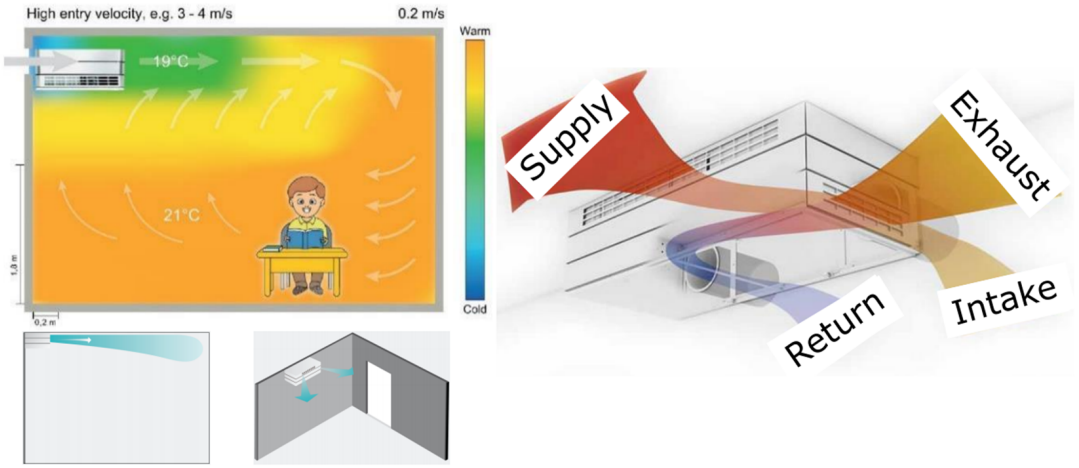

Figure 3.22: Air distribution and schematic principles of the AM 150 (Airmaster, 2018)

The AM 150 datasheet specifications are utilized for a comparison to the energy consumption results found from field measurements in scientific literature (representative DV unit) and to the centralized CAV system for a better understanding of the potential of commercially available DV units. The specification extraction description of the AM 150 DV unit is given in appendix M, while the specific results can be viewed in appendix H.3. The comparison results can be seen under chapter 4.2.4.

4 Results and discussion

Temperature regulation (cases) and air rate regulation control strategies explanations are given in chapter 2.2.1 and 2.2.2 respectively. Floor area of single-person office is 10 m^2.

4.1 Monthly time-step energy analysis

The monthly time-step energy analysis methodology is given in chapter 3.3. The monthly calculations' primary energy consumption are utilized for comparative analysis and discussion concerning building simulation results. The results are only given within operating time, as the main focus is the comparison of control strategies, see figures 4.1 – 4.3:

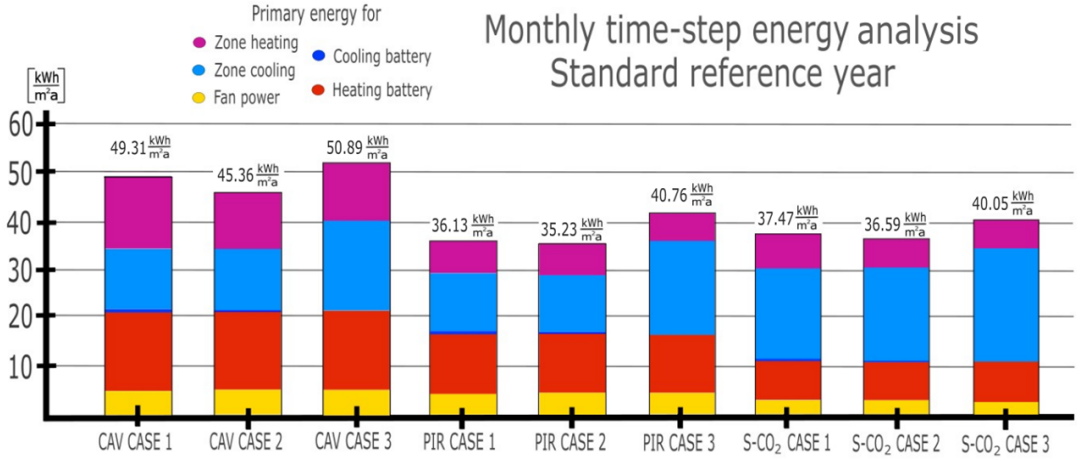

Figure 4.1: The comparison of primary energy for each decentralized ventilation control strategy and case using monthly calculations for the standard reference year weather data, see appendix G.1, tables G.1 – G.3

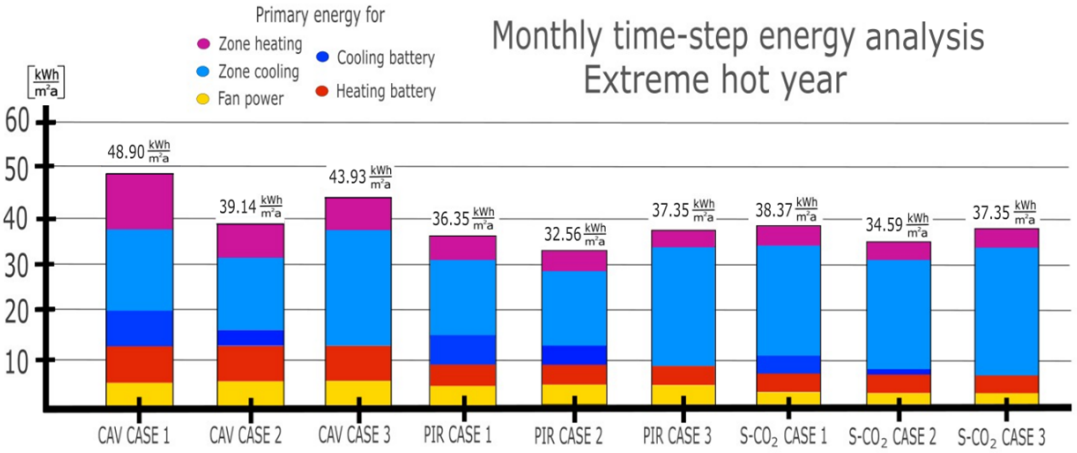

Figure 4.2: The comparison of primary energy for each decentralized ventilation control strategy and case using simple monthly calculations for the extreme hot year weather data, see appendix G.2, tables G.4 – G.6

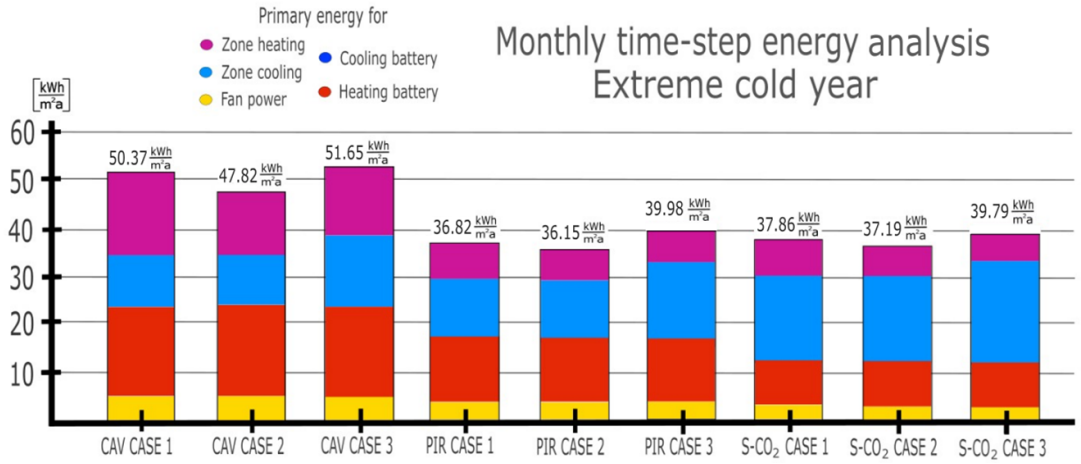

Figure 4.3: The comparison of primary energy for each decentralized ventilation control strategy and case using simple monthly calculations for the extreme cold year weather data, see appendix G.3, tables G.7 – G.9

The exact results for all climate situations and control strategies can be seen under appendix G, which are based on calculations from appendix D.

The monthly energy analysis showed that the decentralized ventilation Passive InfraRed (DV PIR) control strategy case 2 had the best performance during all weather conditions, although case 1 and case 2 during the DV PIR and decentralized ventilation static-CO_2 (DV S-CO_2) control strategy are almost identical, so it is difficult to determine the best performing control strategy solely from the monthly energy analysis. The small differences are thought to be because case 1 creates the issue of high heat loss due to ventilation created by the low supply temperature of 17 °C. Case 2 partially avoids the ventilation heating problem by increasing the supply temperature so that the temperature difference between the zone temperature set-point and the supply temperature is decreased, although the differences are minimal in the DV PIR and S-CO_2 control strategy as aforementioned. These differences are much clearer during the decentralized ventilation constant air volume (DV CAV) control strategy, where there are no internal gains to neutralize the high ventilation cooling effect during vacancy times, so the zone heating is notably decreased during case 2 when higher supply temperatures help decrease the zone heating demand. Case 3 produces higher cooling loads during occupancy times, which is due to the decreased ventilation cooling effect, and the local zone cooling is increased as a consequence, which enables the poorer energy performance of the case 3 regulation strategy during all control strategies.

The DV S-CO_2 control strategy performed worse than the DV PIR strategy due to its increased local zone cooling loads which was caused by smaller intervals of ventilation under max load, which caused the internal loads to be under the same intervals as minimum ventilation loads so that the ventilation cooling performance had much less effect on minimizing the zone temperature, which created higher local zone cooling loads to neutralize the zone (see figure 3.8). Both the DV PIR and S-CO_2 control strategy performed notably better than the DV CAV control strategy overall, which is an expected result (Mysen et al., 2005).

The differences in energy consumption during different weather conditions shows the biggest difference in case 2 and 3 in the DV CAV control strategy from the standard reference year and extreme cold year to the "extreme hot year", where the "extreme hot year" had the lowest energy consumption due to lower heating loads, and cold further neutralize the zone heating demands with higher supply temperatures, and the "extreme cold year" has the highest energy consumption due to high zone heating loads and low supply temperatures. The pattern in energy consumption from control strategy to control strategy is moderately corresponding in each weather condition so that this is potentially not a significant factor. The cases are noted to be converging towards case 1 energy performance as the weather becomes colder.

The wind-induced pressure differences in the façade cause minimal fan energy savings relatively speaking to the total fan energy consumption on the analyzed control strategies during monthly calculations, which were analyzed under optimistic boundary conditions. The fan power energy consumption difference between optimistic wind loading and no wind loading on the DV unit was at most 0.3 $\frac{kWh}{m^2a}$ (which did not make a visual impact in the graphs, hence its exclusion). This is based on a simple addition of free pressure from a constant wind speed, which is a major simplification and was also only analyzed at one office, while other scientific articles performed the analysis on advanced topology network systems containing a surplus of DV units under further increased optimistic boundary conditions so that no conclusions are drawn from the results (Baldini et al., 2008). The fan power savings are potentially higher during the DV S-CO_2 + temperature control strategy since the cooling loads are connected to the fan energy savings, this was not analyzed during the monthly time-step energy analysis.

4.2 Building simulation

The representative DV unit is presented first, which methodology is given in chapter 3.2. Secondly, the comparison of energy performance to a higher occupancy load zone (three-person office) is shown, see appendix J for approach design. Subsequently, the HRU absence and efficiency variations results are given, which is conducted based on the method described in appendix L. Lastly, the energy performance of the AM 150 with datasheet specifications are presented, which simplifications and methodology are given in appendix M.

4.2.1 Representative DV unit

The building simulation methodology of the temperature regulation (cases) and air rate regulation control strategies are given in appendix F.1 and chapter 3.4.2 respectively.

All results are divided into case 1, 2, and 3 for summer, winter, and case 1, 2, and 3 annually, so that seven primary energy consumption results are given in each control strategy figure, and further compared to the centralized CAV system (see figure K.2), which is in the shape of a striped, green line which crosses only its respective seasonal or annual result of relevance. CV CAV S, CV CAV W, and CV CAV A stand for the total primary energy consumption of the centralized ventilation system with the CAV control strategy during the summer season, winter season, and annually respectively. CASE 1, 2, 3 S, WINTER, and CASE 1, 2, 3 A stands for the total primary energy consumption of the representative DV unit with the DV S-CO_2 + temperature control strategy during the summer season, winter season, and annually respectively. The results are also presented as percentages concerning the centralized CAV system, which is a 100 % as default, see figures 4.4 – 4.13:

4.2.1.1 DV CAV control strategy

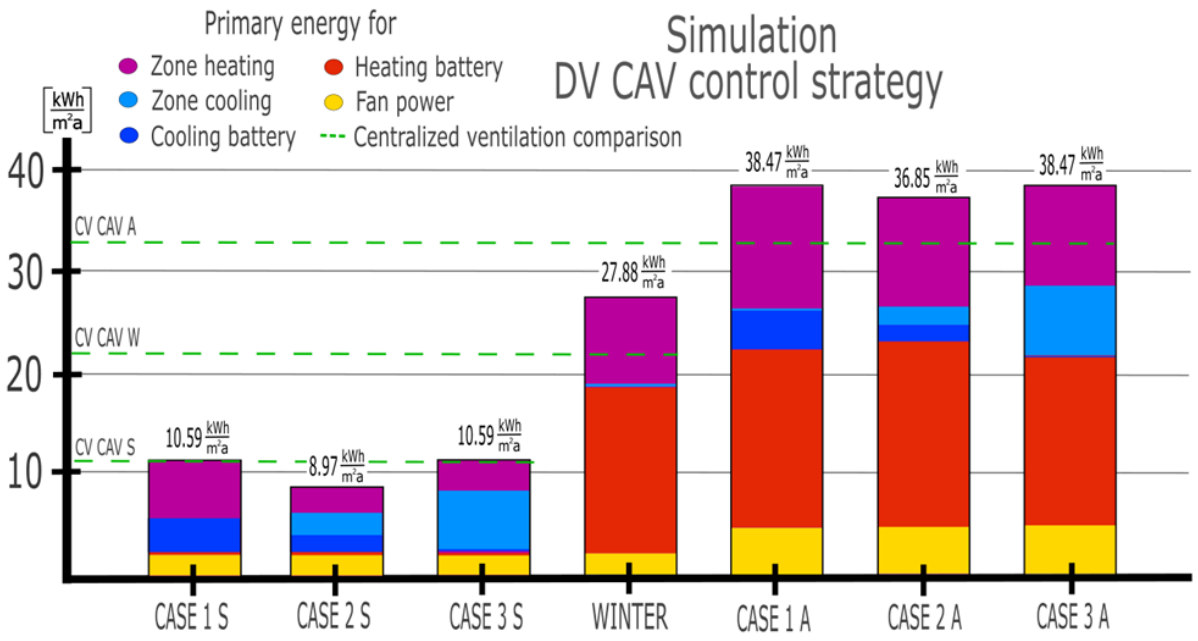

Figure 4.4: Comparison of DV CAV control strategy and cases to centralized CAV system, exact results see appendix H.1.1, table H.1 and H.2. Fanger's comfort indices during hottest and coldest week can be seen in appendix I.1, figures I.1 – I.4

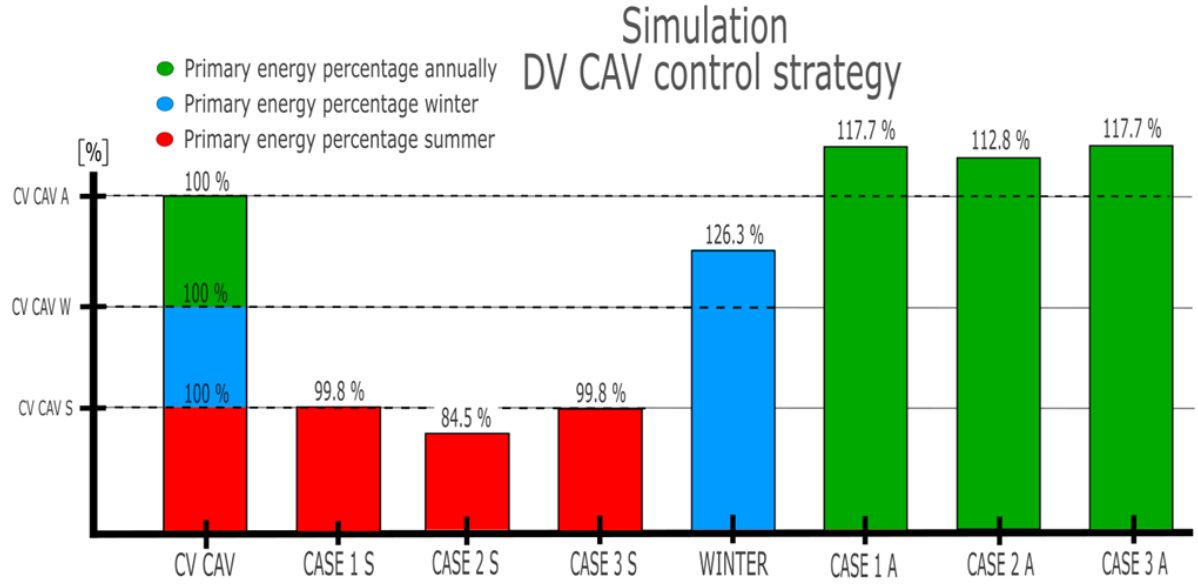

Figure 4.5: Comparison of DV CAV control strategy and cases to centralized CAV system in percentage form

Analyzing the results by summer, the decentralized ventilation constant air volume (DV CAV) control strategy performs best and better than a conventional centralized CAV system under case 2 conditions, similarly to the monthly time-step energy analysis. Case 1 and 3 conditions performed equally well to the centralized CAV system due to higher local zone heating during case 1 and higher local zone cooling during case 3, which both were partially avoided during case 2, with a decrease in AHU cooling as well. Case 2 also performed equally well in thermal comfort to case 1 according to Fanger's comfort indices due to local zone cooling, although the operative temperatures were under the most optimal conditions under case 1. Case 1 conditions also did not require any local zone cooling, so that avoidance of a local cooling unit is a possibility.

During the winter season, the DV CAV control strategy performs notably worse than conventional CAV system (26.3 % increase), which is the consequence of lower HRU efficiency of the DV unit, and so the suffering of thermal energy loss is caused through the exhaust air which has to be further compensated through additional AHU heating energy. The lower SFP value of the DV unit is not enough to compensate for the lower HRU efficiency during the winter season, and so further design and engineering effort, if possible, should be done to augment the recuperative counter flow HRU performance if the DV CAV control strategy is to be better suited for Norwegian climate.

Overall, the annual total primary energy consumption for all cases during the DV CAV control strategy surpasses the centralized CAV system, which is caused by the poor thermal performance of the DV unit during the winter season.

4.2.1.2 DV PIR control strategy

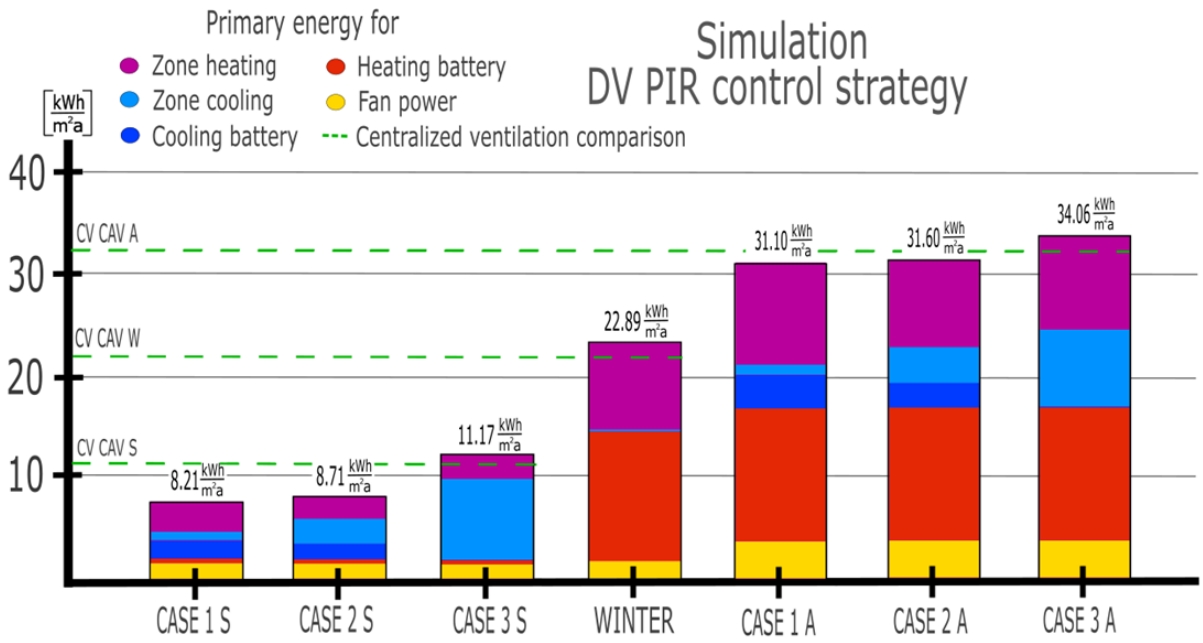

Figure 4.6: Comparison of DV PIR control strategy and cases to centralized CAV system, exact results see appendix H.1.2, table H.3 and H.4. Fanger's comfort indices during hottest and coldest week can be seen in appendix I.2, figures I.5 – I.8

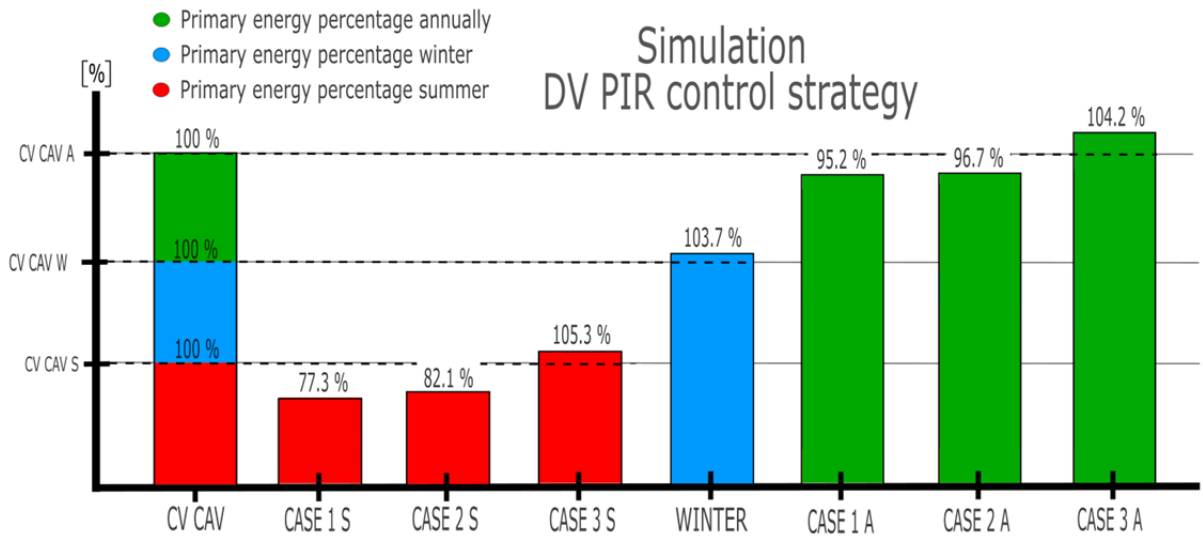

Figure 4.7: Comparison of DV PIR control strategy and cases to centralized CAV system in percentage form

During the summer season, case 1 and 2 conditions of the decentralized ventilation Passive InfraRed (DV PIR) control strategy performed better than the centralized CAV system in energy performance (77.3 % and 82.1 % respectively), where case 1 conditions performed the best. Case 1 performed better since it required significantly less zone cooling than the other two cases, where case 2 had three times as much zone cooling and case 3 had ten times as much zone cooling as case 1. These results correlate with the monthly time-step energy analysis, where cases 1 and 2 showed approximately equal energy performance.

During the winter season, the total primary energy was slightly higher than the centralized CAV system since the lower ventilation loads of the DV PIR control strategy and SFP of the DV unit helped neutralized the additional primary energy from zone heating required to keep thermal comfort at bay.

Annually case 1 and 2 conditions of the DV PIR control strategy performed better in energy performance, which was due to the lower SFP values, less zone heating, and less AHU cooling during summer periods due to lower ventilation loads. Case 1 annually had 95.2 % of the centralized CAV system primary energy consumption which was the product of the aforementioned factors, although this is not a critical difference for any major conclusions. Case 3 had too high local zone cooling loads, which was due to the constantly high supply temperature during the hotter days of the summer season.

Case 1 seems to be the best supply temperature regulation strategy with the DV PIR control strategy, as it requires almost no local zone cooling. The necessity of a local cooling unit is therefore not definite, as there is some zone cooling present, although TEK 17 § 13-4 does allow for some surpassing of the upper limit of operative temperature, so under case 1 condition the local unit could potentially be excluded. Case 1 also requires the least energy consumption out of all case conditions and gives the best ventilation effectiveness due to lower supply temperature.

4.2.1.3 DV S-CO_2 control strategy

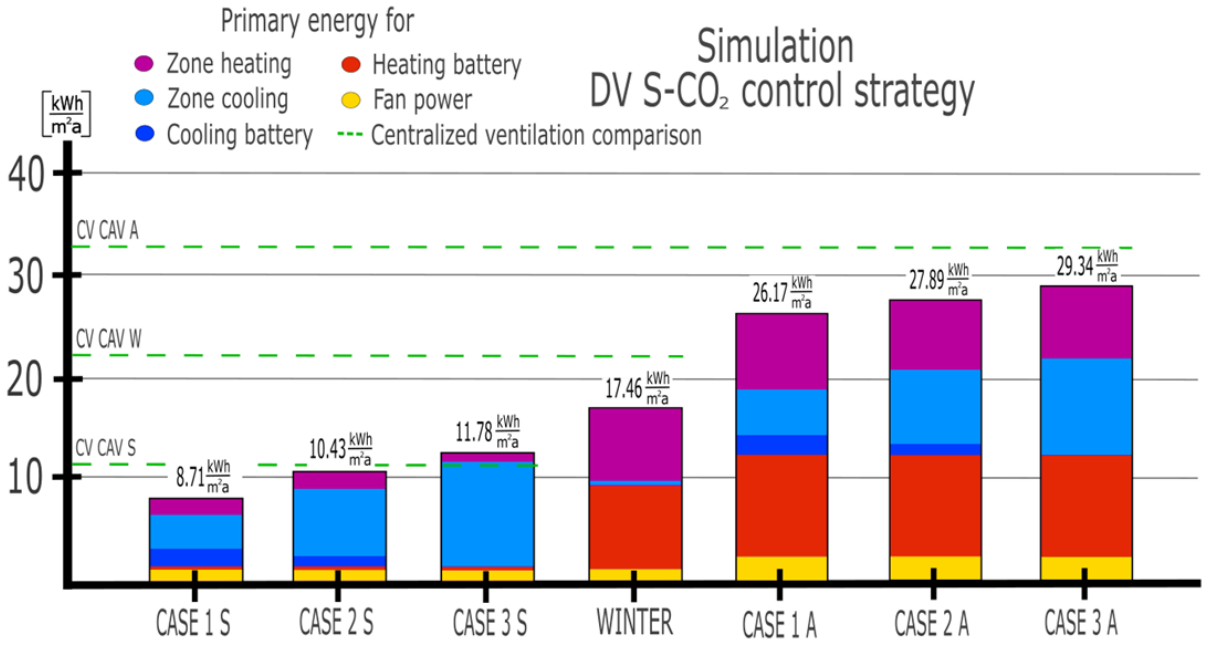

Figure 4.8: Comparison of DV S-CO_2 control strategy and cases to centralized CAV system, exact results see appendix H.1.3, table H.5 and H.6. Fanger's comfort indices during hottest and coldest week can be seen in appendix I.3, figures I.9 – I.12

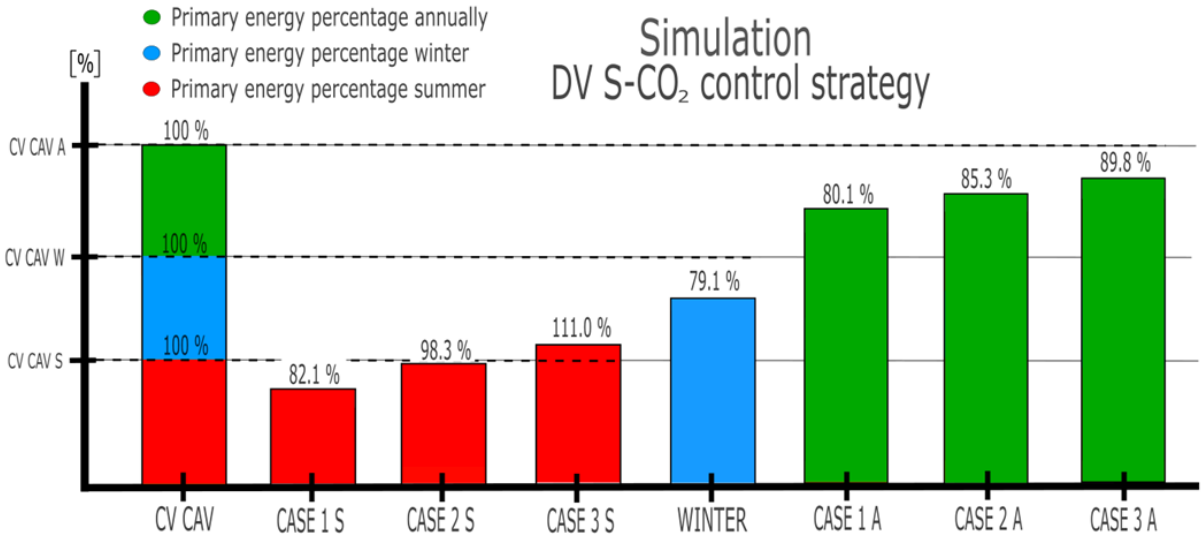

Figure 4.9: Comparison of DV S-CO_2 control strategy and cases to centralized CAV system in percentage form

The decentralized ventilation static-CO_2 (DV S-CO_2) control strategy during summer times performed better than the centralized CAV system during case 1 and 2 conditions, although it performed worse than the DV PIR control strategy, even though the zone heating, AHU cooling, and the fan energy consumption was lower due to fewer ventilation loads. The reason behind the worse performance of the DV S-CO_2 control strategy case 2 and 3 conditions during summer compared to the DV PIR control strategy was the increased energy consumption from local zone cooling, which is the product of the less practical timing of when the cooling load of the ventilation was used, as the strategy is set to use minimum air rates even during occupancy times, which causes a surplus of internal heat gains compared to ventilation cooling at occupancy times (see figure 3.8). This has also been reported in other scientific literature (Bonato et al., 2020). Raising this minimum air rate showed improved energy performance due to diminished local cooling, which correlates with other findings (Schiavon and Melikov, 2009).

During the winter season, the DV S-CO_2 control strategy performs significantly better than the centralized CAV system with only 79.1 % of the total primary energy consumed in comparison. This is a consequence of the lower ventilation loads, creating less fan power, AHU heating, and local zone heating energy consumption so that the lower HRU efficiency of the DV unit becomes less of a weakness due to fewer intervals under heat recovery conditions.

Annually, the DV S-CO_2 control strategy case 1 consumes at the lowest only 80.1 % of the centralized CAV system. This is a significant improvement from both the DV CAV and PIR control strategy in energy performance. These findings correlate with other studies on CAV, PIR, and S-CO_2 control strategies as well (Mysen et al., 2005). The main weakness of the DV S-CO_2 control strategy is the increased local zone cooling under case 1 conditions, so the implementation of a local cooling unit would be a necessity for achieving good thermal comfort. This was potentially avoided in both the DV CAV and PIR control strategy during case 1 conditions, although raising the minimum air rate in the DV S-CO_2 showed better energy performance, and potentially deactivates the need for local zone cooling in the analyzed climate. Furthermore, raising the zone operative temperature set-point could potentially also exclude the local zone cooling, while simultaneously improving energy performance (Schiavon and Melikov, 2009).

4.2.1.4 DV D-CO_2 control strategy

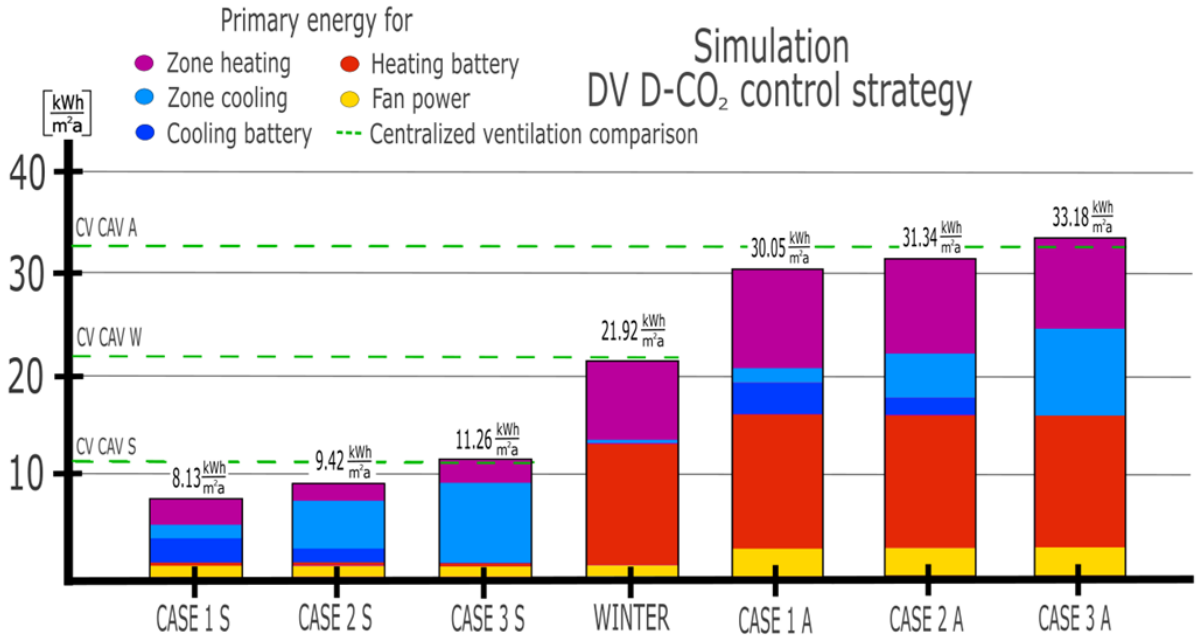

Figure 4.10: Comparison of DV D-CO_2 control strategy and cases to centralized CAV system, exact results see appendix H.1.4, table H.7 and H.8. Fanger's comfort indices during hottest and coldest week can be seen in appendix I.4, figures I.13 – I.16

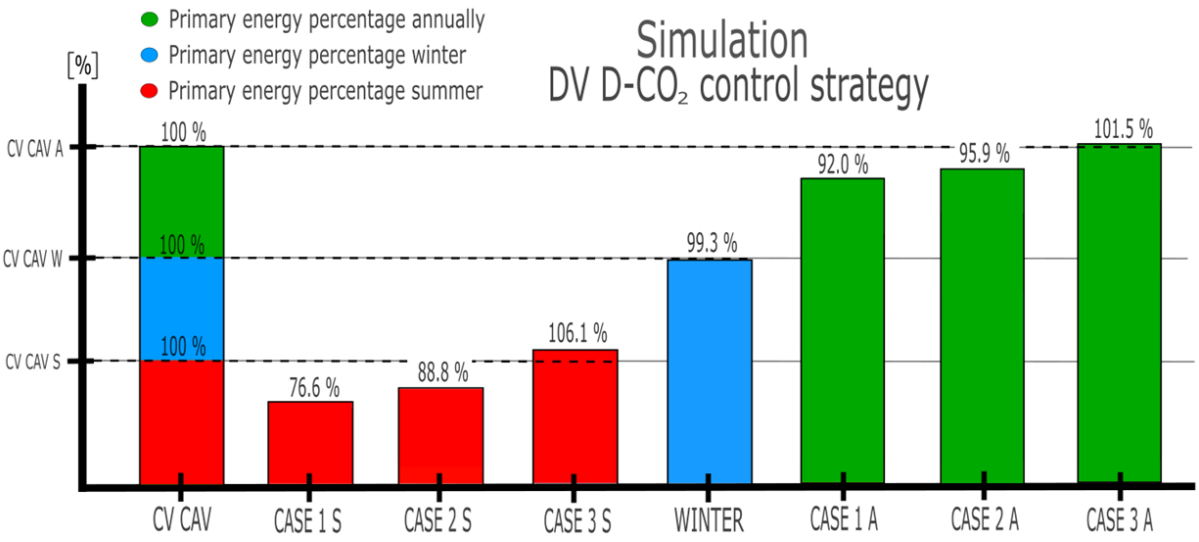

Figure 4.11: Comparison of DV D-CO_2 control strategy and cases to centralized CAV system in percentage form

In summer, the decentralized ventilation dynamic-CO_2 (DV D-CO_2) control strategy performs better than the centralized CAV system under case 1 and 2 conditions, and slightly better than the DV PIR and S-CO_2 control strategy during case 1 condition, which was due to the lower local zone cooling energy required from increased ventilation loads.

The weakness of the D-CO_2 control strategy shows itself during the winter season, where the higher ventilation loads are accumulating more AHU heating and fan power energy consumption, while also contributing to further zone heating, as more ventilation cooling is distributed. It still performs better than the DV PIR and CAV control strategy, as the ventilation loads are smaller, so that less AHU heating is necessary.

If high or special demands are given for atmospheric comfort, the D-CO_2 would be the better choice due to lower CO_2 concentration and air age, as it still performs better than the DV CAV and DV PIR control strategy in energy performance annually. The D-CO_2 control strategy could also potentially avoid the local zone cooling unit, as the zone cooling demand is low during case 1, similarly to the DV PIR control strategy. Potentially a switch of the DV D-CO_2 to the S-CO_2 from summer to winter season respectively, would yield the best energy performance and atmospheric comfort, while simultaneously potentially avoiding the local cooling unit.

4.2.1.5 DV S-CO_2 + temperature control strategy

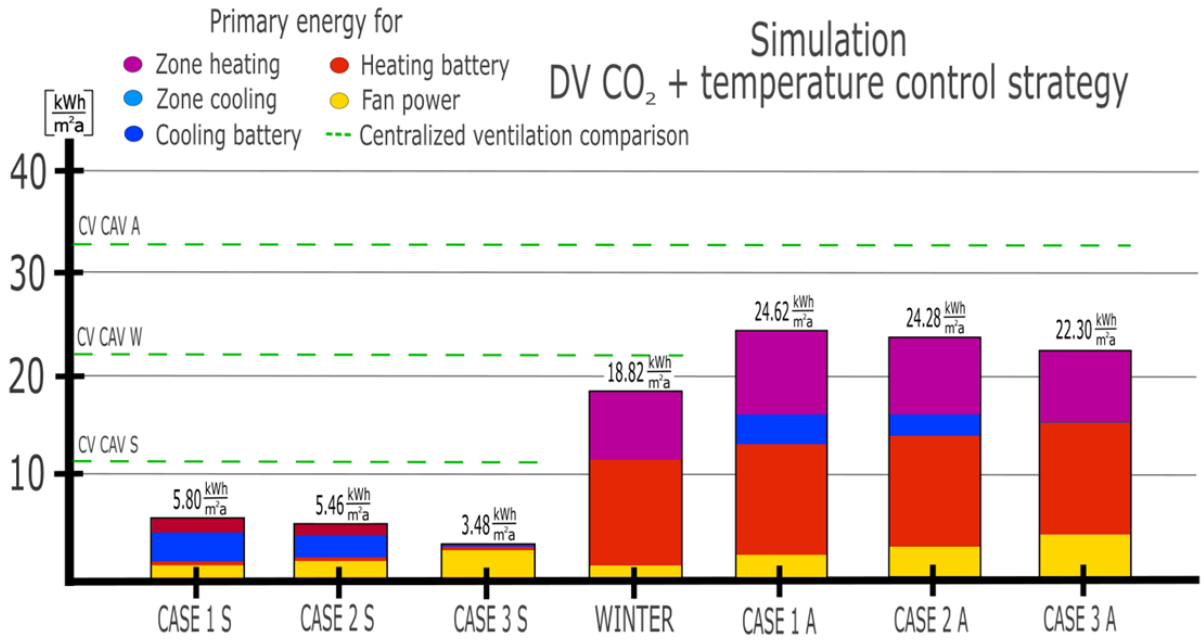

Figure 4.12: Comparison of DV S-CO_2 + temperature control strategy and cases to centralized CAV system, exact results see appendix H.1.5, table H.9 and H.10. Fanger's comfort indices during hottest and coldest week can be seen in appendix I.5, figures I.17 – I.20

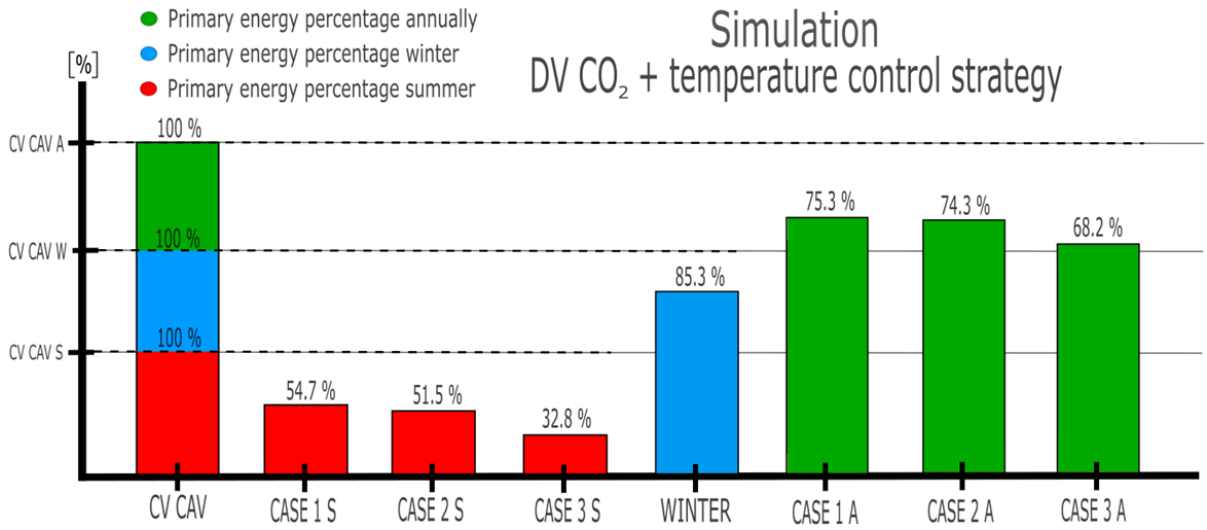

Figure 4.13: Comparison of DV S-CO_2 + temperature control strategy and cases to centralized CAV system in percentage form

During summer, the DV S-CO_2 + temperature control strategy primary energy consumption is significantly reduced during all cases compared to other control strategies, although the results of case 3 are difficult to discuss due to the insufficient cooling. Case 1 and case 2 uses 54.7 % and 51.5 % respectively, which is a significant reduction in comparison to centralized CAV. This reduction comes from less zone heating, as the DV S-CO_2 + temperature control strategy dynamically regulates the ventilation air rates according to the operative temperature, which is affected by the internal heat gains and similarly the absence of any internal heat gains in combination with transmission and infiltration heat losses/gains. The control strategy shows its true potential more extremely as the higher supply temperature of cases 2 and 3 can now more cheaply be compensated through the use of ventilation cooling in combination with the low SFP DV unit. In case 3, the primary energy consumption is almost entirely accumulated by the AHU fan energy consumption, which is energy efficient since cooling with ventilation is highly effective with a low-pressure system. Although case 3 has the greatest energy performance, the absence of the local zone cooling creates operative temperatures outside of the set-points, creating poor thermal comfort, so that the realistic energy consumption cannot be determined. Either rising the upper max ventilation air rate set-point or including local zone cooling during case 3 to further compensate for the overheating would be a necessity for keeping the PPD low. Potentially, if the SvalVent research (SINTEF, 2021, 55:19) approves of the higher zone and supply air temperatures (if compensated accordingly with optimal air supply velocities), case 3 of the DV S-CO_2 + temperature control strategy could yield both high energy performance and sufficient thermal comfort for each person, as individual control is an option in DV units, although this must be further tested using DV units with field measurements.

During winter, the control strategy uses 85.3 % of the total primary energy consumption when compared to a centralized CAV system, which is higher than that of the DV S-CO_2 control strategy, which only used 79.1 %. This is due to the decreased air rates of the DV S-CO_2 control strategy, which subsequently resulted in less AHU heating required, as one can observe from the additional AHU fan energy consumption in the DV S-CO_2 + temperature control strategy. The difference in primary energy consumption during winter is not high, as they are both controlled by a DV S-CO_2 control strategy a majority of the days, but higher air rates of the DV S-CO_2 + temperature control strategy happens during the hotter days of the defined winter season, which gives better thermal comfort, but also higher energy consumption than the pure DV S-CO_2 control strategy.

Annually, case 1 and 2 still performs quite well in energy performance compared to case 3, with only around 75 % of the annual primary energy consumption when comparing it to a centralized CAV system. Comparing the DV S-CO_2 + temperature control strategy to the other four discussed DV control strategies, the greatest energy performance annually is achieved with the DV S-CO_2 + temperature control strategy, while simultaneously keeping the thermal comfort at equal levels during both case 1 and 2 without using local zone cooling. The sound emissions are also kept under acceptable levels due to the max limit of the upper ventilation load, which was decided through DeAL, although a higher upper limit is potentially possible if the AM 150 unit specifications are accepted, which would more efficiently cool the zone. The sound emissions and upper limit of ventilation load will in reality greatly depend on the decentralized ventilation system. A larger system, such as the AM 300 which is dimensioned for larger occupancy zones, could be utilized as well in single-person offices for higher upper limits of ventilation loads, although this would yield higher investment costs.

4.2.2 Comparison of energy performance to three-person office

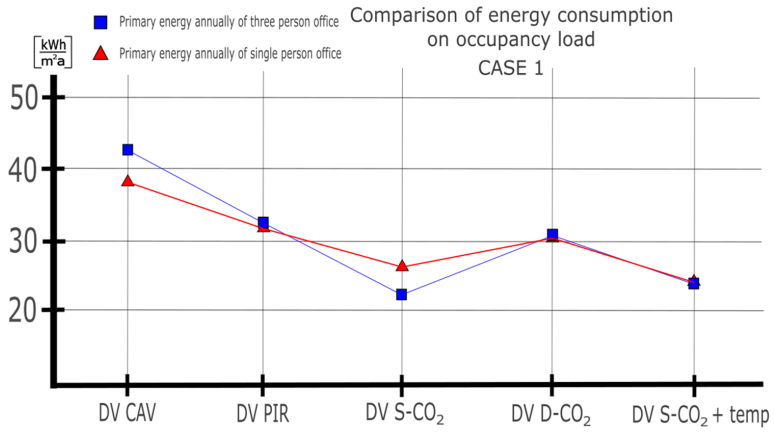

Figure 4.14: Comparison of single-person to three-person office primary energy consumption during case 1, exact results see appendices J.1 - J.5, tables J.1 – J.10

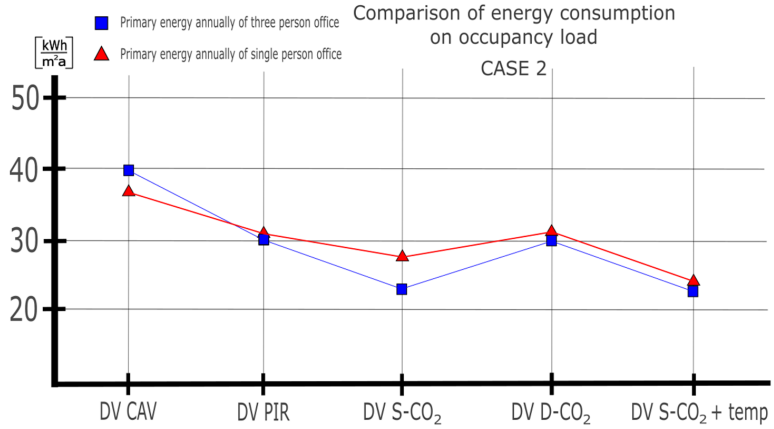

Figure 4.15: Comparison of single-person to three-person office primary energy consumption during case 2, exact results see appendices J.1 - J.5, tables J.1 – J.10

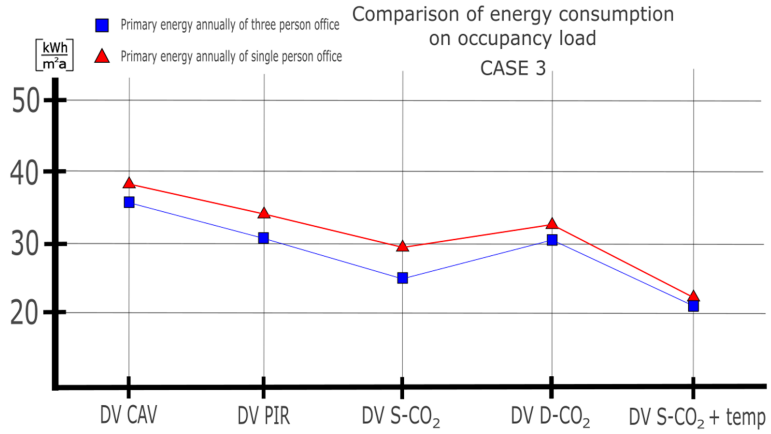

Figure 4.16: Comparison of single-person to three-person office primary energy consumption during case 3, exact results see appendices J.1 - J.5, tables J.1 – J.10

Comparison between the two occupancy patterns for energy results can be difficult, as they are not created equally, so some illogical results are to be expected. The UR of the two occupancy schedules are not identical, and they differ in that they are constructed with different numbers of vertical occupancy factor steps (see figure J.2).

When comparing the DV CAV control strategy between the single and three-person offices, it is observed that there is a lower primary energy demand per area in the single-person office during case 1 and case 2, while in case 3 the three-person office shows better energy performance. This is thought to be a consequence of the high ventilation cooling effect that is dispersed into the zone, so that case 1 and case 2 conditions will yield high local zone heating energy consumption, while case 3 will have little local zone heating since there is little temperature difference between the supply air and zone temperature set-point. If a DV CAV control strategy were to be used in a higher occupancy zone, case 3 could be a potential candidate regulation strategy if the pattern is repeated to other occupancy capacities as well, although the drawbacks of thermal discomfort and worse ventilation effectiveness must be a consideration.

The three-person office DV PIR energy comparison resulted in an equal energy consumption per area during cases 1 and 2 and showed better energy performance during case 3 conditions. Case 1 needed higher AHU cooling energy due to stricter demands for the supply temperature, and also higher local zone heating energy due to the increased ventilation cooling with lower supply temperatures. Case 3 in the single-person office had the problem of having too high supply temperatures, even when the zone energy balance was in need for ventilation cooling, meaning that the free cooling was crippled, and a local zone cooling compensation was necessary, increasing the overall energy consumption. This did not happen to the same degree in the three-person office zone, as it only required half of the total local zone cooling energy consumption per area, as there were relatively fewer internal loads.

The comparison between the single and three-person office showed that the DV S-CO_2 control strategy energy consumption difference remained fairly constant through all cases, where the three-person office showed better energy performance. This is observed to be because of less local zone cooling required during the three-person office analysis, which could be because of longer high ventilation load intervals required to maintain CO_2 under 1000 ppm, which yields more free cooling to the zone (see figure J.4). There is also observed less energy consumption during the winter season, which is because of less AHU heating and zone heating required. Less AHU heating is a small contradiction to what was discussed during summer of higher ventilation loads in three-person office, which should also increase AHU heating during winter as there are increased ventilation loads during winter as well. This could be because of some error in the geometry to occupancy comparison of the two zones, resulting in some undershoots in energy comparison, or it could be that the AHU heating is only necessary at intervals when there are part-load ventilation air rates, as the air rate is statically proportional to the CO_2 generation in the zone, meaning that when there are only one or two persons present, the ventilation load is below maximum load, producing relatively lower AHU heating loads concerning the single-person office energy analysis. The S-CO_2 control strategy seems to improve in energy performance in all cases when occupancy load is increased.

Comparison of the three-person office to single-person office reveals little DV D-CO_2 control strategy energy consumption per area difference on all cases, where the difference is increased by a small amount from case 1 to case 3, respectively. The energy performance of the three-person office does not change during any of the cases, as it is stationary at 30 $\frac{kWh}{m^2a}$, while the energy difference is created from an increment in energy consumption from case 1 – 3 in the single-person office analysis. The stationary energy consumption in the three-person office analysis is simply because the AHU cooling, local zone cooling, and local zone heating always add up to the same amount, even though they are different in all cases. If this pattern repeats, the viability of the D-CO_2 control strategy seems to increase as the occupancy load of the zone gets higher, although this only applies to cases 2 and 3, as case 1 showed equal energy performance.

The single-person office zone to the three-person office zone showed an almost equal DV S-CO_2 + temperature control strategy energy consumption per area during all cases, where the three-person office had the best energy performance during case 2 and 3. The worse energy performance in the single-person office was observed to be that of higher fan energy consumption during summer, which meant higher AHU cooling due to increased ventilation demand during cases 2 and 3. In the winter season, there was also observed more local zone heating energy in the single-person office, which could be due to fewer internal loads or some geometry error previously discussed under the S-CO_2 control strategy. The occupancy patterns effect on the local zone heating during the winter season is most likely what causes the majority of differences. The DV S-CO_2 + temperature control strategy seem to increase in energy performance with increased occupancy load, similar to the S-CO_2 control strategy, which is expected from DCV control strategies as aforementioned (Merema et al., 2018) (Mysen et al., 2003) (Mysen et al., 2005), although even higher occupancy zones and different occupancy schedules should be analyzed as the present results show insignificant differences, so that little conclusion can be drawn.

4.2.3 HRU absence and efficiency variations on energy presence

The primary energy consumption of each HRU efficiency and absence of the HRU from the DV unit is calculated under each case using the S-CO_2 + temperature control strategy. The results are split in the summer season, which is different in each case, the winter season, which is identical in each case, and annually, which has equal primary energy consumption differentials to summer season results due to identical winter results.

CV CAV S, CV CAV W, and CV CAV A stands for the total primary energy consumption of the centralized ventilation system with the CAV control strategy during the summer season, winter season, and annually respectively (yellow lines) (see figure K.2)). DV CASE 1 S, DV WINTER, and DV CASE 1 A stands for the total primary energy consumption of the representative DV unit with the DV S-CO_2 + temperature control strategy case 1 during the summer season, winter season, and annually respectively (pink lines) (see figure 4.12) (only case 1 is shown as a guideline). The results can be viewed in figure 4.17:

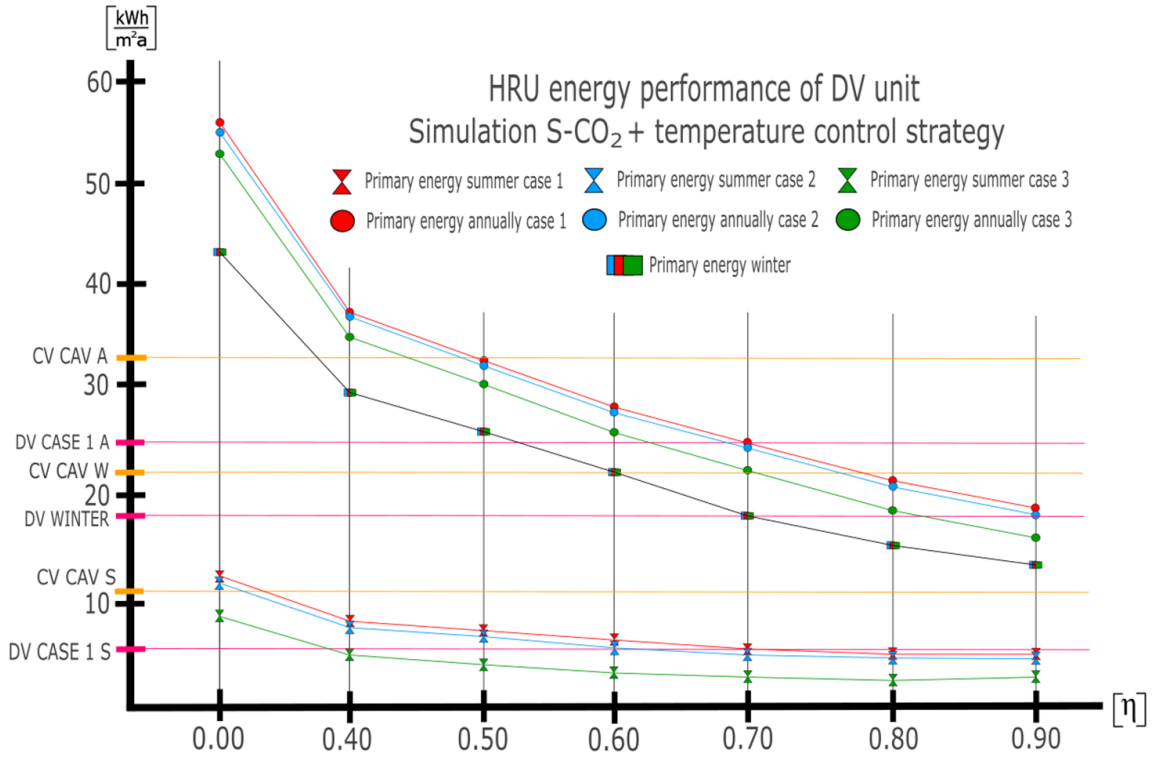

Figure 4.17: HRU energy performance of DV unit under the S-CO_2 + temperature control strategy under each case, exact results see appendix H.2, tables H.11 – H.31

Looking at the primary energy consumption when considering the absence of the HRU and the different HRU efficiencies, the emerging pattern of which case is the best performing is similar to that of the representative DV unit results. It is clear from the results that the absence of the HRU is not an energy-efficient solution in the Norwegian climate due to the cold weather conditions. Even during greater optimistic pressure relationships of 90 %, the HRU efficiency of even 0.4 is superior in energy performance, which is due to the already low SFP in DV units which limits the potential fan energy savings in combination with the thermal savings of the HRU which can be achieved in Norwegian climate. These results could potentially change if the hotter months of June, July, and August were analyzed, which was not conducted. The thermal loads produced from AHU heating necessary in Norwegian climates even during summer times surpass the saved fan power and cooling energy (fan regulation) consumption from avoidance of HRU pressure with the DV S-CO_2 + temperature control strategy. With the boundary conditions and simplifications present, the comparison results show that integrated HRU in DV units year-round in local Norway climate purely from a primary energy consumption perspective based on seasonal analysis is best, although a bypass algorithm when the weather conditions are optimal would produce the highest energy performance if pressure avoidance is the result (Kim and Baldini, 2016).

In hotter climates, more optimistic results are expected to be the outcome of a DV unit without integrated HRU, as the fan regulation from the DV S-CO_2 + temperature control strategy produces cheaper cooling to a greater extent based on hotter weather conditions, and due to the reduced thermal energy savings of the HRU based on the hotter weather conditions, as the temperature difference between the outside and inside converges. As the climate converges to perfect equality of inside and outside temperature, the HRU purpose is left futile, and the only savings concerning the DV unit are that of the reduced SFP from pressure avoidance.

Considering the individual cases, and comparing them to the representative DV unit and the centralized CAV system, increased energy performance is observed when the HRU efficiency is increased. This improvement of energy performance is expected, but it is the slope of improvement that is of interest, as there might be little improvement from 0.8 to 0.9 HRU efficiency and a relatively higher increase in investment cost. Looking at all the cases, the 0.4 HRU efficiency scenario shows worse energy performance than the centralized CAV system, but an HRU efficiency of 0.5 surpasses the centralized CAV system energy performance. Furthermore, an almost constant reduction of annual energy consumption is observed when increasing the HRU efficiency with a step of 0.1. A minor reduction of the annual slope is noted from 0.8 to 0.9 HRU efficiency, which seems to be caused by a global minimum of energy consumption during the summer season at 0.8 HRU efficiency, and a reduction of the slope during the winter season in that interval. The winter season creates the majority of slope improvement of energy performance so that the increased HRU efficiency is therefore still an important factor to optimize for an energy-efficient DV system in Norwegian climate.

During the winter season, the increased energy performance is observed almost constant, with a small reduction in energy savings with each step increase of the HRU efficiency, where all energy savings are accumulated in AHU heating. The increased HRU efficiency is therefore still an important factor to optimize for an energy-efficient DV system in the Norwegian climate.

4.2.4 AM 150 with manufacturer datasheet specifications

Abbreviations are equal to those of the representative DV unit results (see chapter 4.2.1).

The results are shown in figure 4.18 and 4.19:

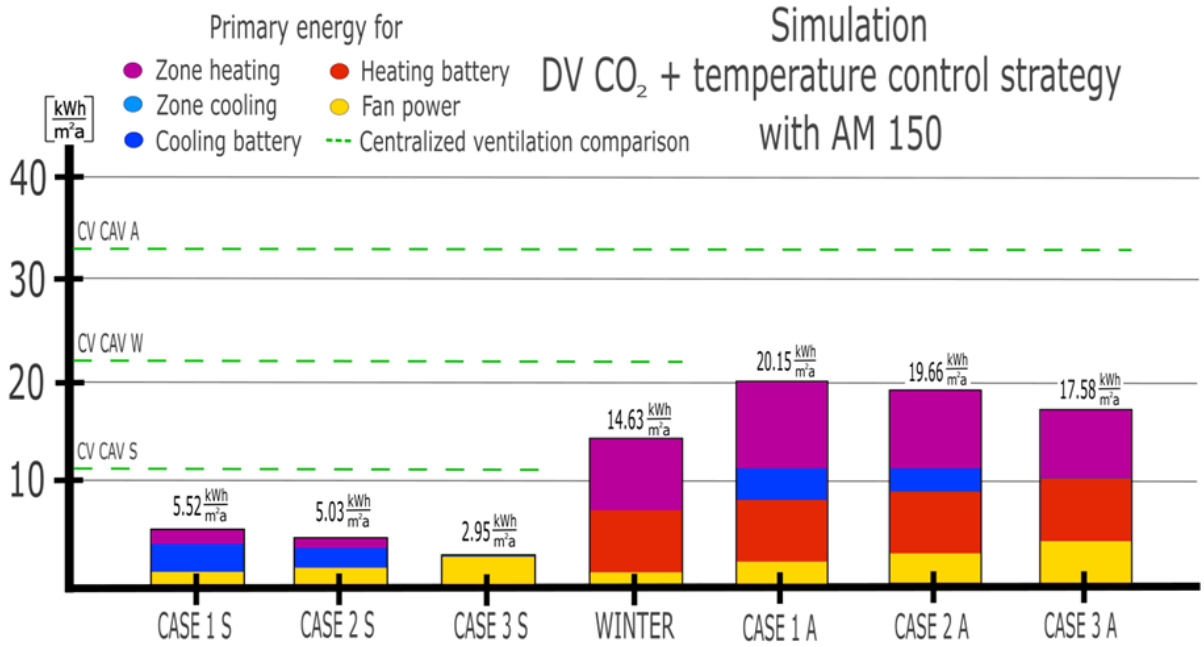

Figure 4.18: Comparison of S-CO_2 + temperature DV unit control strategy and cases with AM 150 specifications to centralized CAV system, exact results see appendix H.3, table H.32 and H.33

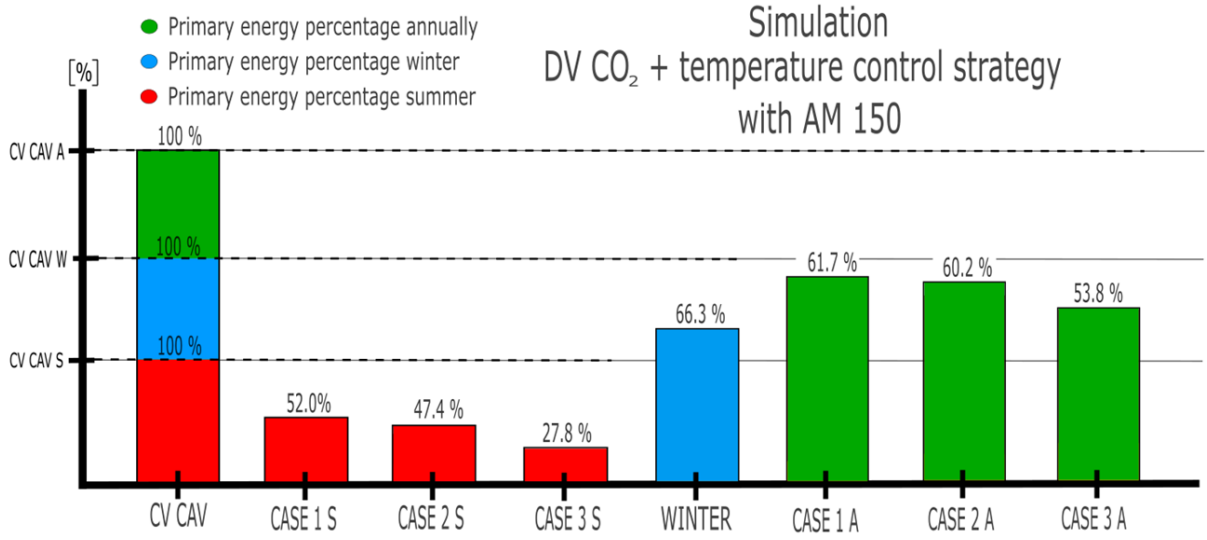

Figure 4.19: Comparison of S-CO_2 + temperature DV unit control strategy and cases with AM 150 specifications to centralized CAV system in percentage form

Looking at the summer season, the results show a significant reduction in primary energy compared to the centralized CAV system, and a small reduction compared to the representative DV unit, which under the given boundary conditions could mean the improved SFP value and HRU efficiency from the AM 150 unit does not create any significant energy savings during summer periods during any cases, which correlates with figure 4.17. The thermal comfort results of case 3 are similar to the representative DV unit findings, so that case 3 still produces a poor indoor climate where many would find the zone temperature too high, although there are improvements of 0.3 PMV during the highest peak, which are because of less operative temperature during the hottest week, which is the result of a higher upper limit of max ventilation load (see figure H.1).

The more important energy reduction is given during the winter season, where instead of using 85.3 % of the primary energy compared to centralized CAV, the AM 150 DV unit only uses 66.3 % of the primary energy compared to the centralized CAV system. This is the result of an increased HRU efficiency, which is the main contributor to the difference between the representative DV unit and the AM 150 DV unit when looking at an annual total primary energy consumption.

Looking at case 2 as the most optimal case concerning energy performance and thermal comfort, the reduction of primary energy consumption compared to the centralized CAV system is lowered from 74.3 % of the representative DV unit to 60.2 % of the AM 150 DV unit, which is a notable difference mainly created by a better thermal performance of the HRU in the AM 150 DV unit. In the Norwegian climate, this thermal performance is of high importance, which can be seen by analyzing how the energy savings change during summer with lower SFP values and higher HRU efficiency, which is not much, and how the results change with lower SFP values and higher HRU efficiency during the winter season, which is of much more significant difference. Under an even colder climate, if a sufficient thermal performance of a DV unit is not possible, the possibility of using DV units instead of a centralized system would be reduced, as the thermal performance is the far more important factor.

This insight also increases the potential of DV units in hotter climates, as the DV S-CO_2 + temperature control strategy uses the SFP values more efficiently since cooling is directly affected by the SFP, and the thermal performance of the HRU is not of as high importance since the supply temperature can be reached far more often under lower HRU efficiencies.

If the datasheet specifications of the AM 150 DV unit is consistent with real-life scenarios, the potential of DV units in Norwegian climates is risen significantly compared to the representative DV unit which was based on scientific data and field measurements. More studies should be conducted to better understand the potential of commercially available DV units in the Norwegian climate from an energy performance perspective, in combination with the economic and comfort perspective.

5 Conclusion

Based on the present analyzed conditions, the following conclusion is presented:

Acoustic demands are most critical utilizing the DV S-CO_2 + temperature control strategy, as the max air rate is of a higher limit to distribute sufficient ventilation cooling to the zone. The S-CO_2 control strategy is the least critical due to low max air rates, and relatively low max air rate intervals. In IDA ICE building simulation the thermal comfort of case 1 and case 2 shows sufficient thermal comfort in all control strategies, although case 3 shows weaknesses during the DV S-CO_2 + temperature control strategy, as the ventilation cooling alone is insufficient in neutralizing the thermal zone balance, and additional zone cooling would be a necessity under the analyzed conditions.

In all control strategies, raising the upper zone temperature set-point would be an effective way of lowering the energy demand, as it would greatly reduce the local zone cooling consumption, which was similarly concluded in other studies (Schiavon and Melikov, 2009) (Yang et al., 2011). This would yield the greatest energy savings on the DV S-CO_2 + temperature control strategy, as it is almost entirely driven by fan power during the summer season, although the thermal comfort would be substandard for a higher number of occupants. A strength of the decentralized ventilation system is that the occupants that are comfortable under higher zone temperatures could subject to this greater energy performing personalized ventilation strategy.

The DV system technology shows potential concerning primary energy performance, although a correct control strategy must be picked accordingly. The decentralized ventilation constant air volume (DV CAV) control strategy performs worse than the centralized CAV system as the centralized system offers the better thermal performance of the HRU, which enables superiority during the winter season. The DV CAV control strategy is therefore not recommended, as its simplicity worsens the energy performance by such an amount that the HRU efficiency of the centralized system surpasses it in energy performance.

The decentralized ventilation Passive InfraRed (DV PIR) control strategy shows improvement from the DV CAV control strategy, although the drawback of the DV PIR control strategy is the necessity of the PIR sensor. The annual performance shows some improvement compared to the centralized CAV system under case 1 conditions, although the savings are not of high significance. Even so, PIR sensors might have difficulty counting the number of occupants in larger areas as single-person offices are not the only concern. The DV PIR control strategy is therefore not recommended.

The decentralized ventilation static-CO_2 (DV S-CO_2) control strategy showed the lowest fan energy consumption of all the strategies due to fewer intervals under max air rate loads, in combination with the reduction of max air rate load. The DV S-CO_2 control strategy had less AHU cooling due to the reduced supply of air that had to be cooled, and similarly less zone heating as there was less ventilation cooling effect being supplied. During the winter season, the energy reduction was a consequence of less fan energy consumption due to lower SFP of the DV system and less supplied air, in combination with less AHU heating energy consumption due to less supplied air, which surpassed the superior efficiency of the HRU of the centralized system. The DV S-CO_2 control strategy is the recommended control strategy if the investment availability of DV units only allows for a discreet number of steps control strategy so that dynamic control strategies are unavailable. This control strategy creates the worst atmospheric inner climate, as it has the least ventilation of all control strategies. It was observed through simulation input combinations that doubling the minimum ventilation load by twice during case 1 resulted in less total energy consumption and local zone cooling, which could avoid the cooling unit and improve the IAQ. Raising the ventilation load has been reported to increase energy performance in a previous study as well (Schiavon and Melikov, 2009).

The decentralized ventilation dynamic-CO_2 (DV D-CO_2) control strategy performed worse than the S-CO_2 control strategy due to the dynamically proportional ventilation control so that more ventilation load is present. This created more AHU heating during the winter season, although better comfort is more than likely the positive outcome of the control strategy compared to the S-CO_2 control strategy. During summer, the DV D-CO_2 control strategy performed better due to the increased ventilation free cooling produced during all cases, so that increased comfort and better energy performance are the results during summer periods. The DV D-CO_2 control strategy is recommended above the S-CO_2 control strategy during summer, although a dynamic DV unit is necessary.

The decentralized ventilation S-CO_2 + temperature control strategy performed the best in energy performance out of all the control strategies. Choosing between cases that showed good thermal comfort, case 2 performed the best in energy performance, which was achieved by the cheap ventilation cooling of the lower SFP of DV units. The difference between case 1 and case 2 was not significant so that if noise is a problem, the recommended case would be case 1, as it produces fewer max loads and therefore less noise. Annually, the energy performance using the DV S-CO_2 + temperature control strategy is the superior control strategy. The DV S-CO_2 + temperature control strategy is the recommended control strategy if a dynamic DV unit is available, such as the AM 150 from Airmaster.

Looking at the comparison of the DV control strategies to a higher occupancy zone, the results showed that the DCV control strategy performed better under higher occupancy load zones, where the DV S-CO_2 and S-CO_2 + temperature control strategy showed the greatest energy performance transition, although the accuracy of the reference zone geometry, occupancy load and occupancy schedule relationship to the single-zone reference model cannot be given. These results correlate to DCV findings on centralized ventilation systems (Merema et al., 2018).

In Norwegian climates, the removal of the HRU is not energy efficient during any season of the year, as the HRU impact on the colder weather conditions is essential for good energy performance, and the reduced pressure from removing the HRU, which results in improved SFP, does not compensate for this thermal energy loss induced. In hotter weather conditions, where the indoor and outdoor climate converges towards equal thermal conditions, the removal of the HRU is a smart choice concerning energy performance, as the HRU is left futile as ΔT approaches 0 kelvin, and so the improved SFP from the reduced pressure through the unit produces additional fan energy savings, as well as cheaper ventilation cooling in the DV S-CO_2 + temperature control strategy. This means that in Norwegian climates, the DV potential is highest in the south of Norway, where heat loss accumulation is of less significance. A sufficiently accurate bypass algorithm is recommended for Norwegian climates instead of total absence, which enables fan-assisted natural ventilation during adequate weather conditions (Kim and Baldini, 2016).

With specifications equal to those of the AM 150, the summer results do not show any significant differences in primary energy consumption, although the increased HRU efficiency shows significant improvements during winter, which further supports the findings of how increased HRU efficiency is important for Norwegian climates in DV units. If the specifications of the AM 150 is reliable to practical scenarios, the DV unit technology is an even stronger contender for energy-efficient HVAC systems in Norway. The AM 150 allows for dynamic operation and bypass automation as well, further increasing its potential for the Norwegian climate.

The main conclusions are as follows:

- The control strategy with ventilation cooling regulation (DV S-CO_2 + temperature) showed the greatest energy performance due to the cheap fan regulation (low SFP/low-pressure loss) of the decentralized ventilation unit. Improving SFP will quicker augment the potential of the S-CO_2 + temperature control strategy than it will with other control strategies. All relevant comfort criteria are upheld under case 1 and case 2, although case 3 has suboptimal performance due to limited cooling possibilities.

- Temperature regulation strategy case 1 showed the greatest energy performance in all control strategies except DV CAV and S-CO_2 + temperature. The higher ventilation cooling from the DV CAV control strategy benefits from the higher case 2 supply temperatures as it further neutralizes the zone, while the higher case 2 supply temperatures from the S-CO_2 + temperature control strategy was more cheaply compensated due to the low SFP of the DV unit, although the difference was low.

- The decentralized ventilation system's potential increases with hotter weather conditions, which is due to increased effectiveness of the temperature regulation of cases and ventilation cooling using the DV S-CO_2 + temperature control strategy, and because the examined DV system has lower HRU efficiency, which substantially increases energy loss compared to centralized systems as the outdoor temperature decreases. Further bypass and subsequently less fan power consumption is also the result of hotter climates.

- Raising the air rates during CO_2 control strategies can improve energy performance during summer periods due to additional ventilation cooling. Doubling the minimum air rates during the S-CO_2 control strategy during summer period moderately lowers the total energy consumption (0.5 $\frac{kWh}{m^2a}$) and substantially lowers the local zone cooling energy consumption (3.37 $\frac{kWh}{m^2a}$).

- Increasing the upper operative temperature set-point increases the energy performance of the system, especially for case 2 and case 3 conditions, as avoidance of local zone cooling is the result.

Further research

The present results can potentially be used as a foundation for further research that can build on the energy comparison findings of the control strategy combinations.

The results are limited to the boundary conditions, assumptions, assessment tools and information found in scientific articles, so that further validation of the produced results by using field measurements with a sufficiently similar approach is of value, considering the present results can be correlated to the field measurement findings for better credibility. The field measurements could also disprove the present findings, which would be of equal importance in the field of DV unit technology.

The results are all based on primary energy comparison of the control strategy combinations, so that an interesting next step could be to include the economic perspective, as this too is of vital importance for determining the optimal control strategy combination for decentralized ventilation. Comparing investments cost of all the necessary equipment and DV unit designs and different combinatorics of all analyzed control strategies could show interesting patterns, and bring forth which control strategy is most optimal with all factors considered. The economic analysis would have to include investment costs, operational costs and maintenance costs, and also the cost savings of lowered ceilings due to absence of centralized ventilation system ductwork.

Investigation on the total building level should be included in future studies, which also includes non-perimeter zones, as analysis on individual perimeter reference zones alone cannot support the practicality of the decentralized ventilation technology.

Environmental impact are also of interest, as better overview of the environmental footprint of each control strategy and centralized system could be compared to each other, as this is also of importance.

References

Airmaster (2018). Desentralisert ventilasjon v/ trond jensen. innlegg presentert ved driftskonkuransen 2018 [presentation]. http://www.driftskonferansen.com/uploads/4/9/7/8/49783435/3._trond_jensen_driftskonferansen_2018_trond_onsdag.pdf.

Airmaster (2020a). Datablad am 150 med cc 150 [data sheet]. https://www.airmaster-as.no/media/4348/15600-am-150-cc-no.pdf.

Airmaster (2020b). Instruksjonsbok am 150 [instruction manual]. https://www.airmaster-as.no/media/4356/14021-rev01-ib-62-no.pdf.

Arbeidstilsynet (2016). Veiledning om klima og luftkvalitet på arbeidsplassen. *Veiledning, best.nr. 444*, https://www.arbeidstilsynet.no/contentassets/3f86f6d2038348d18540404144f76a22/luftkvalitet-pa-arbeidsplassen.pdf.

Baldini, L. and Meggers, F. (2008). Advanced distribution and decentralized supply: a network approach for minimum pressure losses and maximum comfort. In *29th AIVC Conference " Advanced building ventilation and environmental technology for addressing climate change issues", Kyoto, Japan, 14-16 October 2008*, pages 117–122. https://www.researchgate.net/publication/256547423_Advanced_Distribution_and_Decentralized_Supply_A_Network_Approach_for_Minimum_Pressure_Losses_and_Maximum_Comfort.

Baldini, L., Meggers, F., and Leibundgut, H. (2008). 584: Advanced decentralized ventilation: How wind pressure can be used to improve system performance and energy efficiency. *PLEA 2008 – 25th Conference on Passive and Low Energy Architecture. At: Dublin. 22.-24. October*, https://www.researchgate.net/publication/228909220_Advanced_Decentralized_Ventilation_How_Wind_Pressure_Can_Be_Used_to_Improve_System_Performance_and_Energy_Efficiency.

Beattie, C., Fazio, P., Zmeureanu, R., and Rao, J. (2018). Experimental study of air-to-air heat exchangers for use in arctic housing. *Applied Thermal Engineering*, 129:1281–1291. https://doi.org/10.1016/j.applthermaleng.2017.10.112.

Bonato, P., D'Antoni, M., and Fedrizzi, R. (2020). Modelling and simulation-based analysis of a façade-integrated decentralized ventilation unit. *Journal of Building Engineering*, 29:101183. https://doi.org/10.1016/j.jobe.2020.101183.

Calì, D., Matthes, P., Huchtemann, K., Streblow, R., and Müller, D. (2015). Co2 based occupancy detection algorithm: Experimental analysis and validation for office and residential buildings. *Building and Environment*, 86:39–49. https://doi.org/10.1016/j.buildenv.2014.12.011.

Carbonare, N., Fugmann, H., Asadov, N., Pflug, T., Schnabel, L., and Bongs, C. (2020). Simulation and measurement of energetic performance in decentralized regenerative ventilation systems. *Energies*, 13(22):6010. https://doi.org/10.3390/en13226010.

Chenari, B., Lamas, F. B., Gaspar, A. R., and da Silva, M. G. (2017). Simulation of occupancy and co2-based demand-controlled mechanical ventilation strategies in an office room using energyplus. *Energy Procedia*, 113:51–57. https://doi.org/10.1016/j.egypro.2017.04.013.

Coydon, F., Herkel, S., Kuber, T., Pfafferott, J., and Himmelsbach, S. (2015). Energy performance of façade integrated decentralised ventilation systems. *Energy and Buildings*, 107:172–180. https://doi.org/10.1016/j.enbuild.2015.08.015.

Cui, S., Kim, M. K., and Papadikis, K. (2017). Performance evaluation of hybrid radiant cooling system integrated with decentralized ventilation system in hot and humid climates. *Procedia Engineering*, 205:1245–1252. https://doi.org/10.1016/j.proeng.2017.10.367.

Emmerich, S. J. and Persily, A. K. (2003). State-of-the-art review of co2 demand controlled ventilation technology and application. *NIST Interagency/Internal Report (NISTIR) - 6729*, https://www.nist.gov/publications/state-art-review-co2-demand-controlled-ventilation-technology-and-application.

EQUA Simulation AB (2013). *User Manual. IDA Indoor Climate and Energy (4.5)*, http://www.equaonline.com/iceuser/pdf/ice45eng.pdf.

Gendebien, S., Parthoens, A., and Lemort, V. (2019). Investigation of a single room ventilation heat recovery exchanger under frosting conditions: Modeling, experimental validation and operating strategies evaluation. *Energy and Buildings*, 186:1–16. https://doi.org/10.1016/j.enbuild.2018.12.039.

Gendebien, S., Prieels, L., and Lemort, V. (2012). Experimental investigation on a decentralized air handling terminal: procedure of aeraulic and thermal performance determination of the entire unit in several operating conditions. 395(1):012061. https://doi.org/10.1088/1742-6596/395/1/012061.

Grini, C., Sartori, I., Haase, M., Wigenstad, T., Mathisen, H.-M., Wøhlk, H., Sørensen, J., Pettersen, A., and Bryn, I. (2010). Leco - energibruk i fem kontorbygg i norge. befaring og rapportering. *SINTEF Byggforsk*, page 3. https://www.sintefbok.no/book/index/579/leco_energibruk_i_fem_kontorbygg_i_norge.

Gruner, M. and Haase, M. (2012). The potential of façade-integrated ventilation systems in nordic climate. *Advanced decentralised ventilation systems as sustainable alternative to conventional systems,* [Master's thesis, Norges teknisk-naturvitenskapelige universitet], 1. http://hdl.handle.net/11250/230459.

Halvarsson, J. (2012). Occupancy pattern in office buildings: Consequences for hvac system design and operation. [Doctoral dissertation, Norges teknisk-naturvitenskapelige universitet], http://hdl.handle.net/11250/234598.

Haynes, B. P. (2008). The impact of office comfort on productivity. *Journal of facilities management*, 6(1):37–51. https://doi.org/10.1108/14725960810847459.

Hepbasli, A. (2012). Low exergy (lowex) heating and cooling systems for sustainable buildings and societies. *Renewable and Sustainable Energy Reviews*, 16(1):73–104. https://doi.org/10.1016/j.rser.2011.07.138.

Ingebrigtsen, S. (2017). *Ventilasjonsteknikk Del 1.* Skarland Press AS, Hagegata 22, 0653 Oslo, 2019 edition.

Jones, A. P. (1999). Indoor air quality and health. *Atmospheric environment*, 33(28):4535–4564. https://doi.org/10.1016/S1352-2310(99)00272-1.

Kim, H., Park, K.-s., Kim, H.-y., and Song, Y.-h. (2018). Study on variation of internal heat gain in office buildings by chronology. *Energies*, 11(4):1013. https://doi.org/10.3390/en11041013.

Kim, M. K. and Baldini, L. (2016). Energy analysis of a decentralized ventilation system compared with centralized ventilation systems in european climates: Based on review of analyses. *Energy and Buildings*, 111:424–433. https://doi.org/10.1016/j.enbuild.2015.11.044.

Kim, M. K., Leibundgut, H., and Choi, J.-H. (2014). Energy and exergy analyses of advanced decentralized ventilation system compared with centralized cooling and air ventilation systems in the hot and humid climate. *Energy and Buildings*, 79:212–222. https://doi.org/10.1016/j.enbuild.2014.05.009.

Kingma, B. and van Marken Lichtenbelt, W. (2015). Energy consumption in buildings and female thermal demand. *Nature Climate Change*, 5(12):1054–1056. https://doi.org/10.1038/nclimate2741.

Krajčík, M., Simone, A., and Olesen, B. W. (2012). Air distribution and ventilation effectiveness in an occupied room heated by warm air. *Energy and Buildings*, 55:94–101. https://doi.org/10.1016/j.enbuild.2012.08.015.

Lu, L. and Ip, K. Y. (2009). Investigation on the feasibility and enhancement methods of wind power utilization in high-rise buildings of hong kong. *Renewable and Sustainable Energy Reviews*, 13(2):450–461. https://doi.org/10.1016/j.rser.2007.11.013.

Mahler, B. and Himmler, R. (2008). Results of the evaluation study deal decentralized facade integrated ventilation systems. *Energy Systems Laboratory (http://esl.tamu.edu)*, https://hdl.handle.net/1969.1/90808.

Manz, H., Huber, H., Schälin, A., Weber, A., Ferrazzini, M., and Studer, M. (2000). Performance of single room ventilation units with recuperative or regenerative heat recovery. *Energy and Buildings*, 31(1):37–47. https://doi.org/10.1016/S0378-7788(98)00077-2.

Merema, B., Delwati, M., Sourbron, M., and Breesch, H. (2018). Demand controlled ventilation (dcv) in school and office buildings: Lessons learnt from case studies. *Energy and Buildings*, 172:349–360. https://doi.org/10.1016/j.enbuild.2018.04.065.

Merzkirch, A., Maas, S., Scholzen, F., and Waldmann, D. (2016). Field tests of centralized and decentralized ventilation units in residential buildings–specific fan power, heat recovery efficiency, shortcuts and volume flow unbalances. *Energy and buildings*, 116:376–383. https://doi.org/10.1016/j.enbuild.2015.12.008.

Mikola, A., Simson, R., and Kurnitski, J. (2019). The impact of air pressure conditions on the performance of single room ventilation units in multi-story buildings. *Energies*, 12(13):2633. https://doi.org/10.3390/en12132633.

Modera, M. (2013). Field experience with sealing large-building duct leakage with an aerosol-based sealing process. *Proc. 3rd TightVent Workshop on Building and Ductwork Airtightness, Rockville, USA*, https://www.aivc.org/sites/default/files/7-3%20a.pdf.

Mysen, M., Berntsen, S., Nafstad, P., and Schild, P. G. (2005). Occupancy density and

benefits of demand-controlled ventilation in norwegian primary schools. *Energy and Buildings*, 37(12):1234–1240. https://doi.org/10.1016/j.enbuild.2005.01.003.

Mysen, M., Rydock, J., and Tjelflaat, P. (2003). Demand controlled ventilation for office cubicles—can it be profitable? *Energy and buildings*, 35(7):657–662. https://doi.org/10.1016/S0378-7788(02)00212-8.

Mysen, M. and Schild, P. G. (2014). Behovsstyrt ventilasjon, dcv – forutsetninger og utforming. *SINTEF FAG*, https://www.sintef.no/globalassets/project/reduceventilation/behovsstyrt_ventilasjon_dcv-forutsetninger_og_utforming.pdf.

SINTEF [Studio NemiTek] (2021). *Webinar: SvalVent* [video]. Youtube. https://www.youtube.com/watch?v=qwgFu5F7ykg.

Okochi, G. S. and Yao, Y. (2016). A review of recent developments and technological advancements of variable-air-volume (vav) air-conditioning systems. *Renewable and Sustainable Energy Reviews*, 59:784–817. https://doi.org/10.1016/j.rser.2015.12.328.

Rabani, M., Madessa, H. B., Nord, N., Schild, P., and Mysen, M. (2019). Performance assessment of all-air heating in an office cubicle equipped with an active supply diffuser in a cold climate. *Building and Environment*, 156:123–136. https://doi.org/10.1016/j.buildenv.2019.04.017.

Santos, H. R. and Leal, V. M. (2012). Energy vs. ventilation rate in buildings: A comprehensive scenario-based assessment in the european context. *Energy and Buildings*, 54:111–121. https://doi.org/10.1016/j.enbuild.2012.07.040.

Schiavon, S. and Melikov, A. K. (2009). Energy-saving strategies with personalized ventilation in cold climates. *Energy and Buildings*, 41(5):543–550. https://doi.org/10.1016/j.enbuild.2008.11.018.

Schiavon, S., Melikov, A. K., and Sekhar, C. (2010). Energy analysis of the personalized ventilation system in hot and humid climates. *Energy and buildings*, 42(5):699–707. https://doi.org/10.1016/j.enbuild.2009.11.009.

Schild, P. and Mysen, M. (2009). Recommendations on specific fan power and fan system efficiency. *Technical Note AIVC*, 65. https://www.aivc.org/sites/default/files/members_area/medias/pdf/Technotes/TN65_Specific%20Fan%20Power.pdf.

Byggforsk 421.421 (2010). Byggforskserien 421.421. *Grenseverdier for innendørs og utendørs lydnivåer*, https://www.byggforsk.no/dokument/3037/grenseverdier_for_innendoers_og_utendoers_lydnivaaer.

Byggforsk 421.503 (2017). Byggforskserien 421.503. *Luftmengder i ventilasjonsanlegg. Krav og anbefalinger*, https://www.byggforsk.no/dokument/2753/luftmengder_i_ventilasjonsanlegg_krav_og_anbefalinger.

NS 3701:2012 (2012). *Kriterier for passivhus og lavenergibygninger - Yrkesbygninger.* Standard Norge., https://www.standard.no/no/Nettbutikk/produktkatalogen/Produktpresentasjon/?ProductID=587802.

NS-EN 13141-8:2014 (2014). *Ventilasjon i bygninger - Ytelsesprøving av komponenter/produkter for boligventilasjon - Del 8: Ytelsesprøving av mekaniske tillufts- og avtrekksaggregater (inkludert varmegjenvinning) uten kanaltilkopling for mekanisk*

ventilasjon beregnet for ett enkelt rom. STANDARD NORGE., https://www.standard.no/no/Nettbutikk/produktkatalogen/Produktpresentasjon/?ProductID=1029915.

NS-EN 13779:2007 (2007). *Ventilasjon i yrkesbygninger — Ytelseskrav for ventilasjons- og romklimatiseringssystemer.* STANDARD NORGE., https://www.standard.no/no/nettbutikk/produktkatalogen/Produktpresentasjon/?ProductID=468513.

NS-EN 15193-1:2017 (2017). *Bygningers energiytelse - Energikrav i lysanlegg - Del 1: Spesifikasjoner, Modul M9.* STANDARD NORGE., https://www.standard.no/no/Nettbutikk/produktkatalogen/Produktpresentasjon/?ProductID=924632.

NS-EN 15251:2007+NA:2014 (2014). *Inneklimaparametere for dimensjonering og vurdering av bygningers energiytelse inkludert inneluftkvalitet, termisk miljø, belysning og akustikk.* STANDARD NORGE., https://www.standard.no/no/Nettbutikk/produktkatalogen/Produktpresentasjon/?ProductID=703200.

NS-EN ISO 7730:2005 (2005). *Ergonomi i termisk miljø - Analytisk bestemmelse og tolkning av termisk velbefinnende ved kalkulering av PMV- og PPD-indeks og lokal termisk komfort (ISO 7730:2005),* STANDARD NORGE., https://www.standard.no/no/Nettbutikk/produktkatalogen/Produktpresentasjon/?ProductID=158329.

TEK 17 § 12-7 (2020). *§ 12-7. Krav til utforming av rom og annet oppholdsareal.* DIREKTORATET FOR BYGGKVALITET., https://dibk.no/regelverk/byggteknisk-forskrift-tek17/12/ii/12-7/.

TEK 17 § 13-1 (2017). *§ 13-1. Generelle krav til ventilasjon.* DIREKTORATET FOR BYGGKVALITET., https://dibk.no/regelverk/byggteknisk-forskrift-tek17/13/i/13-1/.

TEK 17 § 13-3 (2017). *§ 13-3. Ventilasjon i byggverk for publikum og arbeidsbygning.* DIREKTORATET FOR BYGGKVALITET., https://dibk.no/regelverk/byggteknisk-forskrift-tek17/13/i/13-3/.

TEK 17 § 13-4 (2017). *§ 13-4. Termisk inneklima.* DIREKTORATET FOR BYGGKVALITET., https://dibk.no/regelverk/byggteknisk-forskrift-tek17/13/ii/13-4/.

TEK 17 § 13-6 (2017). *§ 13-6. Lyd og vibrasjoner.* DIREKTORATET FOR BYGGKVALITET., https://dibk.no/regelverk/byggteknisk-forskrift-tek17/13/iv/13-6/.

TEK 17 § 13-7 (2017). *§ 13-7. Lys.* DIREKTORATET FOR BYGGKVALITET., https://dibk.no/regelverk/byggteknisk-forskrift-tek17/13/v/13-7/.

TEK 17 § 14-2 (2020). *§ 14-2. Krav til energieffektivitet.* DIREKTORATET FOR BYGGKVALITET., https://dibk.no/regelverk/byggteknisk-forskrift-tek17/14/14-2/.

TEK 17 § 14-3 (2018). *§ 14-3. Minimumskrav til energieffektivitet.* DIREKTORATET FOR BYGGKVALITET., https://dibk.no/regelverk/byggteknisk-forskrift-tek17/14/14-3/.

Thyholt, M., Lien, A. G., and Dokka, T. H. (2001). Kartlegging av mekanisk kjøling i nye kontor- og forretningsbygg. *SINTEF RAPPORT*, https://www.sintef.no/globalassets/upload/a01525_mekanisk_kjoeling.pdf.

Turanjanin, V., Vučićević, B., Jovanović, M., Mirkov, N., and Lazović, I. (2014). Indoor co2 measurements in serbian schools and ventilation rate calculation. *Energy*, 77:290–296. https://doi.org/10.1016/j.energy.2014.10.028.

Wang, D., Federspiel, C. C., and Rubinstein, F. (2005). Modeling occupancy in single person offices. *Energy and buildings*, 37(2):121–126. https://doi.org/10.1016/j.enbuild.2004.06.015.

Yang, X.-B., Jin, X.-Q., Du, Z.-M., Fan, B., and Chai, X.-F. (2011). Evaluation of four control strategies for building vav air-conditioning systems. *Energy and Buildings*, 43(2-3):414–422. https://doi.org/10.1016/j.enbuild.2010.10.004.

Appendices

A System description of reference zone

Table A.1: Geometry of reference zone (Ørnulf Kristiansen, project leader at Multiconsult)

Parameter	**Value**	**Comments**
External wall (diabatic)	U-value: 0.22 $\frac{W}{m^2K}$ Area: 4.98 m^2 (2.4 m * 2.7 m - 1.5 m^2)	TEK 17 § 14-3 minimum demand Direction south
Internal wall (adiabatic)	U-value: 0.62 $\frac{W}{m^2K}$ Area: 29.16 m^2 (2.4 m * 2.7 m + 4.2 m * 2.7 m * 2)	Interior wall with insulation (from IDA ICE database)
Internal floor (adiabatic) (Net floor area)	U-value: 2.39 $\frac{W}{m^2K}$ Area: 10.08 m^2 (assumed 10.00 m^2) (x_1 = 4.2 m, x_2 = 2.4 m)	Concrete floor 150mm (from IDA ICE database) x_1 = depth of room x_2 = width of room
Internal roof (adiabatic)	U-value: 2.39 $\frac{W}{m^2K}$ Area: 10.08 m^2 (4.2 m * 2.4 m)	Concrete floor 150mm (from IDA ICE database)
External window (diabatic)	U-value: 0.80 $\frac{W}{m^2K}$ Area: 1.50 m^2 (x = 1.2 m, y = 1.25 m)	NS 3701:2012 minimum demand Direction south
Height to ceiling	2.70 m	Minimum 2.4 m (TEK 17 § 12-7) 2.7 m is typical
Net room volume	27.00 m^3	(Net floor area) * (Height to ceiling)

Table A.2: Energy relevant specifications of reference zone

Parameter	**Value**	**Comments**
Occupancy load	1 person	Recurring occupancy schedule (Single-person office)
Operating time	07:00 - 17:00	2500 $\frac{hours}{year}$ NS-EN 15193-1:2017 (17:00 - 07:00 = nighttime)
Utilization rate (UR)	0.60 within operating time	NS-EN 15193-1:2017 Occupancy schedule derivation (Wang et al., 2005)
Occupancy schedule	08:00 - 09:19, 09:48 - 11:12, 11:56 - 12:35, 13:19 - 15:07, 15:34 - 16:28	(Wang et al., 2005)
Internal load of person	120 watt	(Ingebrigtsen, 2017, p. 346) (office activity = 1.2 met) (occupancy schedule (figure 3.1))
Internal load of equipment	85 watt	Desktop + monitor 53 watt + 32 watt = 85 watt (Kim et al., 2018) Power consumption = heat gain (occupancy schedule (figure 3.1))
Internal load of lighting	34 watt	LED + LED 17 watt + 17 watt = 34 watt (Kim et al., 2018) Power consumption = heat gain (occupancy schedule (figure 3.1))
Air change per hour (ACH)	0.1 h^{-1}	TEK 17 § 14-3 (Kim et al., 2014) (Cui et al., 2017)
Minimum ventilation load	8.0 $\frac{m^3}{h}$ (2.22 $\frac{l}{s}$)	TEK 17 § 13-3 With recirculation compensation of 13 % (Merzkirch et al., 2016) Constant all control strategies
Maximum ventilation load	58.0 $\frac{m^3}{h}$ (16.11 $\frac{l}{s}$)	TEK 17 § 13-3 With recirculation compensation of 13 % (Merzkirch et al., 2016) Varies on control strategies
Lower CO_2 set-point	400 ppm	Ambient CO_2 concentration (IDA ICE default)
Upper CO_2 set-point	1000 ppm	"Adequate ventilation" (Arbeidstilsynet, 2016)
Operative temperature (summer season) (April - September)	24.5 ± 1.0 °C	NS-EN ISO 7730:2005 Office metabolism (1.2 MET) clo value = 0.5
Operative temperature (winter season) (October - Mars)	22.0 ± 1.0 °C	NS-EN ISO 7730:2005 Office metabolism (1.2 MET) clo value = 1.0

B Occupancy schedule derivation

An occupancy schedule for single-person offices could not be found, so one is derived from the scientific peer-reviewed article; «Modeling occupancy in single-person offices» (Wang et al., 2005). The occupancy schedule can be seen in figure 3.1.

For extraction of the predictive model and the number of occupancy's to vacancy situations each day the referenced article is utilized. The study analyses vacancy and occupancy intervals, and can model these intervals as a function of time using a variety of statistical methods. The study only covers one office building, with 1 year period of measurements of 35 single-person offices, and should therefore only be considered for those conditions of statistical accuracy.

The following derivation contains relevant contents from the referenced scientific article (Wang et al., 2005):

The number of arrival- and depart situations (figure 2 from referenced study) is calculated with:

$$\bar{\Upsilon} = \sum_{i=1}^{n} P_i * \Upsilon_i$$

The arrival- and depart situations throughout the day are referred to as Υ, and there are n = 12 values of Υ with 12 different possibilities P.

From measurements an average arrival- and depart number was 4.93 $\pm$ 2.06, and from simulations the average arrival- and depart number was 5.51 $\pm$ 1.36. It is assumed from this that the average arrival- and depart number each day is 5.

The morning arrival time is normally at 8:12 with a standard deviation of 11 min, so it is assumed that the occupant arrives at the office at 08:00 for simplification. Figure 8 from the referenced article is used to decide what the typical time interval for both occupancy and vacancy in the office is for that respective time of the day. The figure 8 model is constructed with 1-hour intervals, and a total of 5 arrival- and depart situations is implemented in series to construct the occupancy schedule (see figure 3.1).

The total amount of occupied time from the construction is 364 minutes or 6.07 hours. Measurements of the 35 single-person offices over 171 days showed that the average occupied hours per day was 6.17 ± 2.56 hours. The simulation gave an average occupied hours per day to be 6.47 ± 1.38 hours.

The calculated utilization rate within the 07:00 - 17:00 operating time is $\frac{364\ min\ occupancy}{600\ min\ operating\ time} = 0.607 \approx 0.60$. This is also the utilization rate found using the comprehensive method for calculation of annual energy used for lighting (NS-EN 15193-1:2017) to recalculate the F_A (fraction of time a room or zone is unoccupied) from the utilization rate (Halvarsson, 2012).

The UR is stated to be 0.6 for one-person cellular offices, with 6 hours occupation in a 10 hour office day, which is the default value for annual operating hours for offices. UR is either 0 or 1 for the office room, which stands for vacant or occupied (Halvarsson, 2012).

With these correlating arguments using utilization rate, the occupancy is assumed sufficient for the present work, although conclusions drawn from using the occupancy schedule must be treated by how it was derived, and by the assumptions and simplifications which followed.

C Derivation of the S-CO_2 control strategy timeline for monthly time-step energy analysis

The S-CO_2 control strategy under non-simulation scenarios requires calculations of when and how long the CO_2 concentration is below the 1000 ppm mark, which is a function of occupancy schedule, ventilation load, and occupant CO_2-generation.

The derived occupancy schedule (figure 3.1) is used for the determination of occupant CO_2-generation intervals. The following timeline (figure C.1) is a visual illustration of the different time intervals and CO_2 concentrations that will occur in a typical working day and will be used to predict the air rates.

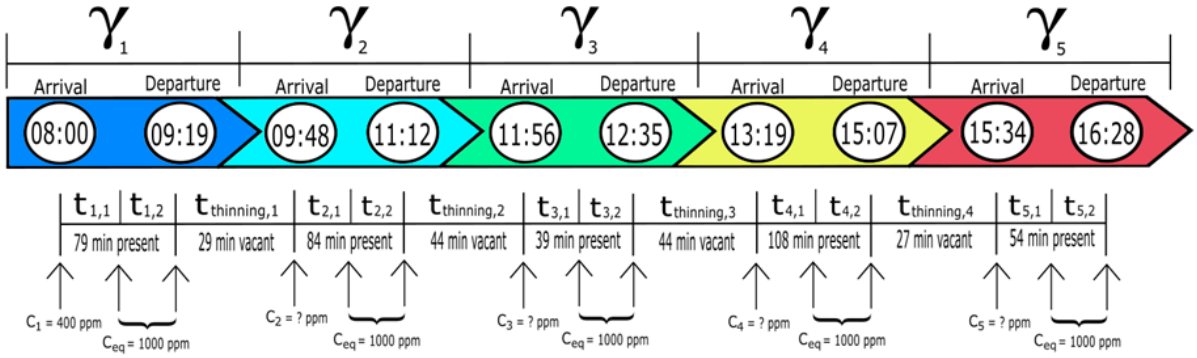

Figure C.1: Incomplete CO_2 concentration timeline

$\dot{Q}_{min}$ is used at times $t_{1,1}$, $t_{thinning,1}$, $t_{2,1}$, $t_{thinning,2}$, $t_{3,1}$, $t_{thinning,3}$, $t_{4,1}$, $t_{thinning,4}$ and $t_{5,1}$, which are the times where the CO_2 concentration has not reached 1000 ppm or has dropped below it. $\dot{Q}_{equilibrium}$ is used at times $t_{1,2}$, $t_{2,2}$, $t_{3,2}$, $t_{4,2}$ and $t_{5,2}$, which are the times when the CO_2 concentration lies at 1000 ppm, and is ventilated at equilibrium. $\dot{Q}_{min}$ is the minimum ventilation load according to TEK 17 § 13-3, while $\dot{Q}_{equilibrium}$ is calculated using the following equation according to Byggforsk 421.503:

$$\dot{Q}_{equilibrium} = 15000 * N_{occupants} * M * \frac{T_{s,a}}{T_{zone}(C_{equilibrium} - C_e)} * \frac{1}{\varepsilon_v} \left[\frac{m^3}{h}\right]$$

With 1 occupant, 1.2 MET, 17 °C (summer) and 20 °C (winter) supply temperature on all cases as simplification, 24.5 °C (summer) and 22 °C (winter) zone temperature, 600 ppm CO_2 concentration differential and a 0.7 mixing ventilation effectiveness. Including recirculation and 0.1 ACH, both equilibrium ventilation loads for summer and winter is set to 40 $\frac{m^3}{h}$, while the minimum ventilation load is set to 12.7 $\frac{m^3}{h}$.

Solving for $t_{\Upsilon,1}$ using:

$$\frac{(C_{equilibrium} - C_{\Upsilon}) * \dot{Q}_{min}}{N_{occupants} * \dot{m}_{CO_2}} = 1 - e^{-\frac{\dot{Q}_{min} * t_{\Upsilon,1}}{V_{zone}}}$$

Which leads to the solution:

$$t_{\Upsilon,1} = -\frac{V_{zone}}{\dot{Q}_{min}} * \log_e \left(1 - \frac{(C_{equilibrium} - C_{\Upsilon}) * \dot{Q}_{min}}{N_{occupants} * \dot{m}_{CO_2)}}\right) [s]$$

With zone volume 27.0 m^3, $\dot{Q}_{min}$ at $3.53 * 10^{-3}$ $\frac{m^3}{s}$ including recirculation and 0.1 ACH, $C_{equilibrium}$ at 1800 $\frac{mg}{m^3}$, C_{Υ} at 720 $\frac{mg}{m^3}$, and one occupant (Emmerich and Persily, 2003). The CO_2 mass production of the occupant is calculated using:

$$\dot{m}_{CO_2} = \dot{V}_{CO_2} * \frac{m^3}{1000\ L} * \rho_{CO_2} * 10^6\ \frac{mg}{kg}$$

With $\dot{V}_{CO_2}$ at 0.0052 $\frac{l}{s}$ and ρ_{CO_2} at 1.98 $\frac{kg}{m^3}$ (Emmerich and Persily, 2003).

Furthermore, the next CO_2 concentration starting point $C_{\Upsilon+1}$ of the cycle can be found with:

$$C_{\Upsilon+1} = (C_{equilibrium} - C_e) * e^{\frac{\dot{Q}_{min} * t_{thinning,\Upsilon}}{V_{zone}}} + C_e\,[ppm]$$

With $t_{thinning,\Upsilon}$ equal to its respective vacancy interval (Turanjanin et al., 2014).

The following table contains the relevant exact values:

Table C.1: Time periods and CO_2 concentration during cycles (see figure 3.7)

Cycle:	**Cycle Υ_1**	**Cycle Υ_2**	**Cycle Υ_3**	**Cycle Υ_4**	**Cycle Υ_5**
Initial C_{Υ}	$C_1 = 400$ ppm	$C_1 = 878$ ppm	$C_1 = 825$ ppm	$C_1 = 825$ ppm	$C_1 = 885$ ppm
$\dot{Q}_{min}$ interval	$t_{1,1} = 3536$ s	$t_{2,1} = 600$ s	$t_{3,1} = 874$ s	$t_{4,1} = 874$ s	$t_{5,1} = 563$ s
$\dot{Q}_{max}$ interval	$t_{1,2} = 1204$ s	$t_{2,2} = 4440$ s	$t_{3,2} = 1466$ s	$t_{4,2} = 5606$ s	$t_{5,2} = 2677$ s

During a day, the total ventilation load is given (3.6 $\left[\frac{\frac{m^3}{h}}{\frac{l}{s}}\right]$ conversion factor):

$$Q_{total} = \dot{Q}_{max} \sum_{i=1}^{\Upsilon} (t_i - t_{i,1})_i + \dot{Q}_{min} \left((86400 - 30480) + \left(30480 - \sum_{i=1}^{\Upsilon} (t_i - t_{i,1})_i\right)\right) \left[\frac{m^3}{day}\right]$$

This equation is used in monthly time-step energy analysis, see appendix D.3.

D Energy equations for monthly time-step energy analysis

A simplified zone energy balance is described (not including $\dot{E}_{inf}$ in referenced article) (Okochi and Yao, 2016), so the zone energy balance equation becomes (calculates local heating or cooling energy consumption):

$$\rho_{zone} V_{zone} C_{zone} \left(\frac{dT_{zone}}{dt} \right) = \dot{E}_{s,a} + \dot{E}_{inf} + \dot{E}_{ex,wl} + \dot{E}_{ex,wd} + \dot{E}_{internal} + \dot{E}_{external} \, [W]$$

Which expands to:

$$\dot{E}_{heating\ or\ cooling} = \frac{\dot{Q}_{s,a} \rho_{s,a} C_{p,a} \left(T_{s,a} - T_{zone} \right)}{3600 \frac{s}{h}} + \frac{(ACH) \, V_{zone} \rho_{s,a} C_{p,a} \left(T_e - T_{zone} \right)}{3600 \frac{s}{h}} +$$

$$U_{ex,wl} A_{ex,wl} \left(T_{ex,wl} - T_{zone} \right) + U_{ex,wd} A_{ex,wd} \left(T_{ex,wd} - T_{zone} \right) + \dot{E}_{person} + \dot{E}_{equipment} + \dot{E}_{lighting} \; [W]$$

- ρ_{zone} = Air density inside zone $\left[\frac{kg}{m^3} \right]$
- V_{zone} = Volume of zone $[m^3]$
- C_{zone} = Zone thermal capacitance $\left[\frac{J}{kg} \right]$
- $\frac{dT_{zone}}{dt}$ = Change in zone temperature with respect to time $[K]$
- $\dot{Q}_{s,a}$ = Volume flow of supply air into zone ($\dot{Q}_{min}$ or $\dot{Q}_{max}$) $\left[\frac{m^3}{h} \right]$
- $\rho_{s,a}$ = Supply air density $\left[\frac{kg}{m^3} \right]$
- $C_{p,a}$ = Specific heat capacity of the supply air $\left[\frac{J}{kgK} \right]$
- $(T_{s,a} - T_{zone})$ = Temperature difference between supply air and zone $[K]$
- $(T_{ex,wl} - T_{zone})$ = Temperature difference between outside and zone $[K]$
- $U_{ex,wl/wd}$ = U-value of external wall / window $\left[\frac{W}{m^2 K} \right]$
- $A_{ex,wl/wd}$ = Area of external wall / window $[m^2]$
- $\left(T_{ex,wl/wd} - T_{zone} \right)$ = Temperature difference of external wall surface (assumed equal to outside temperature) and zone $[K]$

The equation calculates the local heating or cooling energy load necessary to achieve zone energy balance. The solar radiation load $\dot{E}_{solar,\ rad}$ is excluded due to its complexity.

Enthalpies (h) are decided using Mollier diagram (cooling coil), see appendix D.1 - D.3:

D.1 DV CAV control strategy

Firstly, the zone energy consumption equations based on aforementioned scenarios are given (see figure 3.5):

$$E_{scenario\ 1} = \left(\dot{E}_{s,a,max} + \dot{E}_{inf} + \dot{E}_{tr,wl} + \dot{E}_{tr,wd} + \dot{E}_{internal}\right) * t_{scenario\ 1,\ CAV} * \frac{1kW}{1000W} \left[\frac{kWh}{month}\right]$$

Where $t_{scenario\ 1,\ CAV} = \frac{2500\frac{h}{year}}{12\frac{months}{year}} * \frac{6\ h}{10\ h} = 125\ \frac{h}{month}$

$$E_{scenario\ 2} = \left(\dot{E}_{s,a,max} + \dot{E}_{inf} + \dot{E}_{tr,wl} + \dot{E}_{tr,wd}\right) * t_{scenario\ 2,\ CAV} * \frac{1kW}{1000W} \left[\frac{kWh}{month}\right]$$

Where $t_{scenario\ 2,\ CAV} = \frac{2500\frac{h}{year}}{12\frac{months}{year}} * \frac{4\ h}{10\ h} = 83.333\ \frac{h}{month}$

$$E_{scenario\ 3} = \left(\dot{E}_{s,a,min} + \dot{E}_{inf} + \dot{E}_{tr,wl} + \dot{E}_{tr,wd}\right) * t_{scenario\ 3,\ CAV} * \frac{1kW}{1000W} \left[\frac{kWh}{month}\right]$$

Where $t_{scenario\ 3,\ CAV} = \frac{8760\ -\ 2500\frac{h}{year}}{12\frac{months}{year}} * \frac{14\ h}{14\ h} = 521.667\ \frac{h}{month}$ (Scenario 3 is excluded from results)

Ventilation loads, fan energy, and heating and cooling coil energy consumption:

$$Q_{total,\ CAV} = ((N_{occupant} * \dot{q}_{occupant} + A_{zone} * \dot{q}_{area}) * t_{max,\ CAV}) +$$

$$((A_{zone} * \dot{q}_{area}) * (8760 - t_{max,\ CAV})) * 1.13 \left[\frac{m^3}{year}\right]$$

$$E_{fan,\ no\ wind} = Q_{total,\ CAV} * SFP_{no,\ wind} * \frac{1\ h}{3600\ s} \left[\frac{kWh}{year}\right]$$

$$E_{fan,\ wind} = Q_{total,\ CAV} * SFP_{wind} * \frac{1\ h}{3600\ s} \left[\frac{kWh}{year}\right]$$

$$E_{heating\ coil} = C_{p,a} * \rho_{air} * Q_{total,\ CAV/12} * \Delta T_{s,a} * \frac{1\ kWh}{3.6 * 10^6\ J} \left[\frac{kWh}{month}\right]$$

$$\Delta T_{s,a} = T_{s,a} - T_{HRU} = T_{s,a} - \eta_{HRU}(T_{zone} - T_e) - T_e\,[K]$$

$$E_{cooling\ coil} = \rho_{air} * \left(h_1\left[\frac{kJ}{kg}\right] - h_2\left[\frac{kJ}{kg}\right]\right) * \left(Q_{total,\ CAV/12}\right) * \frac{1\ kWh}{3600\ kJ} \left[\frac{kWh}{month}\right]$$

D.2 DV PIR control strategy

Firstly, the zone energy consumption equations based on aforementioned scenarios are given (see figure 3.6):

$$E_{scenario\ 1} = \left(\dot{E}_{s,a,max} + \dot{E}_{inf} + \dot{E}_{tr,wl} + \dot{E}_{tr,wd} + \dot{E}_{internal}\right) * t_{scenario\ 1,\ PIR} * \frac{1kW}{1000W}\ \left[\frac{kWh}{month}\right]$$

Where $t_{scenario\ 1,\ PIR} = \frac{1500\frac{h}{year}}{12\frac{months}{year}} * \frac{6\ h}{6\ h} = 125\ \frac{h}{month}$

$$E_{scenario\ 2} = \left(\dot{E}_{s,a,min} + \dot{E}_{inf} + \dot{E}_{tr,wl} + \dot{E}_{tr,wd}\right) * t_{scenario\ 2,\ PIR} * \frac{1kW}{1000W}\ \left[\frac{kWh}{month}\right]$$

Where $t_{scenario\ 2,\ PIR} = \frac{8760\ -\ 1500\frac{h}{year}}{12\frac{months}{year}} * \frac{18\ h}{18\ h} = 605\ \frac{h}{month}$ (83.33 hours are within operating times and included in results, 521.667 hours are excluded)

Ventilation loads, fan energy, and heating and cooling coil energy consumption:

$$Q_{total,\ PIR} = ((N_{occupant} * \dot{q}_{occupant} + A_{zone} * \dot{q}_{area}) * t_{max,\ PIR}) +$$

$$((A_{zone} * \dot{q}_{area}) * (8760 - t_{max,\ PIR})) * 1.13\ \left[\frac{m^3}{year}\right]$$

$$E_{fan,\ no\ wind} = Q_{total,\ PIR} * SFP_{no,\ wind} * \frac{1\ h}{3600\ s}\ \left[\frac{kWh}{year}\right]$$

$$E_{fan,\ wind} = Q_{total,\ PIR} * SFP_{wind} * \frac{1\ h}{3600\ s}\ \left[\frac{kWh}{year}\right]$$

$$E_{heating\ coil} = C_{p,a} * \rho_{air} * Q_{total,\ PIR/12} * \Delta T_{s,a} * \frac{1\ kWh}{3.6 * 10^6\ J}\ \left[\frac{kWh}{month}\right]$$

$$\Delta T_{s,a} = T_{s,a} - T_{HRU} = T_{s,a} - \eta_{HRU}(T_{zone} - T_e) - T_e\,[K]$$

$$E_{cooling\ coil} = \rho_{air} * \left(h_1\left[\frac{kJ}{kg}\right] - h_2\left[\frac{kJ}{kg}\right]\right) * \left(Q_{total,\ PIR/12}\right) * \frac{1\ kWh}{3600\ kJ}\ \left[\frac{kWh}{month}\right]$$

D.3 DV S-CO_2 control strategy

Firstly, the zone energy consumption equations based on aforementioned scenarios are given (see figure 3.8):

$$E_{scenario\ 1} = \left(\dot{E}_{s,a,max} + \dot{E}_{inf} + \dot{E}_{tr,wl} + \dot{E}_{tr,wd} + \dot{E}_{internal}\right) * t_{scenario\ 1,\ CO_2} * \frac{1kW}{1000W}\ \left[\frac{kWh}{month}\right]$$

Where $t_{scenario\ 1,\ CO_2} = \frac{4.276\frac{h}{day} * 250\frac{days}{year}}{12\frac{months}{year}} = 89.083\ \frac{h}{month}$

$$E_{scenario\ 2} = \left(\dot{E}_{s,a,min} + \dot{E}_{inf} + \dot{E}_{tr,wl} + \dot{E}_{tr,wd}\ \dot{E}_{internal}\right) * t_{scenario\ 2,\ CO_2} * \frac{1kW}{1000W}\ \left[\frac{kWh}{month}\right]$$

Where $t_{scenario\ 2,\ CO_2} = \frac{1.724\frac{h}{day} * 250\frac{days}{year}}{12\frac{months}{year}} = 35.917\ \frac{h}{month}$

$$E_{scenario\ 3} = \left(\dot{E}_{s,a,min} + \dot{E}_{inf} + \dot{E}_{tr,wl} + \dot{E}_{tr,wd}\right)\ *\ t_{scenario\ 3,\ CO_2}\ *\ \frac{1kW}{1000W}\ \left[\frac{kWh}{month}\right]$$

Where $t_{scenario\ 3,\ CO_2} = \frac{8760\ -\ 1500\frac{h}{year}}{12\frac{months}{year}} = 605\ \frac{h}{month}$ (83.33 hours are within operating times and included in results, 521.667 hours are excluded)

Ventilation loads, fan energy, and heating and cooling coil energy consumption:

$$Q_{total,\ CO_2} = \dot{Q}_{max} \sum_{i=1}^{\Upsilon} (t_i - t_{i,1})_i + \dot{Q}_{min} \left((86400 - \sum_{i=1}^{\Upsilon} (t_i - t_{i,1})_i\right)\ *\ \frac{250\ days}{year}\ \left[\frac{m^3}{year}\right]$$

$$E_{fan,\ no\ wind} = Q_{total,\ CO_2} * SFP_{no,\ wind} * \frac{1\ h}{3600\ s}\ \left[\frac{kWh}{year}\right]$$

$$E_{fan,\ wind} = Q_{total,\ CO_2} * SFP_{wind} * \frac{1\ h}{3600\ s}\ \left[\frac{kWh}{year}\right]$$

$$E_{heating\ coil} = C_{p,a}\ *\ \rho_{air}\ *\ Q_{total,\ CO_2/12} * \Delta T_{s,a}\ *\ \frac{1\ kWh}{3.6 * 10^6\ J}\ \left[\frac{kWh}{month}\right]$$

$$\Delta T_{s,a} = T_{s,a} - T_{HRU} = T_{s,a} - \eta_{HRU}(T_{zone} - T_e) - T_e\,[K]$$

$$E_{cooling\ coil} = \rho_{air} * \left(h_1\left[\frac{kJ}{kg}\right] - h_2\left[\frac{kJ}{kg}\right]\right) * \left(Q_{total,\ CO_2/12}\right)\ *\ \frac{1\ kWh}{3600\ kJ}\ \left[\frac{kWh}{month}\right]$$

E Boundary conditions and input parameters for building simulation

Table E.1: General specifications in IDA ICE building simulation, relevant for all control strategy simulations

General (non-mentioned parameters are remained as standard settings)	
Global data	
Location	Oslo/Gardemoen
Climate	Oslo/Fornebu_ASHRAE
Wind profile	City center
Holidays	Public holiday in Sweden (14 days)
Defaults	
External wall	0.22 $\frac{W}{m^2K}$ (connects to face f.3). TEK 17 § 14-3 minimum demand. South (180°)
Interior wall	0.62 $\frac{W}{m^2K}$ (ignores heat transmission). Interior wall with insulation
Floor	2.39 $\frac{W}{m^2K}$ (ignores heat transmission). Concrete floor 150mm
Roof	2.39 $\frac{W}{m^2K}$ (ignores heat transmission). Concrete floor 150mm
Window passive house	Glazing U-value = 0.80 $\frac{W}{m^2K}$, g = 0.68 (solar heat gain), T = 0.6 (solar transmittance), T_{vis} = 0.74 (visible transmittance), Internal and external emissivity = 0.837
Infiltration	
Fixed infiltration	0.1 h^{-1}
System parameters	
Degree of automatic schedule smoothing	Set to 0 (no smoothing)
Air handling unit	
Supply and exhaust fans	Fan efficiency = 0.164 and Δp = 65.6 Pa on both fans. SFP = 0.800 $\frac{kWs}{m^3}$. Air temperature rise = 0.0 °C. Performance = Unlimited (constant SFP)
HRU efficiency	0.70
Supply temperature	Controlled after case 1, case 2 and case 3. See chapter 2.2.1

Table E.2: Zone details in IDA ICE building simulation, relevant for all control strategy simulations

Zone details (non-mentioned parameters are remained as standard settings)	
Office cell zone geometry	
Zone x (width)	2.4 m
Zone y (depth)	4.2 m
Zone z (height)	2.7 m
Zone area	10.08 m^2
Zone volume	27.22 m^3
Window x (horizontal)	1.2 m
Window y (vertical)	1.25 m
Window area	1.50 m^2
Window	
External window shading	Markisolette. Controlled by Sun
Frame U-value	0.80 $\frac{W}{m^2K}$
Direction	South (180°)
Internal loads	
Occupant load	1.2 met = 126 watt. Follows occupancy schedule (see figure 3.1). Occupant load = 1 person. 0.5 clo in summer. 1.0 clo in winter
Equipment load	34 watt. Follows occupancy schedule (see figure 3.1)
Lighting load	85 watt. Follows occupancy schedule (see figure 3.1)
Controller set-points	
Heating set-point	23.5 °C in summer during occupancy. 21.0 °C in winter during occupancy. 19.0 °C year around during vacancy
Cooling set-point	25.5 °C in summer during occupancy. 23.0 °C in winter during occupancy. 26.0 °C year around during vacancy
Room units	
Ideal heating	1000 W, COP = 1, PI controller
Ideal cooling	1000 W, COP = 1, PI controller

F AHU control of supply temperature regulation

F.1 AHU control of DV units with HRU

The AHU control for DV units with HRU is given, see figure F.1 – F.4. The AHU control is equal for all HRU efficiencies, and the temperature pattern can be seen in figure 2.8 – 2.10.

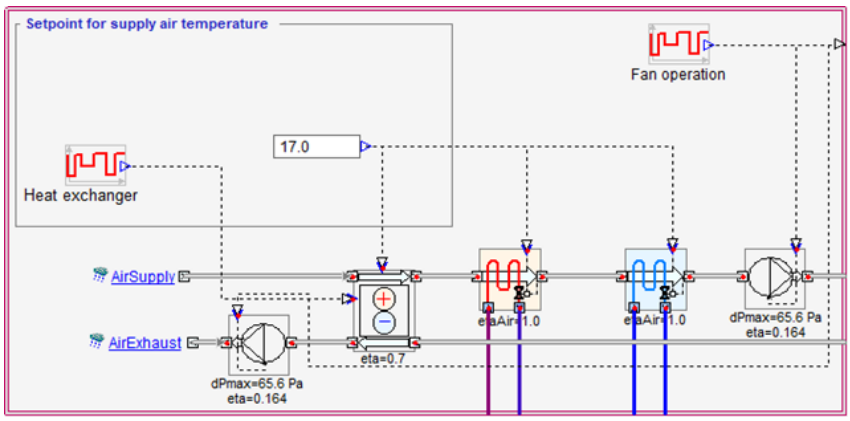

Figure F.1: Case 1 AHU control schematic for summer with HRU

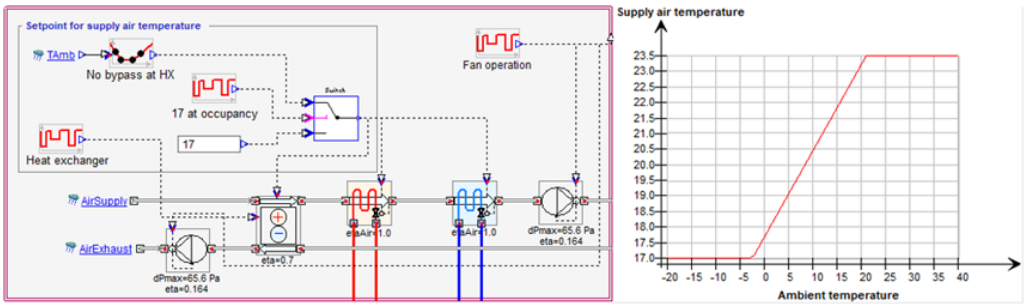

Figure F.2: Case 2 AHU control schematic for summer (left) with supply temperature regulation (right) with HRU

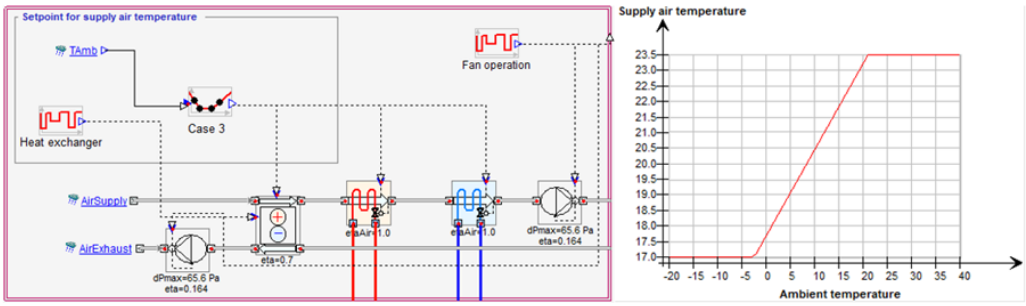

Figure F.3: Case 3 AHU control schematic for summer (left) with supply temperature regulation (right) with HRU

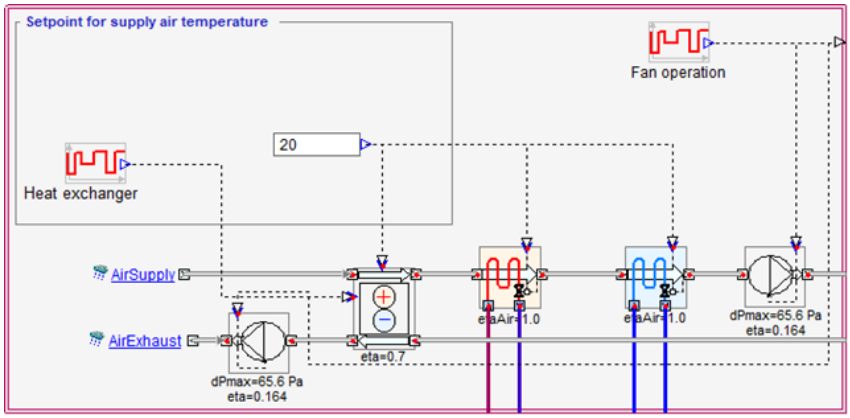

Figure F.4: AHU control schematic for winter with HRU

F.2 AHU control of DV units with no HRU or complete bypass of the HRU

The AHU control with no HRU (or complete bypass) and the temperature pattern is given, see figure F.5 – F.10:

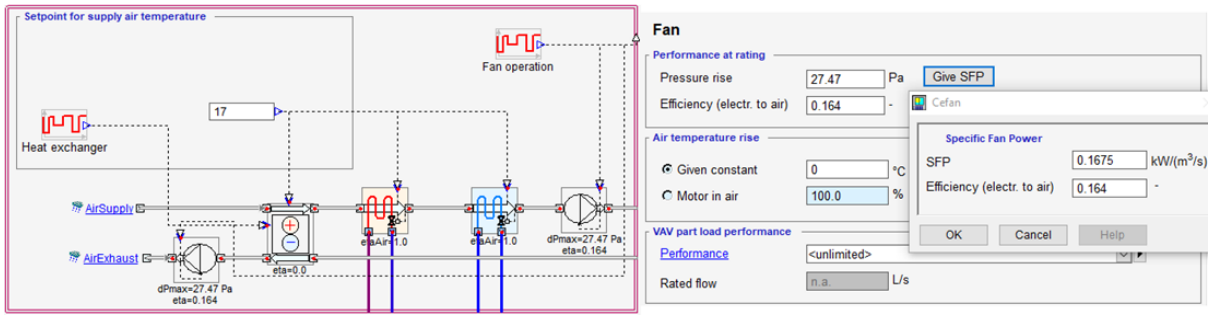

Figure F.5: Case 1 AHU custom control with no HRU

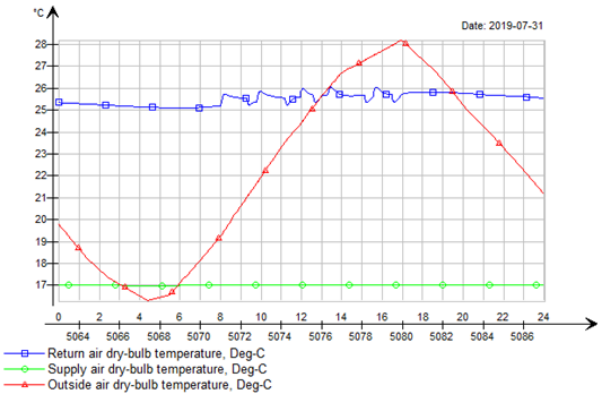

Figure F.6: Case 1 AHU temperatures with no HRU, hottest day

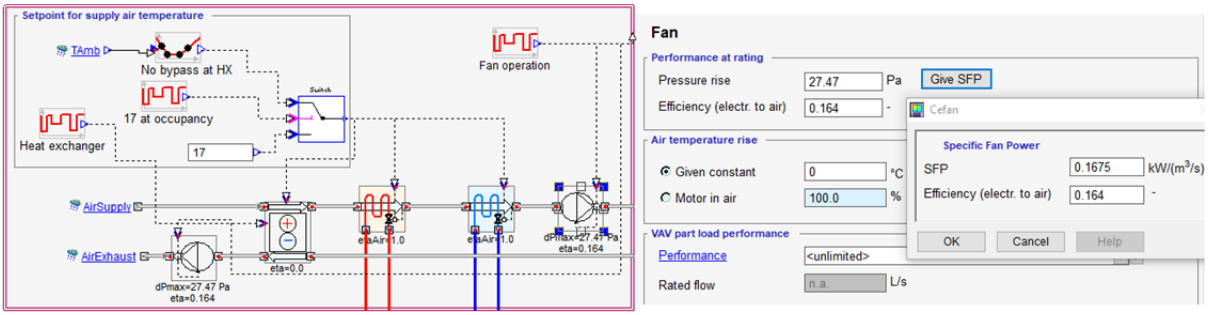

Figure F.7: Case 2 AHU custom control with no HRU

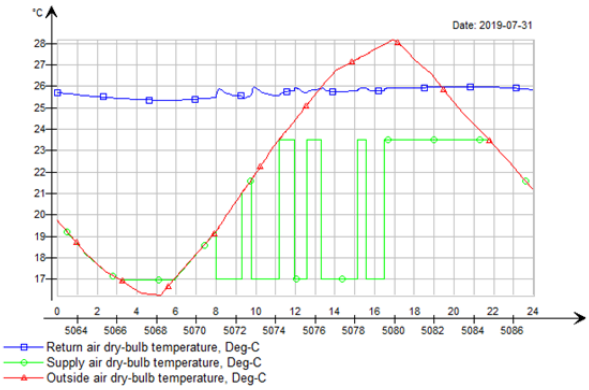

Figure F.8: Case 2 AHU temperatures with no HRU, hottest day

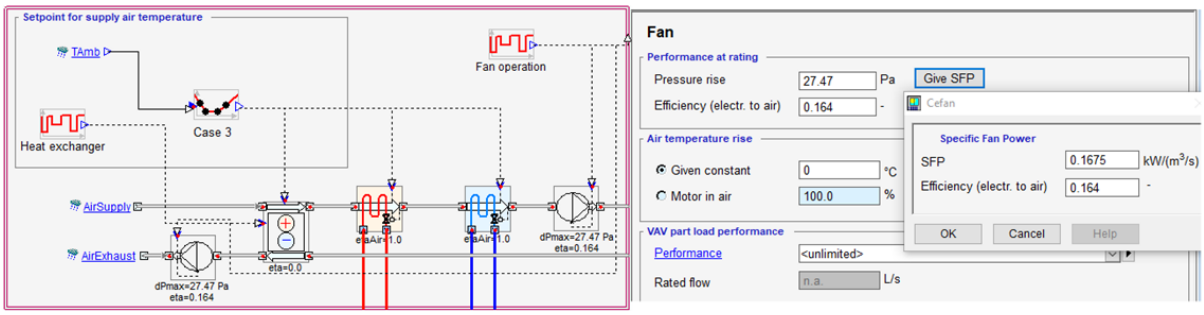

Figure F.9: Case 3 AHU custom control with no HRU

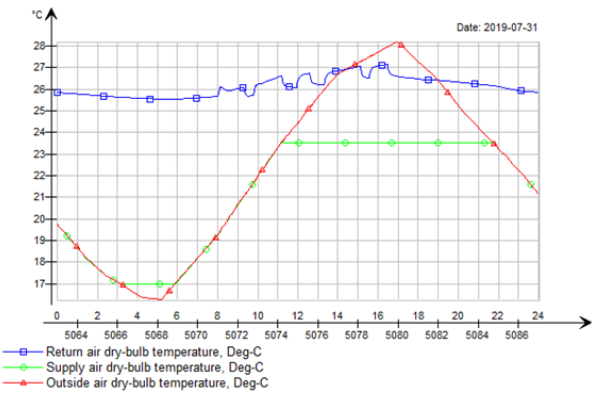

Figure F.10: Case 3 AHU temperatures with no HRU, hottest day

G Monthly time-step energy analysis results

G.1 Standard reference year

Table G.1: Standard reference year DV CAV control strategy annually primary energy results (monthly calculations)

DV CAV control strategy (annually)			
Monthly calculations	Case 1	Case 2	Case 3
AHU fan power	3.93 $\frac{kWh}{m^2a}$	3.93 $\frac{kWh}{m^2a}$	3.93 $\frac{kWh}{m^2a}$
AHU heating	16.62 $\frac{kWh}{m^2a}$	16.62 $\frac{kWh}{m^2a}$	16.62 $\frac{kWh}{m^2a}$
AHU cooling	0.29 $\frac{kWh}{m^2a}$	0.12 $\frac{kWh}{m^2a}$	0.00 $\frac{kWh}{m^2a}$
Local zone cooling	13.67 $\frac{kWh}{m^2a}$	13.67 $\frac{kWh}{m^2a}$	19.32 $\frac{kWh}{m^2a}$
Local zone heating	14.80 $\frac{kWh}{m^2a}$	11.02 $\frac{kWh}{m^2a}$	11.02 $\frac{kWh}{m^2a}$
Total primary energy	49.31 $\frac{kWh}{m^2a}$	45.36 $\frac{kWh}{m^2a}$	50.89 $\frac{kWh}{m^2a}$

Table G.2: Standard reference year DV PIR control strategy annually primary energy results (monthly calculations)

DV PIR control strategy (annually)			
Monthly calculations	Case 1	Case 2	Case 3
AHU fan power	2.92 $\frac{kWh}{m^2a}$	2.92 $\frac{kWh}{m^2a}$	2.92 $\frac{kWh}{m^2a}$
AHU heating	12.13 $\frac{kWh}{m^2a}$	12.13 $\frac{kWh}{m^2a}$	12.13 $\frac{kWh}{m^2a}$
AHU cooling	0.23 $\frac{kWh}{m^2a}$	0.12 $\frac{kWh}{m^2a}$	0.00 $\frac{kWh}{m^2a}$
Local zone cooling	13.67 $\frac{kWh}{m^2a}$	13.67 $\frac{kWh}{m^2a}$	19.32 $\frac{kWh}{m^2a}$
Local zone heating	7.18 $\frac{kWh}{m^2a}$	6.39 $\frac{kWh}{m^2a}$	6.39 $\frac{kWh}{m^2a}$
Total primary energy	36.13 $\frac{kWh}{m^2a}$	35.23 $\frac{kWh}{m^2a}$	40.76 $\frac{kWh}{m^2a}$

Table G.3: Standard reference year DV S-CO_2 control strategy annually primary energy results (monthly calculations)

DV S-CO_2 control strategy (annually)			
Monthly calculations	Case 1	Case 2	Case 3
AHU fan power	2.30 $\frac{kWh}{m^2a}$	2.30 $\frac{kWh}{m^2a}$	2.30 $\frac{kWh}{m^2a}$
AHU heating	8.15 $\frac{kWh}{m^2a}$	8.15 $\frac{kWh}{m^2a}$	8.15 $\frac{kWh}{m^2a}$
AHU cooling	0.17 $\frac{kWh}{m^2a}$	0.07 $\frac{kWh}{m^2a}$	0.00 $\frac{kWh}{m^2a}$
Local zone cooling	19.67 $\frac{kWh}{m^2a}$	19.67 $\frac{kWh}{m^2a}$	23.21 $\frac{kWh}{m^2a}$
Local zone heating	7.18 $\frac{kWh}{m^2a}$	6.39 $\frac{kWh}{m^2a}$	6.39 $\frac{kWh}{m^2a}$
Total primary energy	37.47 $\frac{kWh}{m^2a}$	36.59 $\frac{kWh}{m^2a}$	40.05 $\frac{kWh}{m^2a}$

G.2 Extreme hot year

Table G.4: Extreme hot year DV CAV control strategy annually primary energy results (monthly calculations)

DV CAV control strategy (annually)			
Monthly calculations	Case 1	Case 2	Case 3
AHU fan power	3.93 $\frac{kWh}{m^2a}$	3.93 $\frac{kWh}{m^2a}$	3.93 $\frac{kWh}{m^2a}$
AHU heating	7.80 $\frac{kWh}{m^2a}$	7.80 $\frac{kWh}{m^2a}$	7.80 $\frac{kWh}{m^2a}$
AHU cooling	7.61 $\frac{kWh}{m^2a}$	3.13 $\frac{kWh}{m^2a}$	0.00 $\frac{kWh}{m^2a}$
Local zone cooling	16.97 $\frac{kWh}{m^2a}$	16.97 $\frac{kWh}{m^2a}$	24.89 $\frac{kWh}{m^2a}$
Local zone heating	12.59 $\frac{kWh}{m^2a}$	7.31 $\frac{kWh}{m^2a}$	7.31 $\frac{kWh}{m^2a}$
Total primary energy	48.90 $\frac{kWh}{m^2a}$	39.14 $\frac{kWh}{m^2a}$	43.93 $\frac{kWh}{m^2a}$

Table G.5: Extreme hot year DV PIR control strategy annually primary energy results (monthly calculations)

DV PIR control strategy (annually)			
Monthly calculations	Case 1	Case 2	Case 3
AHU fan power	2.92 $\frac{kWh}{m^2a}$	2.92 $\frac{kWh}{m^2a}$	2.92 $\frac{kWh}{m^2a}$
AHU heating	5.56 $\frac{kWh}{m^2a}$	5.56 $\frac{kWh}{m^2a}$	5.56 $\frac{kWh}{m^2a}$
AHU cooling	5.88 $\frac{kWh}{m^2a}$	3.13 $\frac{kWh}{m^2a}$	0.00 $\frac{kWh}{m^2a}$
Local zone cooling	16.97 $\frac{kWh}{m^2a}$	16.97 $\frac{kWh}{m^2a}$	24.89 $\frac{kWh}{m^2a}$
Local zone heating	5.02 $\frac{kWh}{m^2a}$	3.98 $\frac{kWh}{m^2a}$	3.98 $\frac{kWh}{m^2a}$
Total primary energy	36.35 $\frac{kWh}{m^2a}$	32.56 $\frac{kWh}{m^2a}$	37.35 $\frac{kWh}{m^2a}$

Table G.6: Extreme hot year DV S-CO_2 control strategy annually primary energy results (monthly calculations)

DV S-CO_2 control strategy (annually)			
Monthly calculations	Case 1	Case 2	Case 3
AHU fan power	2.30 $\frac{kWh}{m^2a}$	2.30 $\frac{kWh}{m^2a}$	2.30 $\frac{kWh}{m^2a}$
AHU heating	3.58 $\frac{kWh}{m^2a}$	3.58 $\frac{kWh}{m^2a}$	3.58 $\frac{kWh}{m^2a}$
AHU cooling	4.55 $\frac{kWh}{m^2a}$	1.81 $\frac{kWh}{m^2a}$	0.00 $\frac{kWh}{m^2a}$
Local zone cooling	22.92 $\frac{kWh}{m^2a}$	22.92 $\frac{kWh}{m^2a}$	27.49 $\frac{kWh}{m^2a}$
Local zone heating	5.02 $\frac{kWh}{m^2a}$	3.98 $\frac{kWh}{m^2a}$	3.98 $\frac{kWh}{m^2a}$
Total primary energy	38.37 $\frac{kWh}{m^2a}$	34.59 $\frac{kWh}{m^2a}$	37.35 $\frac{kWh}{m^2a}$

G.3 Extreme cold year

Table G.7: Extreme cold year DV CAV control strategy annually primary energy results (monthly calculations)

DV CAV control strategy (annually)			
Monthly calculations	Case 1	Case 2	Case 3
AHU fan power	3.93 $\frac{kWh}{m^2a}$	3.93 $\frac{kWh}{m^2a}$	3.93 $\frac{kWh}{m^2a}$
AHU heating	18.47 $\frac{kWh}{m^2a}$	18.47 $\frac{kWh}{m^2a}$	18.47 $\frac{kWh}{m^2a}$
AHU cooling	0.00 $\frac{kWh}{m^2a}$	0.00 $\frac{kWh}{m^2a}$	0.00 $\frac{kWh}{m^2a}$
Local zone cooling	12.26 $\frac{kWh}{m^2a}$	12.26 $\frac{kWh}{m^2a}$	16.09 $\frac{kWh}{m^2a}$
Local zone heating	15.71 $\frac{kWh}{m^2a}$	13.16 $\frac{kWh}{m^2a}$	13.16 $\frac{kWh}{m^2a}$
Total primary energy	50.37 $\frac{kWh}{m^2a}$	47.82 $\frac{kWh}{m^2a}$	51.65 $\frac{kWh}{m^2a}$

Table G.8: Extreme cold year DV PIR control strategy annually primary energy results (monthly calculations)

DV PIR control strategy (annually)			
Monthly calculations	Case 1	Case 2	Case 3
AHU fan power	2.92 $\frac{kWh}{m^2a}$	2.92 $\frac{kWh}{m^2a}$	2.92 $\frac{kWh}{m^2a}$
AHU heating	13.48 $\frac{kWh}{m^2a}$	13.48 $\frac{kWh}{m^2a}$	13.48 $\frac{kWh}{m^2a}$
AHU cooling	0.00 $\frac{kWh}{m^2a}$	0.00 $\frac{kWh}{m^2a}$	0.00 $\frac{kWh}{m^2a}$
Local zone cooling	12.26 $\frac{kWh}{m^2a}$	12.26 $\frac{kWh}{m^2a}$	16.09 $\frac{kWh}{m^2a}$
Local zone heating	8.16 $\frac{kWh}{m^2a}$	7.49 $\frac{kWh}{m^2a}$	7.49 $\frac{kWh}{m^2a}$
Total primary energy	36.82 $\frac{kWh}{m^2a}$	36.15 $\frac{kWh}{m^2a}$	39.98 $\frac{kWh}{m^2a}$

Table G.9: Extreme cold year DV S-CO_2 control strategy annually primary energy results (monthly calculations)

DV S-CO_2 control strategy (annually)			
Monthly calculations	Case 1	Case 2	Case 3
AHU fan power	2.30 $\frac{kWh}{m^2a}$	2.30 $\frac{kWh}{m^2a}$	2.30 $\frac{kWh}{m^2a}$
AHU heating	9.15 $\frac{kWh}{m^2a}$	9.15 $\frac{kWh}{m^2a}$	9.15 $\frac{kWh}{m^2a}$
AHU cooling	0.00 $\frac{kWh}{m^2a}$	0.00 $\frac{kWh}{m^2a}$	0.00 $\frac{kWh}{m^2a}$
Local zone cooling	18.25 $\frac{kWh}{m^2a}$	18.25 $\frac{kWh}{m^2a}$	20.85 $\frac{kWh}{m^2a}$
Local zone heating	8.16 $\frac{kWh}{m^2a}$	7.49 $\frac{kWh}{m^2a}$	7.49 $\frac{kWh}{m^2a}$
Total primary energy	37.86 $\frac{kWh}{m^2a}$	37.19 $\frac{kWh}{m^2a}$	39.79 $\frac{kWh}{m^2a}$

H Building simulation tool IDA ICE results

H.1 Representative DV unit

H.1.1 DV CAV control strategy (representative DV unit)

Table H.1: DV CAV control strategy primary energy results for summer and winter (simulation)

DV CAV control strategy (seasons)				
IDA ICE simulation	Summer case 1	Summer case 2	Summer case 3	Winter
AHU fan power	2.15 $\frac{kWh}{m^2a}$	2.15 $\frac{kWh}{m^2a}$	2.15 $\frac{kWh}{m^2a}$	2.12 $\frac{kWh}{m^2a}$
AHU heating	0.32 $\frac{kWh}{m^2a}$	0.32 $\frac{kWh}{m^2a}$	0.32 $\frac{kWh}{m^2a}$	16.90 $\frac{kWh}{m^2a}$
AHU cooling	3.53 $\frac{kWh}{m^2a}$	1.86 $\frac{kWh}{m^2a}$	0.04 $\frac{kWh}{m^2a}$	0.00 $\frac{kWh}{m^2a}$
Local zone cooling	0.00 $\frac{kWh}{m^2a}$	1.66 $\frac{kWh}{m^2a}$	6.15 $\frac{kWh}{m^2a}$	0.16 $\frac{kWh}{m^2a}$
Local zone heating	4.59 $\frac{kWh}{m^2a}$	2.98 $\frac{kWh}{m^2a}$	1.93 $\frac{kWh}{m^2a}$	8.70 $\frac{kWh}{m^2a}$
Total primary energy	10.59 $\frac{kWh}{m^2a}$	8.97 $\frac{kWh}{m^2a}$	10.59 $\frac{kWh}{m^2a}$	27.88 $\frac{kWh}{m^2a}$

Table H.2: DV CAV control strategy primary energy results annually (simulation)

DV CAV control strategy (annually)			
IDA ICE simulation	Case 1	Case 2	Case 3
AHU fan power	4.27 $\frac{kWh}{m^2a}$	4.27 $\frac{kWh}{m^2a}$	4.27 $\frac{kWh}{m^2a}$
AHU heating	17.22 $\frac{kWh}{m^2a}$	17.22 $\frac{kWh}{m^2a}$	17.22 $\frac{kWh}{m^2a}$
AHU cooling	3.53 $\frac{kWh}{m^2a}$	1.86 $\frac{kWh}{m^2a}$	0.04 $\frac{kWh}{m^2a}$
Local zone cooling	0.16 $\frac{kWh}{m^2a}$	1.82 $\frac{kWh}{m^2a}$	6.31 $\frac{kWh}{m^2a}$
Local zone heating	13.29 $\frac{kWh}{m^2a}$	11.68 $\frac{kWh}{m^2a}$	10.63 $\frac{kWh}{m^2a}$
Total primary energy	38.47 $\frac{kWh}{m^2a}$	36.85 $\frac{kWh}{m^2a}$	38.47 $\frac{kWh}{m^2a}$

H.1.2 DV PIR control strategy (representative DV unit)

Table H.3: DV PIR control strategy primary energy results for summer and winter (simulation)

DV PIR control strategy (seasons)				
IDA ICE simulation	Summer case 1	Summer case 2	Summer case 3	Winter
AHU fan power	1.63 $\frac{kWh}{m^2a}$	1.63 $\frac{kWh}{m^2a}$	1.63 $\frac{kWh}{m^2a}$	1.60 $\frac{kWh}{m^2a}$
AHU heating	0.20 $\frac{kWh}{m^2a}$	0.20 $\frac{kWh}{m^2a}$	0.20 $\frac{kWh}{m^2a}$	12.58 $\frac{kWh}{m^2a}$
AHU cooling	2.65 $\frac{kWh}{m^2a}$	1.80 $\frac{kWh}{m^2a}$	0.03 $\frac{kWh}{m^2a}$	0.00 $\frac{kWh}{m^2a}$
Local zone cooling	0.79 $\frac{kWh}{m^2a}$	2.85 $\frac{kWh}{m^2a}$	7.90 $\frac{kWh}{m^2a}$	0.21 $\frac{kWh}{m^2a}$
Local zone heating	2.94 $\frac{kWh}{m^2a}$	2.23 $\frac{kWh}{m^2a}$	1.41 $\frac{kWh}{m^2a}$	8.50 $\frac{kWh}{m^2a}$
Total primary energy	8.21 $\frac{kWh}{m^2a}$	8.71 $\frac{kWh}{m^2a}$	11.17 $\frac{kWh}{m^2a}$	22.89 $\frac{kWh}{m^2a}$

Table H.4: DV PIR control strategy primary energy results annually (simulation)

DV PIR control strategy (annually)			
IDA ICE simulation	Case 1	Case 2	Case 3
AHU fan power	3.23 $\frac{kWh}{m^2a}$	3.23 $\frac{kWh}{m^2a}$	3.23 $\frac{kWh}{m^2a}$
AHU heating	12.78 $\frac{kWh}{m^2a}$	12.78 $\frac{kWh}{m^2a}$	12.78 $\frac{kWh}{m^2a}$
AHU cooling	2.65 $\frac{kWh}{m^2a}$	1.80 $\frac{kWh}{m^2a}$	0.03 $\frac{kWh}{m^2a}$
Local zone cooling	1.00 $\frac{kWh}{m^2a}$	3.06 $\frac{kWh}{m^2a}$	8.11 $\frac{kWh}{m^2a}$
Local zone heating	11.44 $\frac{kWh}{m^2a}$	10.73 $\frac{kWh}{m^2a}$	9.91 $\frac{kWh}{m^2a}$
Total primary energy	31.10 $\frac{kWh}{m^2a}$	31.60 $\frac{kWh}{m^2a}$	34.06 $\frac{kWh}{m^2a}$

H.1.3 DV S-CO_2 control strategy (representative DV unit)

Table H.5: DV S-CO_2 control strategy primary energy results for summer and winter (simulation)

DV S-CO_2 control strategy (seasons)				
IDA ICE simulation	Summer case 1	Summer case 2	Summer case 3	Winter
AHU fan power	1.05 $\frac{kWh}{m^2a}$	1.05 $\frac{kWh}{m^2a}$	1.05 $\frac{kWh}{m^2a}$	1.04 $\frac{kWh}{m^2a}$
AHU heating	0.15 $\frac{kWh}{m^2a}$	0.15 $\frac{kWh}{m^2a}$	0.15 $\frac{kWh}{m^2a}$	8.47 $\frac{kWh}{m^2a}$
AHU cooling	1.67 $\frac{kWh}{m^2a}$	0.85 $\frac{kWh}{m^2a}$	0.02 $\frac{kWh}{m^2a}$	0.00 $\frac{kWh}{m^2a}$
Local zone cooling	4.60 $\frac{kWh}{m^2a}$	7.53 $\frac{kWh}{m^2a}$	9.93 $\frac{kWh}{m^2a}$	0.38 $\frac{kWh}{m^2a}$
Local zone heating	1.24 $\frac{kWh}{m^2a}$	0.85 $\frac{kWh}{m^2a}$	0.63 $\frac{kWh}{m^2a}$	7.57 $\frac{kWh}{m^2a}$
Total primary energy	8.71 $\frac{kWh}{m^2a}$	10.43 $\frac{kWh}{m^2a}$	11.78 $\frac{kWh}{m^2a}$	17.46 $\frac{kWh}{m^2a}$

Table H.6: DV S-CO_2 control strategy primary energy results annually (simulation)

DV S-CO_2 control strategy (annually)			
IDA ICE simulation	Case 1	Case 2	Case 3
AHU fan power	2.09 $\frac{kWh}{m^2a}$	2.09 $\frac{kWh}{m^2a}$	2.09 $\frac{kWh}{m^2a}$
AHU heating	8.62 $\frac{kWh}{m^2a}$	8.62 $\frac{kWh}{m^2a}$	8.62 $\frac{kWh}{m^2a}$
AHU cooling	1.67 $\frac{kWh}{m^2a}$	0.85 $\frac{kWh}{m^2a}$	0.02 $\frac{kWh}{m^2a}$
Local zone cooling	4.98 $\frac{kWh}{m^2a}$	7.91 $\frac{kWh}{m^2a}$	10.31 $\frac{kWh}{m^2a}$
Local zone heating	8.81 $\frac{kWh}{m^2a}$	8.42 $\frac{kWh}{m^2a}$	8.20 $\frac{kWh}{m^2a}$
Total primary energy	26.17 $\frac{kWh}{m^2a}$	27.89 $\frac{kWh}{m^2a}$	29.24 $\frac{kWh}{m^2a}$

H.1.4 DV D-CO_2 control strategy (representative DV unit)

Table H.7: DV D-CO_2 control strategy primary energy results for summer and winter (simulation)

DV D-CO_2 control strategy (seasons)				
IDA ICE simulation	Summer case 1	Summer case 2	Summer case 3	Winter
AHU fan power	1.51 $\frac{kWh}{m^2a}$	1.51 $\frac{kWh}{m^2a}$	1.51 $\frac{kWh}{m^2a}$	1.48 $\frac{kWh}{m^2a}$
AHU heating	0.20 $\frac{kWh}{m^2a}$	0.20 $\frac{kWh}{m^2a}$	0.20 $\frac{kWh}{m^2a}$	12.20 $\frac{kWh}{m^2a}$
AHU cooling	2.59 $\frac{kWh}{m^2a}$	1.29 $\frac{kWh}{m^2a}$	0.03 $\frac{kWh}{m^2a}$	0.00 $\frac{kWh}{m^2a}$
Local zone cooling	1.44 $\frac{kWh}{m^2a}$	4.75 $\frac{kWh}{m^2a}$	8.35 $\frac{kWh}{m^2a}$	0.35 $\frac{kWh}{m^2a}$
Local zone heating	2.39 $\frac{kWh}{m^2a}$	1.67 $\frac{kWh}{m^2a}$	1.17 $\frac{kWh}{m^2a}$	7.89 $\frac{kWh}{m^2a}$
Total primary energy	8.13 $\frac{kWh}{m^2a}$	9.42 $\frac{kWh}{m^2a}$	11.26 $\frac{kWh}{m^2a}$	21.92 $\frac{kWh}{m^2a}$

Table H.8: DV D-CO_2 control strategy primary energy results annually (simulation)

DV D-CO_2 control strategy (annually)			
IDA ICE simulation	Case 1	Case 2	Case 3
AHU fan power	2.99 $\frac{kWh}{m^2a}$	2.99 $\frac{kWh}{m^2a}$	2.99 $\frac{kWh}{m^2a}$
AHU heating	12.40 $\frac{kWh}{m^2a}$	12.40 $\frac{kWh}{m^2a}$	12.40 $\frac{kWh}{m^2a}$
AHU cooling	2.59 $\frac{kWh}{m^2a}$	1.29 $\frac{kWh}{m^2a}$	0.03 $\frac{kWh}{m^2a}$
Local zone cooling	1.79 $\frac{kWh}{m^2a}$	5.10 $\frac{kWh}{m^2a}$	8.70 $\frac{kWh}{m^2a}$
Local zone heating	10.28 $\frac{kWh}{m^2a}$	9.56 $\frac{kWh}{m^2a}$	9.06 $\frac{kWh}{m^2a}$
Total primary energy	30.05 $\frac{kWh}{m^2a}$	31.34 $\frac{kWh}{m^2a}$	33.18 $\frac{kWh}{m^2a}$

H.1.5 DV S-CO_2 + temperature control strategy (representative DV unit)

Table H.9: DV S-CO_2 + temperature control strategy primary energy results for summer and winter (simulation)

DV S-CO_2 + temperature control strategy (seasons)				
IDA ICE simulation	Summer case 1	Summer case 2	Summer case 3	Winter
AHU fan power	1.36 $\frac{kWh}{m^2a}$	1.76 $\frac{kWh}{m^2a}$	2.69 $\frac{kWh}{m^2a}$	1.22 $\frac{kWh}{m^2a}$
AHU heating	0.15 $\frac{kWh}{m^2a}$	0.15 $\frac{kWh}{m^2a}$	0.15 $\frac{kWh}{m^2a}$	10.18 $\frac{kWh}{m^2a}$
AHU cooling	3.07 $\frac{kWh}{m^2a}$	2.54 $\frac{kWh}{m^2a}$	0.05 $\frac{kWh}{m^2a}$	0.00 $\frac{kWh}{m^2a}$
Local zone cooling	0.00 $\frac{kWh}{m^2a}$	0.00 $\frac{kWh}{m^2a}$	0.00 $\frac{kWh}{m^2a}$	0.00 $\frac{kWh}{m^2a}$
Local zone heating	1.22 $\frac{kWh}{m^2a}$	1.01 $\frac{kWh}{m^2a}$	0.59 $\frac{kWh}{m^2a}$	7.42 $\frac{kWh}{m^2a}$
Total primary energy	5.80 $\frac{kWh}{m^2a}$	5.46 $\frac{kWh}{m^2a}$	3.48 $\frac{kWh}{m^2a}$	18.82 $\frac{kWh}{m^2a}$

Table H.10: DV S-CO_2 + temperature control strategy primary energy results annually (simulation)

DV S-CO_2 + temperature control strategy (annually)			
IDA ICE simulation	Case 1	Case 2	Case 3
AHU fan power	2.58 $\frac{kWh}{m^2a}$	2.98 $\frac{kWh}{m^2a}$	3.91 $\frac{kWh}{m^2a}$
AHU heating	10.33 $\frac{kWh}{m^2a}$	10.33 $\frac{kWh}{m^2a}$	10.33 $\frac{kWh}{m^2a}$
AHU cooling	3.07 $\frac{kWh}{m^2a}$	2.54 $\frac{kWh}{m^2a}$	0.05 $\frac{kWh}{m^2a}$
Local zone cooling	0.00 $\frac{kWh}{m^2a}$	0.00 $\frac{kWh}{m^2a}$	0.00 $\frac{kWh}{m^2a}$
Local zone heating	8.64 $\frac{kWh}{m^2a}$	8.43 $\frac{kWh}{m^2a}$	8.01 $\frac{kWh}{m^2a}$
Total primary energy	24.62 $\frac{kWh}{m^2a}$	24.28 $\frac{kWh}{m^2a}$	22.30 $\frac{kWh}{m^2a}$

H.2 HRU absence and efficiency variations on energy presence

H.2.1 Case 1 scenario

Table H.11: DV S-CO_2 + temperature case 1 control strategy with no integrated HRU, summer + winter + annually primary energy results (simulation)

DV S-CO_2 + temperature control strategy (seasons + annually) HRU efficiency = 0.0, SFP = 0.335 $\frac{kWs}{m^3}$			
IDA ICE simulation	Summer case 1	Winter	Annually
AHU fan power	0.57 $\frac{kWh}{m^2a}$	0.52 $\frac{kWh}{m^2a}$	1.09 $\frac{kWh}{m^2a}$
AHU heating	7.56 $\frac{kWh}{m^2a}$	35.51 $\frac{kWh}{m^2a}$	43.07 $\frac{kWh}{m^2a}$
AHU cooling	3.07 $\frac{kWh}{m^2a}$	0.00 $\frac{kWh}{m^2a}$	3.07 $\frac{kWh}{m^2a}$
Local zone cooling	0.00 $\frac{kWh}{m^2a}$	0.00 $\frac{kWh}{m^2a}$	0.00 $\frac{kWh}{m^2a}$
Local zone heating	1.22 $\frac{kWh}{m^2a}$	7.42 $\frac{kWh}{m^2a}$	8.63 $\frac{kWh}{m^2a}$
Total primary energy	12.42 $\frac{kWh}{m^2a}$	43.44 $\frac{kWh}{m^2a}$	55.86 $\frac{kWh}{m^2a}$

Table H.12: DV S-CO_2 + temperature case 1 control strategy with $\eta_{HRU} = 0.4$, summer + winter + annually primary energy results (simulation)

DV S-CO_2 + temperature control strategy (seasons + annually) HRU efficiency = 0.4, SFP = 0.800 $\frac{kWs}{m^3}$			
IDA ICE simulation	Summer case 1	Winter	Annually
AHU fan power	1.36 $\frac{kWh}{m^2a}$	1.22 $\frac{kWh}{m^2a}$	2.58 $\frac{kWh}{m^2a}$
AHU heating	2.12 $\frac{kWh}{m^2a}$	20.76 $\frac{kWh}{m^2a}$	22.88 $\frac{kWh}{m^2a}$
AHU cooling	3.07 $\frac{kWh}{m^2a}$	0.00 $\frac{kWh}{m^2a}$	3.07 $\frac{kWh}{m^2a}$
Local zone cooling	0.00 $\frac{kWh}{m^2a}$	0.00 $\frac{kWh}{m^2a}$	0.00 $\frac{kWh}{m^2a}$
Local zone heating	1.22 $\frac{kWh}{m^2a}$	7.42 $\frac{kWh}{m^2a}$	8.64 $\frac{kWh}{m^2a}$
Total primary energy	7.77 $\frac{kWh}{m^2a}$	29.40 $\frac{kWh}{m^2a}$	37.17 $\frac{kWh}{m^2a}$

Table H.13: DV S-CO_2 + temperature case 1 control strategy with $\eta_{HRU} = 0.5$, summer + winter + annually primary energy results (simulation)

DV S-CO_2 + temperature control strategy (seasons + annually) HRU efficiency = 0.5, SFP = 0.800 $\frac{kWs}{m^3}$			
IDA ICE simulation	Summer case 1	Winter	Annually
AHU fan power	1.36 $\frac{kWh}{m^2a}$	1.22 $\frac{kWh}{m^2a}$	2.58 $\frac{kWh}{m^2a}$
AHU heating	1.27 $\frac{kWh}{m^2a}$	17.08 $\frac{kWh}{m^2a}$	18.35 $\frac{kWh}{m^2a}$
AHU cooling	3.07 $\frac{kWh}{m^2a}$	0.00 $\frac{kWh}{m^2a}$	3.07 $\frac{kWh}{m^2a}$
Local zone cooling	0.00 $\frac{kWh}{m^2a}$	0.00 $\frac{kWh}{m^2a}$	0.00 $\frac{kWh}{m^2a}$
Local zone heating	1.22 $\frac{kWh}{m^2a}$	7.42 $\frac{kWh}{m^2a}$	8.64 $\frac{kWh}{m^2a}$
Total primary energy	6.92 $\frac{kWh}{m^2a}$	25.72 $\frac{kWh}{m^2a}$	32.64 $\frac{kWh}{m^2a}$

Table H.14: DV S-CO_2 + temperature case 1 control strategy with $\eta_{HRU} = 0.6$, summer + winter + annually primary energy results (simulation)

DV S-CO_2 + temperature control strategy (seasons + annually) HRU efficiency = 0.6, SFP = 0.800 $\frac{kWs}{m^3}$			
IDA ICE simulation	Summer case 1	Winter	Annually
AHU fan power	1.36 $\frac{kWh}{m^2a}$	1.22 $\frac{kWh}{m^2a}$	2.58 $\frac{kWh}{m^2a}$
AHU heating	0.60 $\frac{kWh}{m^2a}$	13.50 $\frac{kWh}{m^2a}$	14.10 $\frac{kWh}{m^2a}$
AHU cooling	3.07 $\frac{kWh}{m^2a}$	0.00 $\frac{kWh}{m^2a}$	3.07 $\frac{kWh}{m^2a}$
Local zone cooling	0.00 $\frac{kWh}{m^2a}$	0.00 $\frac{kWh}{m^2a}$	0.00 $\frac{kWh}{m^2a}$
Local zone heating	1.22 $\frac{kWh}{m^2a}$	7.42 $\frac{kWh}{m^2a}$	8.64 $\frac{kWh}{m^2a}$
Total primary energy	6.25 $\frac{kWh}{m^2a}$	22.14 $\frac{kWh}{m^2a}$	28.39 $\frac{kWh}{m^2a}$

Table H.15: DV S-CO_2 + temperature case 1 control strategy with $\eta_{HRU} = 0.7$, summer + winter + annually primary energy results (simulation)

DV S-CO_2 + temperature control strategy (seasons + annually) HRU efficiency = 0.7, SFP = 0.800 $\frac{kWs}{m^3}$			
IDA ICE simulation	Summer case 1	Winter	Annually
AHU fan power	1.36 $\frac{kWh}{m^2a}$	1.22 $\frac{kWh}{m^2a}$	2.58 $\frac{kWh}{m^2a}$
AHU heating	0.15 $\frac{kWh}{m^2a}$	10.18 $\frac{kWh}{m^2a}$	10.33 $\frac{kWh}{m^2a}$
AHU cooling	3.07 $\frac{kWh}{m^2a}$	0.00 $\frac{kWh}{m^2a}$	3.07 $\frac{kWh}{m^2a}$
Local zone cooling	0.00 $\frac{kWh}{m^2a}$	0.00 $\frac{kWh}{m^2a}$	0.00 $\frac{kWh}{m^2a}$
Local zone heating	1.22 $\frac{kWh}{m^2a}$	7.42 $\frac{kWh}{m^2a}$	8.64 $\frac{kWh}{m^2a}$
Total primary energy	5.80 $\frac{kWh}{m^2a}$	18.82 $\frac{kWh}{m^2a}$	24.62 $\frac{kWh}{m^2a}$

Table H.16: DV S-CO_2 + temperature case 1 control strategy with $\eta_{HRU} = 0.8$, summer + winter + annually primary energy results (simulation)

DV S-CO_2 + temperature control strategy (seasons + annually) HRU efficiency = 0.8, SFP = 0.800 $\frac{kWs}{m^3}$			
IDA ICE simulation	Summer case 1	Winter	Annually
AHU fan power	1.36 $\frac{kWh}{m^2a}$	1.22 $\frac{kWh}{m^2a}$	2.58 $\frac{kWh}{m^2a}$
AHU heating	0.00 $\frac{kWh}{m^2a}$	7.33 $\frac{kWh}{m^2a}$	7.33 $\frac{kWh}{m^2a}$
AHU cooling	3.07 $\frac{kWh}{m^2a}$	0.00 $\frac{kWh}{m^2a}$	3.07 $\frac{kWh}{m^2a}$
Local zone cooling	0.00 $\frac{kWh}{m^2a}$	0.00 $\frac{kWh}{m^2a}$	0.00 $\frac{kWh}{m^2a}$
Local zone heating	1.22 $\frac{kWh}{m^2a}$	7.42 $\frac{kWh}{m^2a}$	8.64 $\frac{kWh}{m^2a}$
Total primary energy	5.65 $\frac{kWh}{m^2a}$	15.97 $\frac{kWh}{m^2a}$	21.62 $\frac{kWh}{m^2a}$

Table H.17: DV S-CO_2 + temperature case 1 control strategy with $\eta_{HRU} = 0.9$, summer + winter + annually primary energy results (simulation)

DV S-CO_2 + temperature control strategy (seasons + annually) HRU efficiency = 0.9, SFP = 0.800 $\frac{kWs}{m^3}$			
IDA ICE simulation	Summer case 1	Winter	Annually
AHU fan power	1.36 $\frac{kWh}{m^2a}$	1.22 $\frac{kWh}{m^2a}$	2.58 $\frac{kWh}{m^2a}$
AHU heating	0.00 $\frac{kWh}{m^2a}$	5.17 $\frac{kWh}{m^2a}$	5.17 $\frac{kWh}{m^2a}$
AHU cooling	3.07 $\frac{kWh}{m^2a}$	0.00 $\frac{kWh}{m^2a}$	3.07 $\frac{kWh}{m^2a}$
Local zone cooling	0.00 $\frac{kWh}{m^2a}$	0.00 $\frac{kWh}{m^2a}$	0.00 $\frac{kWh}{m^2a}$
Local zone heating	1.22 $\frac{kWh}{m^2a}$	7.42 $\frac{kWh}{m^2a}$	8.64 $\frac{kWh}{m^2a}$
Total primary energy	5.65 $\frac{kWh}{m^2a}$	13.81 $\frac{kWh}{m^2a}$	19.46 $\frac{kWh}{m^2a}$

H.2.2 Case 2 scenario

Table H.18: DV S-CO_2 + temperature case 2 control strategy with no integrated HRU, summer + winter + annually primary energy results (simulation)

DV S-CO_2 + temperature control strategy (seasons + annually) HRU efficiency = 0.0, SFP = 0.335 $\frac{kWs}{m^3}$			
IDA ICE simulation	Summer case 2	Winter	Annually
AHU fan power	0.61 $\frac{kWh}{m^2a}$	0.52 $\frac{kWh}{m^2a}$	1.13 $\frac{kWh}{m^2a}$
AHU heating	7.59 $\frac{kWh}{m^2a}$	35.51 $\frac{kWh}{m^2a}$	43.10 $\frac{kWh}{m^2a}$
AHU cooling	2.54 $\frac{kWh}{m^2a}$	0.00 $\frac{kWh}{m^2a}$	2.54 $\frac{kWh}{m^2a}$
Local zone cooling	0.00 $\frac{kWh}{m^2a}$	0.00 $\frac{kWh}{m^2a}$	0.00 $\frac{kWh}{m^2a}$
Local zone heating	1.21 $\frac{kWh}{m^2a}$	7.41 $\frac{kWh}{m^2a}$	8.62 $\frac{kWh}{m^2a}$
Total primary energy	11.65 $\frac{kWh}{m^2a}$	43.44 $\frac{kWh}{m^2a}$	55.09 $\frac{kWh}{m^2a}$

Table H.19: DV S-CO_2 + temperature case 2 control strategy with $\eta_{HRU} = 0.4$, summer + winter + annually primary energy results (simulation)

DV S-CO_2 + temperature control strategy (seasons + annually) HRU efficiency = 0.4, SFP = 0.800 $\frac{kWs}{m^3}$			
IDA ICE simulation	Summer case 2	Winter	Annually
AHU fan power	1.60 $\frac{kWh}{m^2a}$	1.22 $\frac{kWh}{m^2a}$	2.82 $\frac{kWh}{m^2a}$
AHU heating	2.21 $\frac{kWh}{m^2a}$	20.76 $\frac{kWh}{m^2a}$	22.97 $\frac{kWh}{m^2a}$
AHU cooling	2.54 $\frac{kWh}{m^2a}$	0.00 $\frac{kWh}{m^2a}$	2.54 $\frac{kWh}{m^2a}$
Local zone cooling	0.00 $\frac{kWh}{m^2a}$	0.00 $\frac{kWh}{m^2a}$	0.00 $\frac{kWh}{m^2a}$
Local zone heating	1.19 $\frac{kWh}{m^2a}$	7.42 $\frac{kWh}{m^2a}$	8.61 $\frac{kWh}{m^2a}$
Total primary energy	7.54 $\frac{kWh}{m^2a}$	29.40 $\frac{kWh}{m^2a}$	36.94 $\frac{kWh}{m^2a}$

Table H.20: DV S-CO_2 + temperature case 2 control strategy with $\eta_{HRU} = 0.5$, summer + winter + annually primary energy results (simulation)

DV S-CO_2 + temperature control strategy (seasons + annually) HRU efficiency = 0.5, SFP = 0.800 $\frac{kWs}{m^3}$			
IDA ICE simulation	Summer case 2	Winter	Annually
AHU fan power	1.63 $\frac{kWh}{m^2a}$	1.22 $\frac{kWh}{m^2a}$	2.85 $\frac{kWh}{m^2a}$
AHU heating	1.26 $\frac{kWh}{m^2a}$	17.08 $\frac{kWh}{m^2a}$	18.34 $\frac{kWh}{m^2a}$
AHU cooling	2.54 $\frac{kWh}{m^2a}$	0.00 $\frac{kWh}{m^2a}$	2.54 $\frac{kWh}{m^2a}$
Local zone cooling	0.00 $\frac{kWh}{m^2a}$	0.00 $\frac{kWh}{m^2a}$	0.00 $\frac{kWh}{m^2a}$
Local zone heating	1.18 $\frac{kWh}{m^2a}$	7.42 $\frac{kWh}{m^2a}$	8.60 $\frac{kWh}{m^2a}$
Total primary energy	6.61 $\frac{kWh}{m^2a}$	25.72 $\frac{kWh}{m^2a}$	32.33 $\frac{kWh}{m^2a}$

Table H.21: DV S-CO_2 + temperature case 2 control strategy with $\eta_{HRU} = 0.6$, summer + winter + annually primary energy results (simulation)

DV S-CO_2 + temperature control strategy (seasons + annually) HRU efficiency = 0.6, SFP = 0.800 $\frac{kWs}{m^3}$			
IDA ICE simulation	Summer case 2	Winter	Annually
AHU fan power	1.68 $\frac{kWh}{m^2a}$	1.22 $\frac{kWh}{m^2a}$	2.90 $\frac{kWh}{m^2a}$
AHU heating	0.51 $\frac{kWh}{m^2a}$	13.50 $\frac{kWh}{m^2a}$	14.01 $\frac{kWh}{m^2a}$
AHU cooling	2.54 $\frac{kWh}{m^2a}$	0.00 $\frac{kWh}{m^2a}$	2.54 $\frac{kWh}{m^2a}$
Local zone cooling	0.00 $\frac{kWh}{m^2a}$	0.00 $\frac{kWh}{m^2a}$	0.00 $\frac{kWh}{m^2a}$
Local zone heating	1.10 $\frac{kWh}{m^2a}$	7.42 $\frac{kWh}{m^2a}$	8.52 $\frac{kWh}{m^2a}$
Total primary energy	5.83 $\frac{kWh}{m^2a}$	22.14 $\frac{kWh}{m^2a}$	27.92 $\frac{kWh}{m^2a}$

Table H.22: DV S-CO_2 + temperature case 2 control strategy with $\eta_{HRU} = 0.7$, summer + winter + annually primary energy results (simulation)

DV S-CO_2 + temperature control strategy (seasons + annually) HRU efficiency = 0.7, SFP = 0.800 $\frac{kWs}{m^3}$			
IDA ICE simulation	Summer case 2	Winter	Annually
AHU fan power	1.76 $\frac{kWh}{m^2a}$	1.22 $\frac{kWh}{m^2a}$	2.98 $\frac{kWh}{m^2a}$
AHU heating	0.15 $\frac{kWh}{m^2a}$	10.18 $\frac{kWh}{m^2a}$	10.33 $\frac{kWh}{m^2a}$
AHU cooling	2.54 $\frac{kWh}{m^2a}$	0.00 $\frac{kWh}{m^2a}$	2.54 $\frac{kWh}{m^2a}$
Local zone cooling	0.00 $\frac{kWh}{m^2a}$	0.00 $\frac{kWh}{m^2a}$	0.00 $\frac{kWh}{m^2a}$
Local zone heating	1.01 $\frac{kWh}{m^2a}$	7.42 $\frac{kWh}{m^2a}$	8.43 $\frac{kWh}{m^2a}$
Total primary energy	5.46 $\frac{kWh}{m^2a}$	18.82 $\frac{kWh}{m^2a}$	24.28 $\frac{kWh}{m^2a}$

Table H.23: DV S-CO_2 + temperature case 2 control strategy with $\eta_{HRU} = 0.8$, summer + winter + annually primary energy results (simulation)

DV S-CO_2 + temperature control strategy (seasons + annually) HRU efficiency = 0.8, SFP = 0.800 $\frac{kWs}{m^3}$			
IDA ICE simulation	Summer case 2	Winter	Annually
AHU fan power	1.85 $\frac{kWh}{m^2a}$	1.22 $\frac{kWh}{m^2a}$	3.07 $\frac{kWh}{m^2a}$
AHU heating	0.00 $\frac{kWh}{m^2a}$	7.33 $\frac{kWh}{m^2a}$	7.33 $\frac{kWh}{m^2a}$
AHU cooling	2.54 $\frac{kWh}{m^2a}$	0.00 $\frac{kWh}{m^2a}$	2.54 $\frac{kWh}{m^2a}$
Local zone cooling	0.00 $\frac{kWh}{m^2a}$	0.00 $\frac{kWh}{m^2a}$	0.00 $\frac{kWh}{m^2a}$
Local zone heating	0.92 $\frac{kWh}{m^2a}$	7.42 $\frac{kWh}{m^2a}$	8.34 $\frac{kWh}{m^2a}$
Total primary energy	5.31 $\frac{kWh}{m^2a}$	15.97 $\frac{kWh}{m^2a}$	21.28 $\frac{kWh}{m^2a}$

Table H.24: DV S-CO_2 + temperature case 2 control strategy with $\eta_{HRU} = 0.9$, summer + winter + annually primary energy results (simulation)

DV S-CO_2 + temperature control strategy (seasons + annually) HRU efficiency = 0.9, SFP = 0.800 $\frac{kWs}{m^3}$			
IDA ICE simulation	Summer case 2	Winter	Annually
AHU fan power	1.98 $\frac{kWh}{m^2a}$	1.22 $\frac{kWh}{m^2a}$	3.20 $\frac{kWh}{m^2a}$
AHU heating	0.00 $\frac{kWh}{m^2a}$	5.17 $\frac{kWh}{m^2a}$	5.17 $\frac{kWh}{m^2a}$
AHU cooling	2.54 $\frac{kWh}{m^2a}$	0.00 $\frac{kWh}{m^2a}$	2.54 $\frac{kWh}{m^2a}$
Local zone cooling	0.00 $\frac{kWh}{m^2a}$	0.00 $\frac{kWh}{m^2a}$	0.00 $\frac{kWh}{m^2a}$
Local zone heating	0.84 $\frac{kWh}{m^2a}$	7.42 $\frac{kWh}{m^2a}$	8.26 $\frac{kWh}{m^2a}$
Total primary energy	5.36 $\frac{kWh}{m^2a}$	13.81 $\frac{kWh}{m^2a}$	19.17 $\frac{kWh}{m^2a}$

H.2.3 Case 3 scenario

Table H.25: DV S-CO_2 + temperature case 3 control strategy with no integrated HRU, summer + winter + annually primary energy results (simulation)

DV S-CO_2 + temperature control strategy (seasons + annually) HRU efficiency = 0.0, SFP = 0.335 $\frac{kWs}{m^3}$			
IDA ICE simulation	Summer case 3	Winter	Annually
AHU fan power	0.68 $\frac{kWh}{m^2a}$	0.52 $\frac{kWh}{m^2a}$	1.20 $\frac{kWh}{m^2a}$
AHU heating	7.63 $\frac{kWh}{m^2a}$	35.51 $\frac{kWh}{m^2a}$	43.14 $\frac{kWh}{m^2a}$
AHU cooling	0.05 $\frac{kWh}{m^2a}$	0.00 $\frac{kWh}{m^2a}$	0.05 $\frac{kWh}{m^2a}$
Local zone cooling	0.00 $\frac{kWh}{m^2a}$	0.00 $\frac{kWh}{m^2a}$	0.00 $\frac{kWh}{m^2a}$
Local zone heating	1.20 $\frac{kWh}{m^2a}$	7.41 $\frac{kWh}{m^2a}$	8.61 $\frac{kWh}{m^2a}$
Total primary energy	9.56 $\frac{kWh}{m^2a}$	43.44 $\frac{kWh}{m^2a}$	53.00 $\frac{kWh}{m^2a}$

Table H.26: DV S-CO_2 + temperature case 3 control strategy with $\eta_{HRU} = 0.4$, summer + winter + annually primary energy results (simulation)

DV S-CO_2 + temperature control strategy (seasons + annually) HRU efficiency = 0.4, SFP = 0.800 $\frac{kWs}{m^3}$			
IDA ICE simulation	Summer case 3	Winter	Annually
AHU fan power	1.96 $\frac{kWh}{m^2a}$	1.22 $\frac{kWh}{m^2a}$	3.18 $\frac{kWh}{m^2a}$
AHU heating	2.13 $\frac{kWh}{m^2a}$	20.76 $\frac{kWh}{m^2a}$	22.89 $\frac{kWh}{m^2a}$
AHU cooling	0.05 $\frac{kWh}{m^2a}$	0.00 $\frac{kWh}{m^2a}$	0.05 $\frac{kWh}{m^2a}$
Local zone cooling	0.00 $\frac{kWh}{m^2a}$	0.00 $\frac{kWh}{m^2a}$	0.00 $\frac{kWh}{m^2a}$
Local zone heating	1.18 $\frac{kWh}{m^2a}$	7.42 $\frac{kWh}{m^2a}$	8.60 $\frac{kWh}{m^2a}$
Total primary energy	5.32 $\frac{kWh}{m^2a}$	29.40 $\frac{kWh}{m^2a}$	34.72 $\frac{kWh}{m^2a}$

Table H.27: DV S-CO_2 + temperature case 3 control strategy with $\eta_{HRU} = 0.5$, summer + winter + annually primary energy results (simulation)

DV S-CO_2 + temperature control strategy (seasons + annually) HRU efficiency = 0.5, SFP = 0.800 $\frac{kWs}{m^3}$			
IDA ICE simulation	Summer case 3	Winter	Annually
AHU fan power	2.13 $\frac{kWh}{m^2a}$	1.22 $\frac{kWh}{m^2a}$	3.35 $\frac{kWh}{m^2a}$
AHU heating	1.29 $\frac{kWh}{m^2a}$	17.08 $\frac{kWh}{m^2a}$	18.37 $\frac{kWh}{m^2a}$
AHU cooling	0.05 $\frac{kWh}{m^2a}$	0.00 $\frac{kWh}{m^2a}$	0.05 $\frac{kWh}{m^2a}$
Local zone cooling	0.00 $\frac{kWh}{m^2a}$	0.00 $\frac{kWh}{m^2a}$	0.00 $\frac{kWh}{m^2a}$
Local zone heating	1.13 $\frac{kWh}{m^2a}$	7.42 $\frac{kWh}{m^2a}$	8.55 $\frac{kWh}{m^2a}$
Total primary energy	4.60 $\frac{kWh}{m^2a}$	25.72 $\frac{kWh}{m^2a}$	30.32 $\frac{kWh}{m^2a}$

Table H.28: DV S-CO_2 + temperature case 3 control strategy with $\eta_{HRU} = 0.6$, summer + winter + annually primary energy results (simulation)

DV S-CO_2 + temperature control strategy (seasons + annually) HRU efficiency = 0.6, SFP = 0.800 $\frac{kWs}{m^3}$			
IDA ICE simulation	Summer case 3	Winter	Annually
AHU fan power	2.36 $\frac{kWh}{m^2a}$	1.22 $\frac{kWh}{m^2a}$	3.58 $\frac{kWh}{m^2a}$
AHU heating	0.70 $\frac{kWh}{m^2a}$	13.50 $\frac{kWh}{m^2a}$	14.20 $\frac{kWh}{m^2a}$
AHU cooling	0.05 $\frac{kWh}{m^2a}$	0.00 $\frac{kWh}{m^2a}$	0.05 $\frac{kWh}{m^2a}$
Local zone cooling	0.00 $\frac{kWh}{m^2a}$	0.00 $\frac{kWh}{m^2a}$	0.00 $\frac{kWh}{m^2a}$
Local zone heating	0.88 $\frac{kWh}{m^2a}$	7.42 $\frac{kWh}{m^2a}$	8.30 $\frac{kWh}{m^2a}$
Total primary energy	3.99 $\frac{kWh}{m^2a}$	22.14 $\frac{kWh}{m^2a}$	26.13 $\frac{kWh}{m^2a}$

Table H.29: DV S-CO_2 + temperature case 3 control strategy with $\eta_{HRU} = 0.7$, summer + winter + annually primary energy results (simulation)

DV S-CO_2 + temperature control strategy (seasons + annually) HRU efficiency = 0.7, SFP = 0.800 $\frac{kWs}{m^3}$			
IDA ICE simulation	Summer case 3	Winter	Annually
AHU fan power	2.69 $\frac{kWh}{m^2a}$	1.22 $\frac{kWh}{m^2a}$	3.91 $\frac{kWh}{m^2a}$
AHU heating	0.15 $\frac{kWh}{m^2a}$	10.18 $\frac{kWh}{m^2a}$	10.33 $\frac{kWh}{m^2a}$
AHU cooling	0.05 $\frac{kWh}{m^2a}$	0.00 $\frac{kWh}{m^2a}$	0.05 $\frac{kWh}{m^2a}$
Local zone cooling	0.00 $\frac{kWh}{m^2a}$	0.00 $\frac{kWh}{m^2a}$	0.00 $\frac{kWh}{m^2a}$
Local zone heating	0.59 $\frac{kWh}{m^2a}$	7.42 $\frac{kWh}{m^2a}$	8.01 $\frac{kWh}{m^2a}$
Total primary energy	3.48 $\frac{kWh}{m^2a}$	18.82 $\frac{kWh}{m^2a}$	22.30 $\frac{kWh}{m^2a}$

Table H.30: DV S-CO_2 + temperature case 3 control strategy with $\eta_{HRU} = 0.8$, summer + winter + annually primary energy results (simulation)

DV S-CO_2 + temperature control strategy (seasons + annually) HRU efficiency = 0.8, SFP = 0.800 $\frac{kWs}{m^3}$			
IDA ICE simulation	Summer case 3	Winter	Annually
AHU fan power	3.18 $\frac{kWh}{m^2a}$	1.22 $\frac{kWh}{m^2a}$	4.40 $\frac{kWh}{m^2a}$
AHU heating	0.00 $\frac{kWh}{m^2a}$	7.33 $\frac{kWh}{m^2a}$	7.33 $\frac{kWh}{m^2a}$
AHU cooling	0.05 $\frac{kWh}{m^2a}$	0.00 $\frac{kWh}{m^2a}$	0.05 $\frac{kWh}{m^2a}$
Local zone cooling	0.00 $\frac{kWh}{m^2a}$	0.00 $\frac{kWh}{m^2a}$	0.00 $\frac{kWh}{m^2a}$
Local zone heating	0.00 $\frac{kWh}{m^2a}$	7.42 $\frac{kWh}{m^2a}$	7.42 $\frac{kWh}{m^2a}$
Total primary energy	3.23 $\frac{kWh}{m^2a}$	15.97 $\frac{kWh}{m^2a}$	19.20 $\frac{kWh}{m^2a}$

Table H.31: DV S-CO_2 + temperature case 3 control strategy with $\eta_{HRU} = 0.9$, summer + winter + annually primary energy results (simulation)

DV S-CO_2 + temperature control strategy (seasons + annually) HRU efficiency = 0.9, SFP = 0.800 $\frac{kWs}{m^3}$			
IDA ICE simulation	Summer case 3	Winter	Annually
AHU fan power	3.49 $\frac{kWh}{m^2a}$	1.22 $\frac{kWh}{m^2a}$	4.71 $\frac{kWh}{m^2a}$
AHU heating	0.00 $\frac{kWh}{m^2a}$	5.17 $\frac{kWh}{m^2a}$	5.17 $\frac{kWh}{m^2a}$
AHU cooling	0.05 $\frac{kWh}{m^2a}$	0.00 $\frac{kWh}{m^2a}$	0.05 $\frac{kWh}{m^2a}$
Local zone cooling	0.00 $\frac{kWh}{m^2a}$	0.00 $\frac{kWh}{m^2a}$	0.00 $\frac{kWh}{m^2a}$
Local zone heating	0.00 $\frac{kWh}{m^2a}$	7.42 $\frac{kWh}{m^2a}$	7.42 $\frac{kWh}{m^2a}$
Total primary energy	3.54 $\frac{kWh}{m^2a}$	13.81 $\frac{kWh}{m^2a}$	17.35 $\frac{kWh}{m^2a}$

H.3 AM 150 with manufacturer datasheet specifications

Table H.32: DV S-CO_2 + temperature control strategy with AM 150 specifications primary energy results for summer and winter (simulation)

DV S-CO_2 + temperature control strategy (seasons)				
IDA ICE simulation	Summer case 1	Summer case 2	Summer case 3	Winter
AHU fan power	1.19 $\frac{kWh}{m^2a}$	1.57 $\frac{kWh}{m^2a}$	2.92 $\frac{kWh}{m^2a}$	1.07 $\frac{kWh}{m^2a}$
AHU heating	0.00 $\frac{kWh}{m^2a}$	0.00 $\frac{kWh}{m^2a}$	0.00 $\frac{kWh}{m^2a}$	6.17 $\frac{kWh}{m^2a}$
AHU cooling	3.11 $\frac{kWh}{m^2a}$	2.78 $\frac{kWh}{m^2a}$	0.03 $\frac{kWh}{m^2a}$	0.00 $\frac{kWh}{m^2a}$
Local zone cooling	0.00 $\frac{kWh}{m^2a}$	0.00 $\frac{kWh}{m^2a}$	0.00 $\frac{kWh}{m^2a}$	0.00 $\frac{kWh}{m^2a}$
Local zone heating	1.22 $\frac{kWh}{m^2a}$	0.68 $\frac{kWh}{m^2a}$	0.00 $\frac{kWh}{m^2a}$	7.39 $\frac{kWh}{m^2a}$
Total primary energy	5.52 $\frac{kWh}{m^2a}$	5.03 $\frac{kWh}{m^2a}$	2.95 $\frac{kWh}{m^2a}$	14.63 $\frac{kWh}{m^2a}$

Table H.33: DV S-CO_2 + temperature control strategy with AM 150 specifications primary energy results annually (simulation)

DV S-CO_2 + temperature control strategy (annually)			
IDA ICE simulation	Case 1	Case 2	Case 3
AHU fan power	2.26 $\frac{kWh}{m^2a}$	2.64 $\frac{kWh}{m^2a}$	3.99 $\frac{kWh}{m^2a}$
AHU heating	6.17 $\frac{kWh}{m^2a}$	6.17 $\frac{kWh}{m^2a}$	6.17 $\frac{kWh}{m^2a}$
AHU cooling	3.11 $\frac{kWh}{m^2a}$	2.78 $\frac{kWh}{m^2a}$	0.03 $\frac{kWh}{m^2a}$
Local zone cooling	0.00 $\frac{kWh}{m^2a}$	0.00 $\frac{kWh}{m^2a}$	0.00 $\frac{kWh}{m^2a}$
Local zone heating	8.61 $\frac{kWh}{m^2a}$	8.07 $\frac{kWh}{m^2a}$	7.39 $\frac{kWh}{m^2a}$
Total primary energy	20.15 $\frac{kWh}{m^2a}$	19.66 $\frac{kWh}{m^2a}$	17.58 $\frac{kWh}{m^2a}$

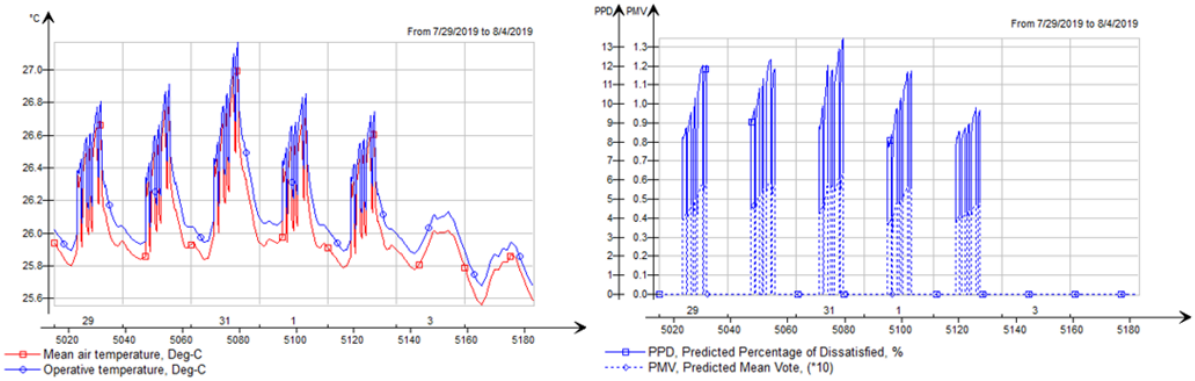

Figure H.1: Hottest week DV S-CO_2 + temperature control strategy case 3 temperatures (left) and Fanger's comfort indices (right) with AM 150

I Thermal comfort of representative DV unit simulations on critical weeks

I.1 DV CAV control strategy

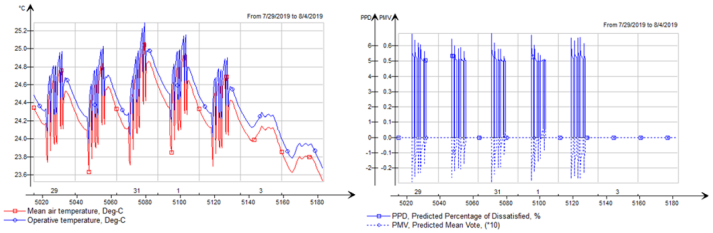

Figure I.1: Hottest week DV CAV control strategy case 1 temperatures (left) and Fanger's comfort indices (right)

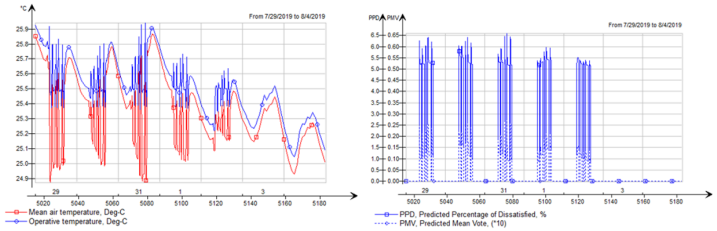

Figure I.2: Hottest week DV CAV control strategy case 2 temperatures (left) and Fanger's comfort indices (right)

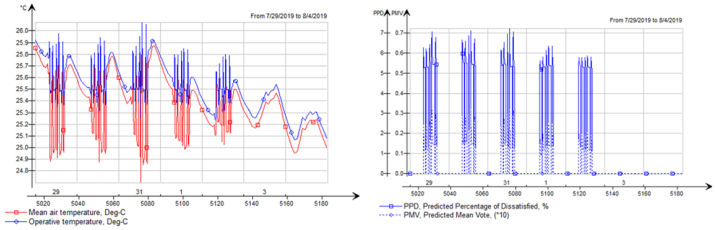

Figure I.3: Hottest week DV CAV control strategy case 3 temperatures (left) and Fanger's comfort indices (right)

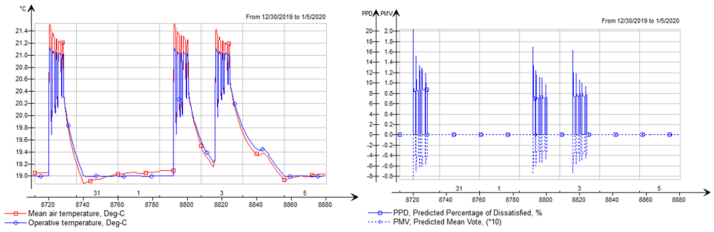

Figure I.4: Coldest week DV CAV control strategy winter temperatures (left) and Fanger's comfort indices (right)

I.2 DV PIR control strategy

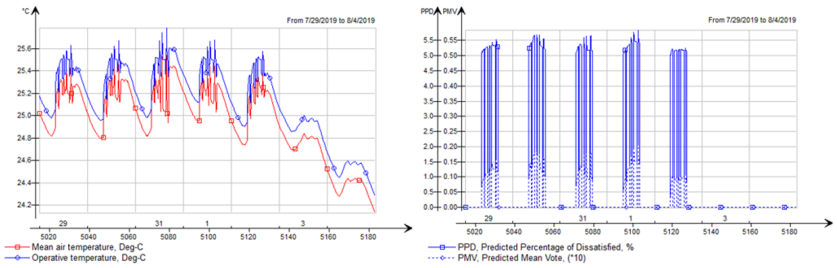

Figure I.5: Hottest week DV PIR control strategy case 1 temperatures (left) and Fanger's comfort indices (right)

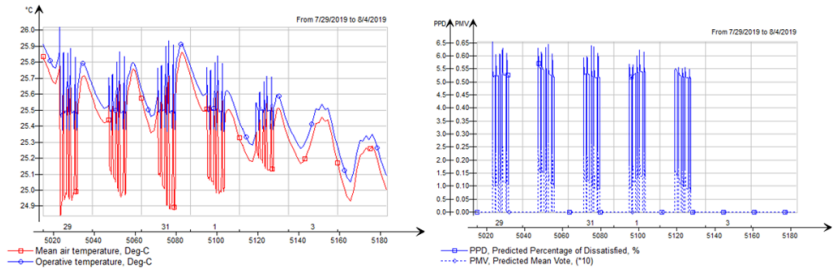

Figure I.6: Hottest week DV PIR control strategy case 2 temperatures (left) and Fanger's comfort indices (right)

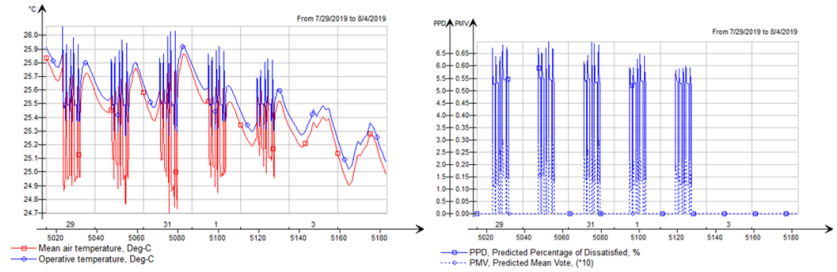

Figure I.7: Hottest week DV PIR control strategy case 3 temperatures (left) and Fanger's comfort indices (right)

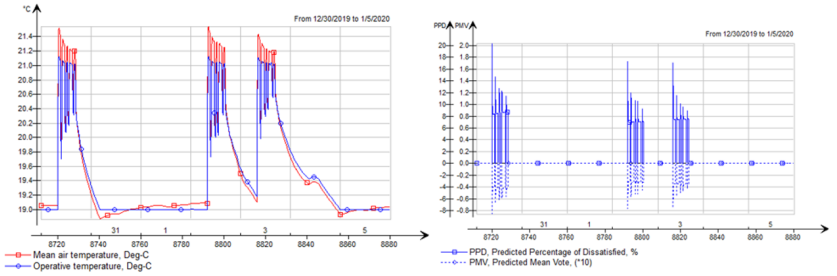

Figure I.8: Coldest week DV PIR control strategy winter temperatures (left) and Fanger's comfort indices (right)

I.3 DV S-CO_2 control strategy

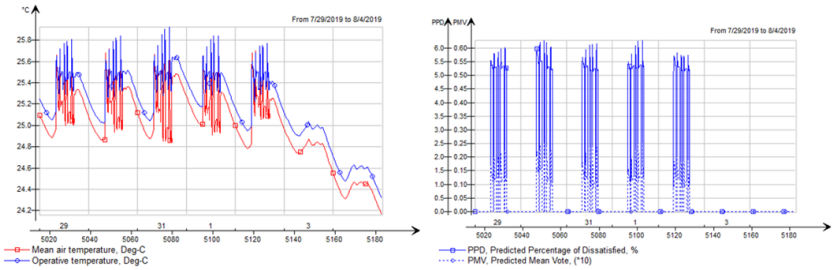

Figure I.9: Hottest week DV S-CO_2 control strategy case 1 temperatures (left) and Fanger's comfort indices (right)

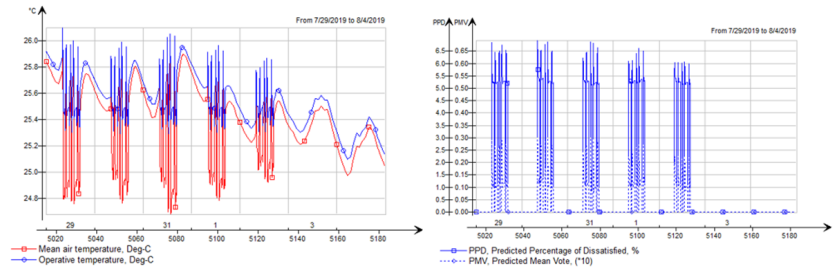

Figure I.10: Hottest week DV S-CO_2 control strategy case 2 temperatures (left) and Fanger's comfort indices (right)

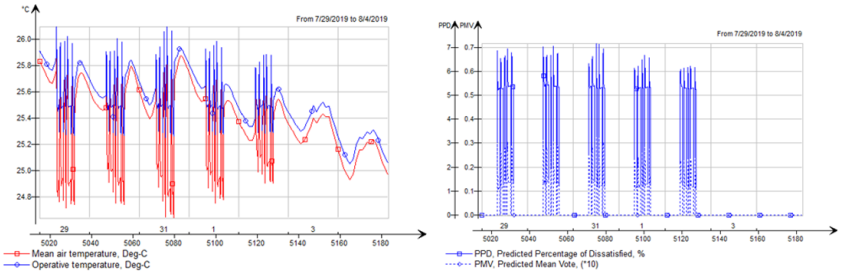

Figure I.11: Hottest week DV S-CO_2 control strategy case 3 temperatures (left) and Fanger's comfort indices (right)

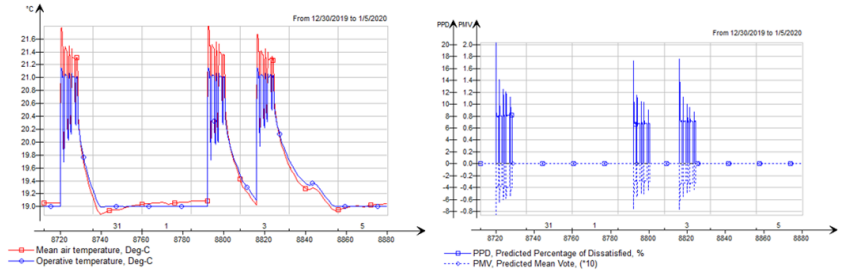

Figure I.12: Coldest week DV S-CO_2 control strategy winter temperatures (left) and Fanger's comfort indices (right)

I.4 DV D-CO_2 control strategy

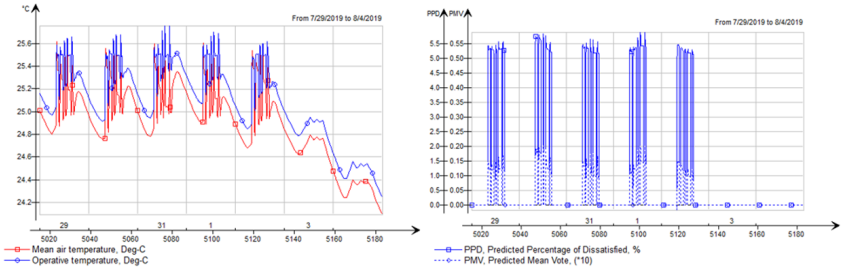

Figure I.13: Hottest week DV D-CO_2 control strategy case 1 temperatures (left) and Fanger's comfort indices (right)

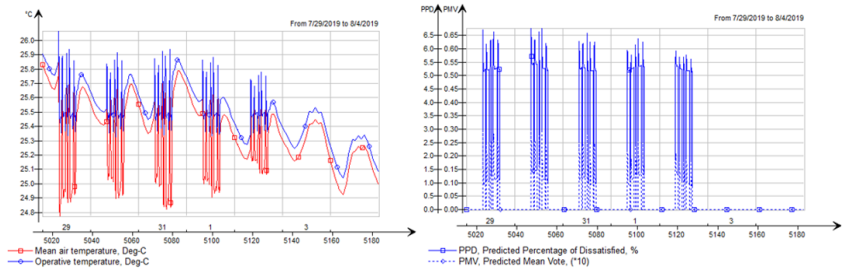

Figure I.14: Hottest week DV D-CO_2 control strategy case 2 temperatures (left) and Fanger's comfort indices (right)

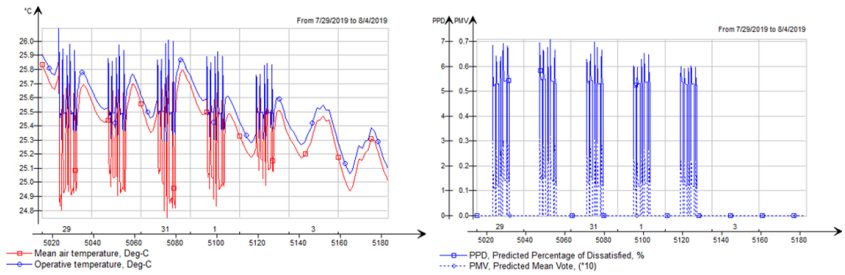

Figure I.15: Hottest week DV D-CO_2 control strategy case 3 temperatures (left) and Fanger's comfort indices (right)

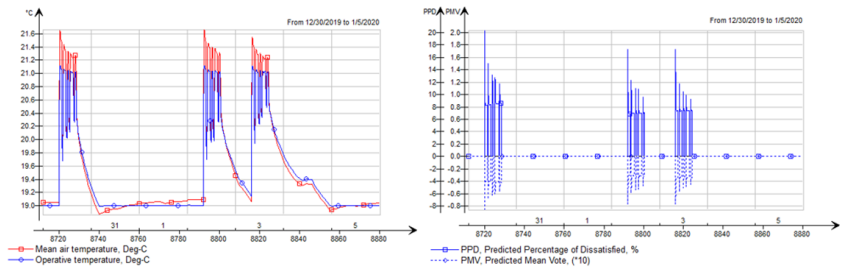

Figure I.16: Coldest week DV D-CO_2 control strategy winter temperatures (left) and Fanger's comfort indices (right)

I.5 DV S-CO_2 + temperature control strategy

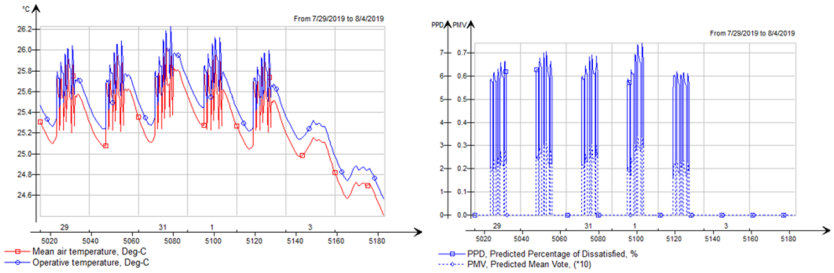

Figure I.17: Hottest week DV S-CO_2 + temperature control strategy case 1 temperatures (left) and Fanger's comfort indices (right)

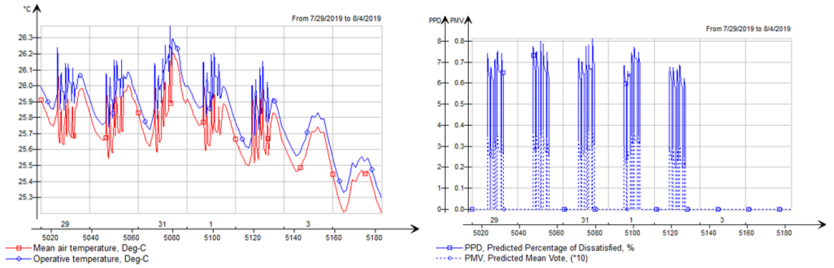

Figure I.18: Hottest week DV S-CO_2 + temperature control strategy case 2 temperatures (left) and Fanger's comfort indices (right)

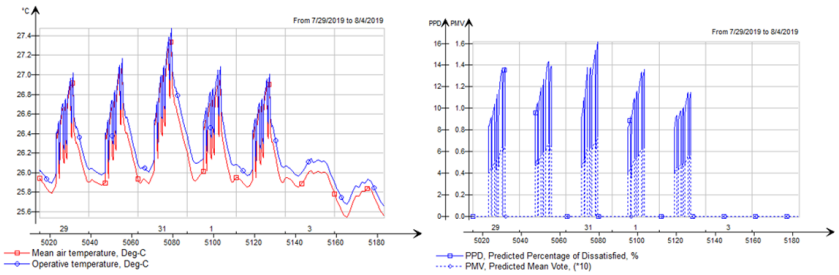

Figure I.19: Hottest week DV S-CO_2 + temperature control strategy case 3 temperatures (left) and Fanger's comfort indices (right)

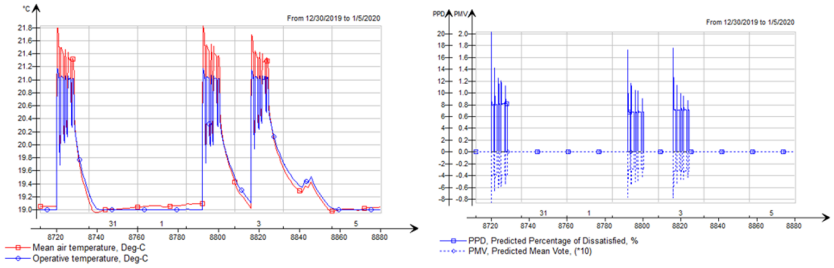

Figure I.20: Coldest week DV S-CO_2 + temperature control strategy winter temperatures (left) and Fanger's comfort indices (right)

J Boundary conditions of three-person office

Certain boundary conditions are extracted from the peer-reviewed scientific article «Modelling and simulation-based analysis of a façade-integrated decentralized ventilation unit» (Bonato et al., 2020). The majority of boundary conditions and assumptions are similar to the present work on a single-person office, although further complexity follows three-person offices, such as the occupancy schedule and the geometric values. The ventilation load must also be altered accordingly to the three-person reference zone with new minimum and maximum ventilation loads according to TEK 17 § 13-3 and considering around 13 % recirculation (Merzkirch et al., 2016). $\dot{Q}_{min}$ is calculated to be 19 $\frac{m^3}{h}$, so that with recirculation, $\dot{Q}_{min}$ becomes $\approx$ 22 $\frac{m^3}{h}$. $\dot{Q}_{max}$ is calculated to be 145.5 $\frac{m^3}{h}$, so that with recirculation, $\dot{Q}_{max}$ becomes $\approx$ 165 $\frac{m^3}{h}$.

The ventilation loads are based on the three-person reference zone, which is further implemented into IDA ICE (see figure J.1) (extracted directly from the referenced article (Bonato et al., 2020)):

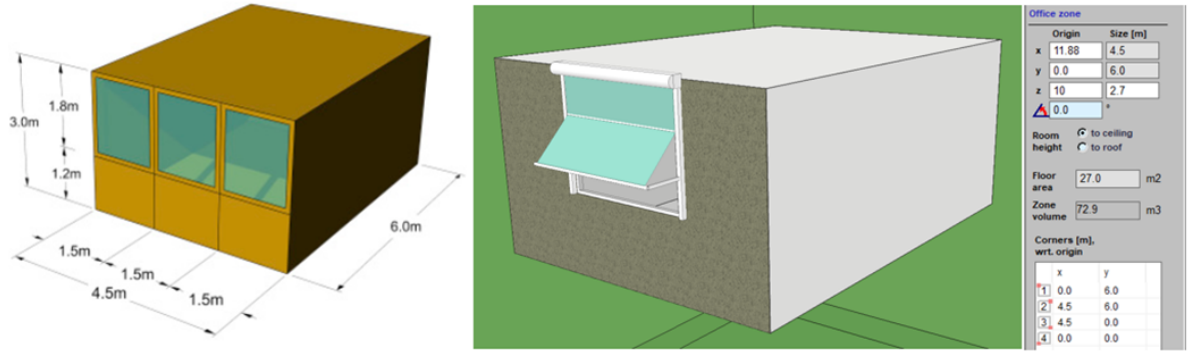

Figure J.1: Reference office zone (left) (Bonato et al., 2020), office zone model and geometric values in IDA ICE (right) for three-person office

The window area is corrected accordingly to $A_g \geq 0.07 * A_{floor}$ / LT (2.7 m^2) from TEK 17 § 13-7, so that the comparison results are compatible with the single-person office model since the relatively larger window area of the extracted model would produce increased cooling percentages concerning geometry and occupancy, as the window to floor area relationship is higher. Extracted DV unit specifications are similarly used on the three-person reference zone, although a higher max ventilation load of the DV unit is necessary without breaking the noise demands based on assumptions from DeAL (Mahler and Himmler, 2008).

An upper ventilation load of 235 $\frac{m^3}{h}$ can be used without breaking 35 dB(A) according to the datasheet of AM 300. On the AM 150, the upper limit was 115 $\frac{m^3}{h}$, and the upper limit according to DeAL was 85 $\frac{m^3}{h}$, which is a relationship of 0.74, which is transferred to the bigger DV unit becomes 174 $\frac{m^3}{h}$. This upper limit of 174 $\frac{m^3}{h}$ is therefore further used in the DV S-CO_2 + temperature control strategy on the three-person reference zone. This mirroring is a major assumption and should be treated as such. This assumption is made since the upper limit of this bigger DV unit cannot be found in articles, so an upper limit based on the smaller unit is done. This assumption is still well below the commercial datasheet value of the AM 300, so there is still a large margin for avoiding optimistic results error.

The extracted occupancy schedule (see figure J.2) (extracted directly from the referenced article (Bonato et al., 2020)):

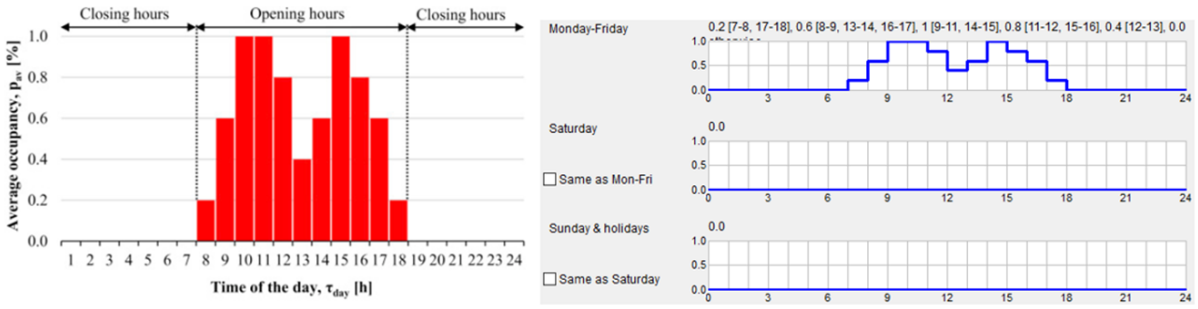

Figure J.2: Occupancy schedule of three-person office room (Bonato et al., 2020) (left), and IDA ICE schedule input (right)

Unlike the single-person reference zone occupancy schedule in the present work, the three-person reference zone occupancy schedule is based on a stochastic approach for modeling the spread of occupancy patterns around a reference average daily occupancy profile, as it is stated to yield a more accurate representation of the annual energy performance (Bonato et al., 2020).

Further internal loads are also added to fit the three-person office, which is simply multiplied by a factor of three from the single-person office internal loads. The internal loads also follow the occupancy schedule shown in figure J.2. Argumentation around having a different schedule for the internal loads can be made, although it is assumed to be sufficient here.

From the DV S-CO_2 + temperature control strategy, the upper limit of the max ventilation load with respect to sound level seems to be sufficient for keeping the temperature within acceptable levels within the zone. It should be noted that this is the most critical day of the year, so that all other days have better thermal comfort if outside dry-bulb temperature is considered, see figure J.3:

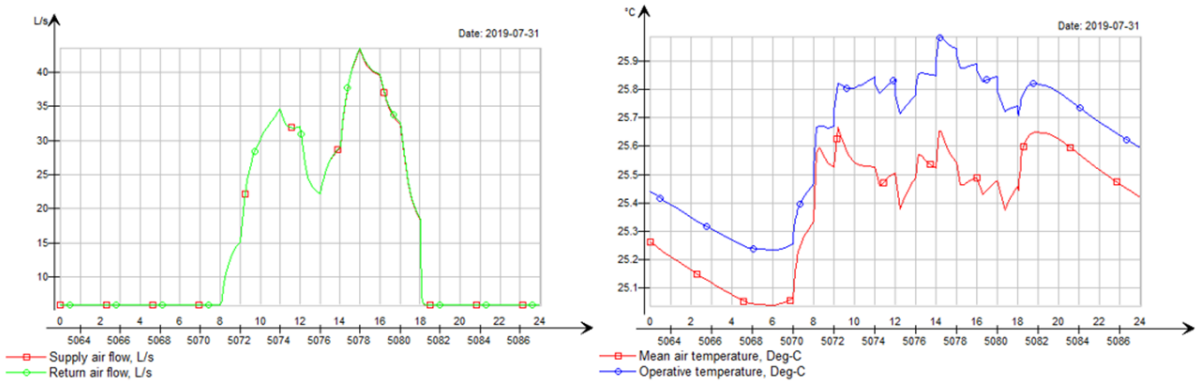

Figure J.3: Ventilation pattern (left) and zone temperatures (right) of DV S-CO_2 + temperature control strategy case 1 with max ventilation load 174 $\frac{m^3}{h}$ (48.3 $\frac{l}{s}$) for three-person office

The DV PIR and DV S-CO_2 control strategy needs a higher number of ventilation air rate modes for zones with more than one occupant, so that the ventilation load is proportionally controlled with a discreet number of steps, equal to that of number of occupants designed for the zone, see figure J.4:

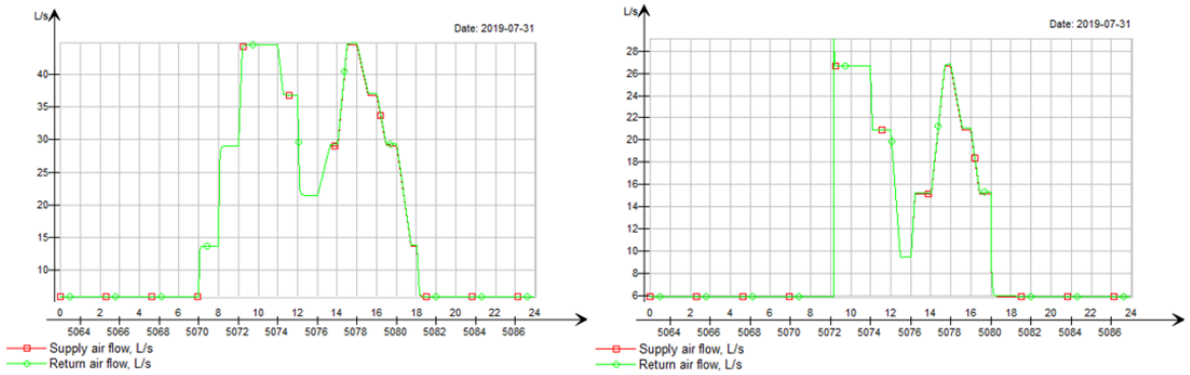

Figure J.4: Proportional ventilation pattern of DV PIR (left) and DV S-CO_2 (right) control strategy in three-person office

It should be noted that in practical circumstances only four vertical steps would be required in the three-person reference zone, unlike the stochastic approach visualized in figure J.4.

J.1 DV CAV control strategy (three-person office)

Table J.1: DV CAV control strategy primary energy results for summer, winter and, annually for three-person office (simulation)

DV CAV control strategy (seasons)				
IDA ICE simulation	Summer case 1	Summer case 2	Summer case 3	Winter
AHU fan power	2.34 $\frac{kWh}{m^2a}$	2.34 $\frac{kWh}{m^2a}$	2.34 $\frac{kWh}{m^2a}$	2.29 $\frac{kWh}{m^2a}$
AHU heating	0.26 $\frac{kWh}{m^2a}$	0.26 $\frac{kWh}{m^2a}$	0.26 $\frac{kWh}{m^2a}$	17.61 $\frac{kWh}{m^2a}$
AHU cooling	4.01 $\frac{kWh}{m^2a}$	3.41 $\frac{kWh}{m^2a}$	0.04 $\frac{kWh}{m^2a}$	0.00 $\frac{kWh}{m^2a}$
Local zone cooling	0.00 $\frac{kWh}{m^2a}$	0.00 $\frac{kWh}{m^2a}$	3.27 $\frac{kWh}{m^2a}$	0.00 $\frac{kWh}{m^2a}$
Local zone heating	8.84 $\frac{kWh}{m^2a}$	6.39 $\frac{kWh}{m^2a}$	2.69 $\frac{kWh}{m^2a}$	7.52 $\frac{kWh}{m^2a}$
Total primary energy	15.45 $\frac{kWh}{m^2a}$	12.40 $\frac{kWh}{m^2a}$	8.60 $\frac{kWh}{m^2a}$	27.42 $\frac{kWh}{m^2a}$

Table J.2: DV CAV control strategy primary energy results annually for three-person office (simulation)

DV CAV control strategy (annually)			
IDA ICE simulation	Case 1	Case 2	Case 3
AHU fan power	4.63 $\frac{kWh}{m^2a}$	4.63 $\frac{kWh}{m^2a}$	4.63 $\frac{kWh}{m^2a}$
AHU heating	17.87 $\frac{kWh}{m^2a}$	17.87 $\frac{kWh}{m^2a}$	17.87 $\frac{kWh}{m^2a}$
AHU cooling	4.01 $\frac{kWh}{m^2a}$	3.41 $\frac{kWh}{m^2a}$	0.04 $\frac{kWh}{m^2a}$
Local zone cooling	0.00 $\frac{kWh}{m^2a}$	0.00 $\frac{kWh}{m^2a}$	3.27 $\frac{kWh}{m^2a}$
Local zone heating	16.36 $\frac{kWh}{m^2a}$	13.91 $\frac{kWh}{m^2a}$	10.21 $\frac{kWh}{m^2a}$
Total primary energy	42.87 $\frac{kWh}{m^2a}$	39.82 $\frac{kWh}{m^2a}$	36.02 $\frac{kWh}{m^2a}$

J.2 DV PIR control strategy (three-person office)

Table J.3: DV PIR control strategy primary energy results for summer, winter, and annually for three-person office (simulation)

DV PIR control strategy (seasons)				
IDA ICE simulation	Summer case 1	Summer case 2	Summer case 3	Winter
AHU fan power	1.80 $\frac{kWh}{m^2a}$	1.80 $\frac{kWh}{m^2a}$	1.80 $\frac{kWh}{m^2a}$	1.77 $\frac{kWh}{m^2a}$
AHU heating	0.20 $\frac{kWh}{m^2a}$	0.20 $\frac{kWh}{m^2a}$	0.20 $\frac{kWh}{m^2a}$	13.63 $\frac{kWh}{m^2a}$
AHU cooling	3.01 $\frac{kWh}{m^2a}$	2.44 $\frac{kWh}{m^2a}$	0.03 $\frac{kWh}{m^2a}$	0.00 $\frac{kWh}{m^2a}$
Local zone cooling	0.00 $\frac{kWh}{m^2a}$	0.05 $\frac{kWh}{m^2a}$	4.63 $\frac{kWh}{m^2a}$	0.07 $\frac{kWh}{m^2a}$
Local zone heating	4.61 $\frac{kWh}{m^2a}$	3.36 $\frac{kWh}{m^2a}$	1.91 $\frac{kWh}{m^2a}$	6.89 $\frac{kWh}{m^2a}$
Total primary energy	9.62 $\frac{kWh}{m^2a}$	7.85 $\frac{kWh}{m^2a}$	8.57 $\frac{kWh}{m^2a}$	22.36 $\frac{kWh}{m^2a}$

Table J.4: DV PIR control strategy primary energy results annually for three-person office (simulation)

DV PIR control strategy (annually)			
IDA ICE simulation	Case 1	Case 2	Case 3
AHU fan power	3.57 $\frac{kWh}{m^2a}$	3.57 $\frac{kWh}{m^2a}$	3.57 $\frac{kWh}{m^2a}$
AHU heating	13.83 $\frac{kWh}{m^2a}$	13.83 $\frac{kWh}{m^2a}$	13.83 $\frac{kWh}{m^2a}$
AHU cooling	3.01 $\frac{kWh}{m^2a}$	2.44 $\frac{kWh}{m^2a}$	0.03 $\frac{kWh}{m^2a}$
Local zone cooling	0.07 $\frac{kWh}{m^2a}$	0.12 $\frac{kWh}{m^2a}$	4.70 $\frac{kWh}{m^2a}$
Local zone heating	11.50 $\frac{kWh}{m^2a}$	10.25 $\frac{kWh}{m^2a}$	8.80 $\frac{kWh}{m^2a}$
Total primary energy	31.98 $\frac{kWh}{m^2a}$	30.21 $\frac{kWh}{m^2a}$	30.93 $\frac{kWh}{m^2a}$

J.3 DV S-CO_2 control strategy (three-person office)

Table J.5: DV S-CO_2 control strategy primary energy results for summer, winter, and annually for three-person office (simulation)

DV S-CO_2 control strategy (seasons)				
IDA ICE simulation	Summer case 1	Summer case 2	Summer case 3	Winter
AHU fan power	1.18 $\frac{kWh}{m^2a}$	1.18 $\frac{kWh}{m^2a}$	1.18 $\frac{kWh}{m^2a}$	1.16 $\frac{kWh}{m^2a}$
AHU heating	0.15 $\frac{kWh}{m^2a}$	0.15 $\frac{kWh}{m^2a}$	0.15 $\frac{kWh}{m^2a}$	9.11 $\frac{kWh}{m^2a}$
AHU cooling	1.90 $\frac{kWh}{m^2a}$	1.31 $\frac{kWh}{m^2a}$	0.02 $\frac{kWh}{m^2a}$	0.00 $\frac{kWh}{m^2a}$
Local zone cooling	1.04 $\frac{kWh}{m^2a}$	2.86 $\frac{kWh}{m^2a}$	6.56 $\frac{kWh}{m^2a}$	0.22 $\frac{kWh}{m^2a}$
Local zone heating	2.00 $\frac{kWh}{m^2a}$	1.53 $\frac{kWh}{m^2a}$	1.06 $\frac{kWh}{m^2a}$	5.98 $\frac{kWh}{m^2a}$
Total primary energy	6.27 $\frac{kWh}{m^2a}$	7.03 $\frac{kWh}{m^2a}$	8.97 $\frac{kWh}{m^2a}$	16.47 $\frac{kWh}{m^2a}$

Table J.6: DV S-CO_2 control strategy primary energy results annually for three-person office (simulation)

DV S-CO_2 control strategy (annually)			
IDA ICE simulation	Case 1	Case 2	Case 3
AHU fan power	2.34 $\frac{kWh}{m^2a}$	2.34 $\frac{kWh}{m^2a}$	2.34 $\frac{kWh}{m^2a}$
AHU heating	9.26 $\frac{kWh}{m^2a}$	9.26 $\frac{kWh}{m^2a}$	9.26 $\frac{kWh}{m^2a}$
AHU cooling	1.90 $\frac{kWh}{m^2a}$	1.31 $\frac{kWh}{m^2a}$	0.02 $\frac{kWh}{m^2a}$
Local zone cooling	1.26 $\frac{kWh}{m^2a}$	3.08 $\frac{kWh}{m^2a}$	6.78 $\frac{kWh}{m^2a}$
Local zone heating	7.98 $\frac{kWh}{m^2a}$	7.51 $\frac{kWh}{m^2a}$	7.04 $\frac{kWh}{m^2a}$
Total primary energy	22.74 $\frac{kWh}{m^2a}$	23.50 $\frac{kWh}{m^2a}$	25.44 $\frac{kWh}{m^2a}$

J.4 DV D-CO_2 control strategy (three-person office)

Table J.7: DV D-CO_2 control strategy primary energy results for summer, winter, and annually for three-person office (simulation)

DV D-CO_2 control strategy (seasons)				
IDA ICE simulation	Summer case 1	Summer case 2	Summer case 3	Winter
AHU fan power	1.71 $\frac{kWh}{m^2a}$	1.71 $\frac{kWh}{m^2a}$	1.71 $\frac{kWh}{m^2a}$	1.66 $\frac{kWh}{m^2a}$
AHU heating	0.26 $\frac{kWh}{m^2a}$	0.26 $\frac{kWh}{m^2a}$	0.26 $\frac{kWh}{m^2a}$	12.94 $\frac{kWh}{m^2a}$
AHU cooling	3.03 $\frac{kWh}{m^2a}$	2.36 $\frac{kWh}{m^2a}$	0.03 $\frac{kWh}{m^2a}$	0.00 $\frac{kWh}{m^2a}$
Local zone cooling	0.00 $\frac{kWh}{m^2a}$	0.66 $\frac{kWh}{m^2a}$	4.90 $\frac{kWh}{m^2a}$	0.00 $\frac{kWh}{m^2a}$
Local zone heating	4.01 $\frac{kWh}{m^2a}$	2.95 $\frac{kWh}{m^2a}$	1.73 $\frac{kWh}{m^2a}$	7.51 $\frac{kWh}{m^2a}$
Total primary energy	9.01 $\frac{kWh}{m^2a}$	7.94 $\frac{kWh}{m^2a}$	8.63 $\frac{kWh}{m^2a}$	22.11 $\frac{kWh}{m^2a}$

Table J.8: DV D-CO_2 control strategy primary energy results annually for three-person office (simulation)

DV D-CO_2 control strategy (annually)			
IDA ICE simulation	Case 1	Case 2	Case 3
AHU fan power	3.37 $\frac{kWh}{m^2a}$	3.37 $\frac{kWh}{m^2a}$	3.37 $\frac{kWh}{m^2a}$
AHU heating	13.20 $\frac{kWh}{m^2a}$	13.20 $\frac{kWh}{m^2a}$	13.20 $\frac{kWh}{m^2a}$
AHU cooling	3.03 $\frac{kWh}{m^2a}$	2.36 $\frac{kWh}{m^2a}$	0.03 $\frac{kWh}{m^2a}$
Local zone cooling	0.00 $\frac{kWh}{m^2a}$	0.66 $\frac{kWh}{m^2a}$	4.90 $\frac{kWh}{m^2a}$
Local zone heating	11.52 $\frac{kWh}{m^2a}$	10.46 $\frac{kWh}{m^2a}$	9.24 $\frac{kWh}{m^2a}$
Total primary energy	31.12 $\frac{kWh}{m^2a}$	30.05 $\frac{kWh}{m^2a}$	30.74 $\frac{kWh}{m^2a}$

J.5 DV S-CO_2 + temperature control strategy (three-person office)

Table J.9: DV S-CO_2 + temperature control strategy primary energy results for summer, winter, and annually for three-person office (simulation)

DV S-CO_2 + temperature control strategy (seasons)				
IDA ICE simulation	Summer case 1	Summer case 2	Summer case 3	Winter
AHU fan power	1.23 $\frac{kWh}{m^2a}$	1.37 $\frac{kWh}{m^2a}$	2.21 $\frac{kWh}{m^2a}$	1.31 $\frac{kWh}{m^2a}$
AHU heating	0.15 $\frac{kWh}{m^2a}$	0.15 $\frac{kWh}{m^2a}$	0.15 $\frac{kWh}{m^2a}$	10.94 $\frac{kWh}{m^2a}$
AHU cooling	2.43 $\frac{kWh}{m^2a}$	2.38 $\frac{kWh}{m^2a}$	0.05 $\frac{kWh}{m^2a}$	0.00 $\frac{kWh}{m^2a}$
Local zone cooling	0.00 $\frac{kWh}{m^2a}$	0.00 $\frac{kWh}{m^2a}$	0.00 $\frac{kWh}{m^2a}$	0.00 $\frac{kWh}{m^2a}$
Local zone heating	1.97 $\frac{kWh}{m^2a}$	1.51 $\frac{kWh}{m^2a}$	1.05 $\frac{kWh}{m^2a}$	5.81 $\frac{kWh}{m^2a}$
Total primary energy	5.78 $\frac{kWh}{m^2a}$	5.41 $\frac{kWh}{m^2a}$	3.46 $\frac{kWh}{m^2a}$	18.06 $\frac{kWh}{m^2a}$

Table J.10: DV S-CO_2 + temperature control strategy primary energy results annually for three-person office (simulation)

DV S-CO_2 + temperature control strategy (annually)			
IDA ICE simulation	Case 1	Case 2	Case 3
AHU fan power	2.54 $\frac{kWh}{m^2a}$	2.68 $\frac{kWh}{m^2a}$	3.52 $\frac{kWh}{m^2a}$
AHU heating	11.09 $\frac{kWh}{m^2a}$	11.09 $\frac{kWh}{m^2a}$	11.09 $\frac{kWh}{m^2a}$
AHU cooling	2.43 $\frac{kWh}{m^2a}$	2.38 $\frac{kWh}{m^2a}$	0.05 $\frac{kWh}{m^2a}$
Local zone cooling	0.00 $\frac{kWh}{m^2a}$	0.00 $\frac{kWh}{m^2a}$	0.00 $\frac{kWh}{m^2a}$
Local zone heating	7.78 $\frac{kWh}{m^2a}$	7.32 $\frac{kWh}{m^2a}$	6.86 $\frac{kWh}{m^2a}$
Total primary energy	23.84 $\frac{kWh}{m^2a}$	23.47 $\frac{kWh}{m^2a}$	21.52 $\frac{kWh}{m^2a}$

K Centralized CAV system for energy comparison

A centralized system with a CAV control strategy is used as the frame of reference for energy savings comparison. Typically, a whole building is used for the frame of reference, although the relevant zone is only a single-person office room, so some simplifications are necessary. The minimum demands according to TEK 17 § 14-2 are used for the centralized air handling unit, and the typical operating hours for the whole building is assumed to be equal to that of the office room, wherein Norway, the typical operating times of an office building is 12 hours in weekdays which equals 3000 hours a year (Mysen et al., 2003). The reduction of percentage from max load to part load is also assumed identical for the whole building and office room, where the office room goes from 51 $\frac{m^3}{h}$ to 7 $\frac{m^3}{h}$ (excluding recirculation due to strategic placing of return and intake air), which has an air rate reduction factor of around 20 % (assumed sufficient) which is typical for office buildings during nighttime. Max loads and part loads of the office room and building are therefore present at equal time periods, with equal air rate reduction factor (Schild and Mysen, 2009).

The centralized system includes a heat recovery unit with 80 % efficiency and a total pressure drop of 1050 Pa, where the total fan efficiency is 70 %, this yields a specific fan power of 1.5 $\frac{kWs}{m^3}$. The part-load performance calculation uses an integrated function, which is calculated accordingly to ASHRAE stnd. 90.1 (2007) app.G in IDA ICE, which then lowers the SFP at lower air rates, and fan energy savings are the result. There is also thermal energy savings present, as a central AHU produces temperature rise over the fans according to $\Delta T_{fan\ rise} = 0.0011 * \Delta p = 0.5$K. The system set-up in IDA ICE can be seen in figure K.1:

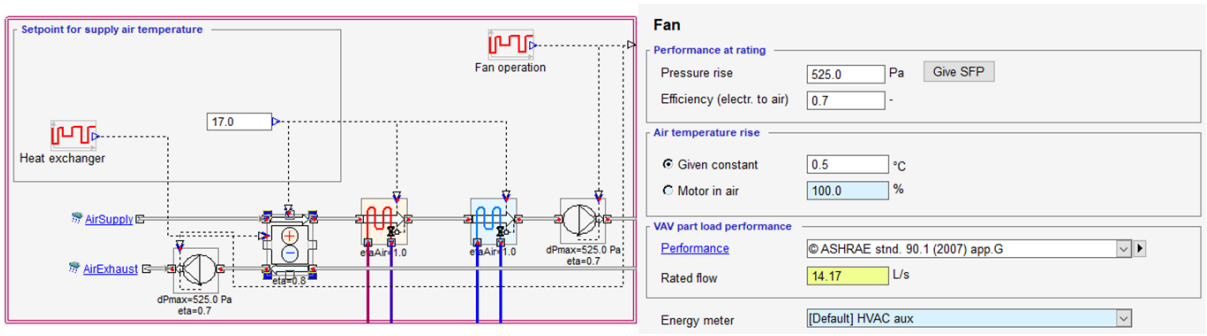

Figure K.1: Centralized CAV ventilation system AHU control in IDA ICE

The results are divided into the summer season, winter season, and annually, and are tested under case 1 condition as case 2 and 3 are not typical during a centralized system, see table K.1 and figure K.2:

Table K.1: Primary energy consumption for centralized ventilation under CAV control strategy by season and annually (simulation)

Centralized CAV case 1 conditions			
IDA ICE simulation	Summer	Winter	Annually
AHU fan power	3.30 $\frac{kWh}{m^2a}$	3.17 $\frac{kWh}{m^2a}$	6.47 $\frac{kWh}{m^2a}$
AHU heating	0.01 $\frac{kWh}{m^2a}$	11.20 $\frac{kWh}{m^2a}$	11.21 $\frac{kWh}{m^2a}$
AHU cooling	3.54 $\frac{kWh}{m^2a}$	0.00 $\frac{kWh}{m^2a}$	3.54 $\frac{kWh}{m^2a}$
Local zone cooling	0.04 $\frac{kWh}{m^2a}$	0.22 $\frac{kWh}{m^2a}$	0.26 $\frac{kWh}{m^2a}$
Local zone heating	3.72 $\frac{kWh}{m^2a}$	7.48 $\frac{kWh}{m^2a}$	11.20 $\frac{kWh}{m^2a}$
Total primary energy	10.61 $\frac{kWh}{m^2a}$	22.07 $\frac{kWh}{m^2a}$	32.68 $\frac{kWh}{m^2a}$

The additional zone cooling energy during winter is thought to be a consequence of the lower zone temperature set-points in combination with internal heat gains during some specific hot days during the winter season, although this is rare. During summer there are higher temperature set-points, and so the constant ventilation cooling load is sufficient for thermal maintenance.

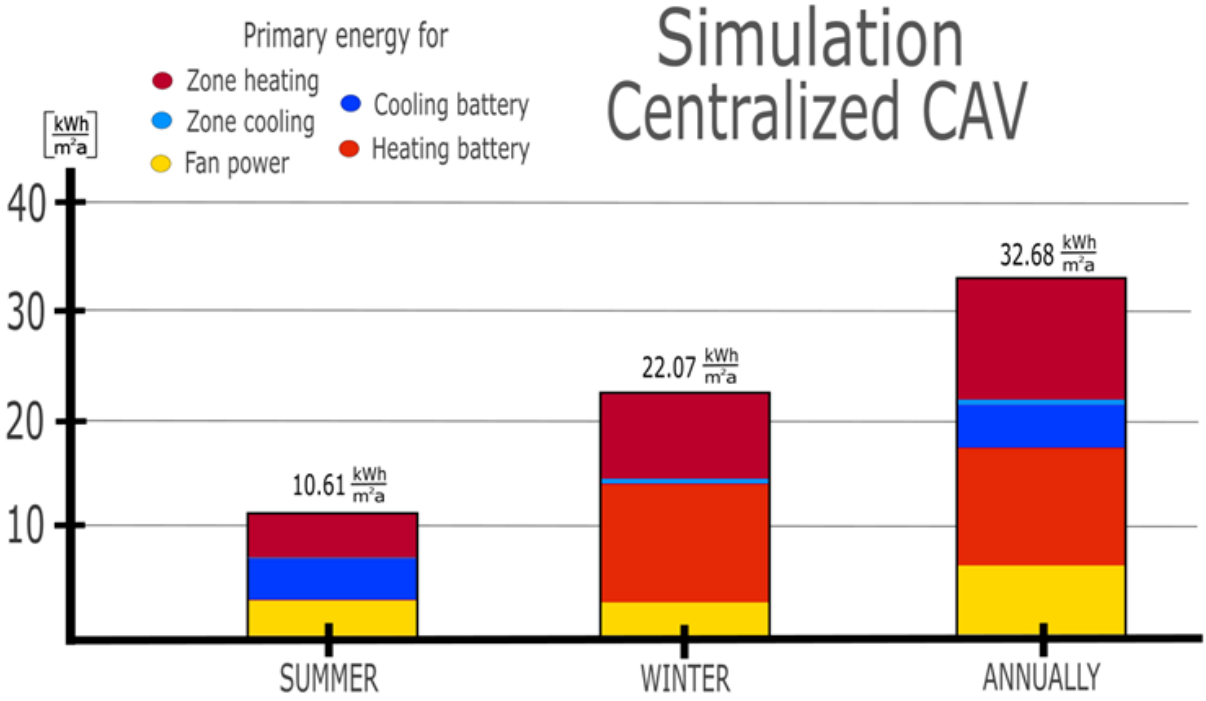

Figure K.2: Primary energy consumption for centralized ventilation under CAV strategy by season and annually

L HRU absence and efficiency variations on energy presence

Firstly, determination of the pressure drop across the HRU is necessary as this is the decider of fan power energy savings. Any disturbance of the flow will cause a pressure drop, and it is the velocity of the flow that determines the amount of pressure drop in combination with the disturbance pattern. The velocity is further determined by the air rate so that minimum air rates will have fewer pressure drops, and maximum air rates will have high-pressure drops. The amount of minimum and maximum air rates are further controlled by the ventilation control strategies, so that these strategies will also have an important saying in whether or not it is favorable to keep or remove the HRU, although this analysis cannot be given here.

An article did an experimental investigation on the aeraulic performance of a decentralized AHU, where the pressure drop across the HRU and the total pressure drop across the unit have been measured (Gendebien et al., 2012). The DV unit is a double-flow recuperative HR AHU, which is similar to the investigated design, and the air rates were kept under a 100 $\frac{m^3}{h}$, which is within the boundaries of the present conditions. The pressure drop was measured with a pressure sensor of $\pm$ 1 Pa error for pressures under 100 Pa. The coalescence of the pressure drop of this specific HRU, and the SFP and HRU efficiency used from the FTDVS study are not possible to determine so that the accuracy of the produced results must be treated with this limitation in mind. With the absence of certain coalescence, simplifications for determining the HRU pressure drop can be made without knowingly sacrificing accuracy of energy calculations, but still keeping the accuracy within acceptable limits, which is favorable in the present research as accurate pressure drops must be measured for each DV unit and air rate, which cannot be given in this study anyway. The simplified extraction of pressure drops across the HRU is done by comparing the HRU pressure drop to the total pressure drop and using this relationship factor for the DV unit measurements done in the FTDVS study, which is the measurements used for energy calculations. There are two measurements for each matrix given with some discrepancies, so the average is taken and compared to the total pressure drop measured with the filter (Gendebien et al., 2012).

At an air rate of 35 $\frac{m^3}{h}$, the pressure drop across the HRU was measured to be 30 Pa, while the total pressure drop was measured at 50 Pa. This gives a pressure relationship of 0.6 at this specific air rate. This relationship seems to be reoccurring at each air rate with some minor discrepancies. Some other relationships are: 50 $\frac{m^3}{h}$ gives 45 Pa / 75 Pa = 0.6, and 80 m$\frac{m^3}{h}$ gives 90 Pa / 155 Pa = 0.58. This specific relationship of 0.6 is therefore used further with FTDVS measurements when deciding SFP values without the HRU pathing disturbance.

In building simulation, a constant SFP of 0.800 $\frac{kWs}{m^3}$ is used, which is the result of a total fan efficiency of 0.164 and a total pressure drop of 0.1312 kPa. By not integrating the HRU in this specific DV unit, the new theoretical total pressure drop is 0.1312 kPa - 0.6 * 0.1312 kPa = 0.055 kPa in accordance with the simplified extraction of the pressure relationship. This new total pressure drop yields a new DV unit $SFP_{no\,HRU}$ of 0.335 $\frac{kWs}{m^3}$. The remaining pressure drop is caused by filters, friction, and collision towards walls and other present obstacles. The HRU is a major pressure drop contributor due to its specific corrugations which causes more collision intensity and turbulence, which favors the thermal performance in heat exchange.

The $SFP_{no\,HRU}$ value is used in calculations of HRU efficiency = 0, while at the other HRU efficiencies of 0.4 – 0.9 (step increase 0.1), the original SFP value 0.800 $\frac{kWs}{m^3}$ is used, as the relationship of thermal efficiency and pressure drop is not possible to determine due to complications and lack of data. The aeraulic and thermal performance study only measured the already known phenomenon of decreased heat exchange performance when increasing the air rate, as aforementioned (Gendebien et al., 2012).

The HRU efficiencies with their respective SFP values will be investigated through the use of IDA ICE building simulation tool while using the DV S-CO_2 + temperature control strategy, while case 1, 2 and 3 (summer) and winter is all investigated, see appendix H.2, table H.11 – H.31 for energy performance results. The AHU control under the scenarios with bypass function HRU's or absence of HRU can be seen in appendix F.2, figure F.5 – F.10, while the AHU control under different HRU efficiencies are similarly to appendix F.1, figure F.1 – F.4, although with different HRU efficiencies.

Ignoring the HRU is also not the only consideration when discussing the energy performance of the DV unit, according to work done on natural fan-assisted ventilation (Kim and Baldini, 2016), the DV unit can run on bypass mode to avoid the HRU pressure resistance whenever the outside air conditions allow it, resulting in lower SFP and improved energy performance. It is stated "During the period when fan-assisted NV can be used, heating, cooling and pumping energy are not required to run the HVAC system, and the fan loads alone deal with the entire HVAC energy demand in buildings" (Kim and Baldini, 2016), where it was also concluded that the DV system saves around 76 % of fan energy consumption compared to the CV system based on the specific boundary conditions in the article (Kim and Baldini, 2016).

A simple method of deciding acceptable outside dry bulb temperatures can be made from the energy balance equation based on internal heat gains and thermal comfort, which is between 13 °C and 25 °C, although this is based on the boundary conditions described in the article (Kim and Baldini, 2016). Analyzing the specific Fornebu weather data file, the number of hours of which this temperature limit is achieved can be decided, which decides the number of hours the DV unit can run on HRU bypass mode. The number of hours is 2074, and is accumulated between April and September, and is decided without consideration to any humidity limits, unlike the referenced article (Kim and Baldini, 2016). This is a total availability of 23.7 % of fan-assisted natural ventilation, which is similar to the findings which found that European countries have availability of around 22.0 – 32.0 % each year (Kim and Baldini, 2016). The amount of energy saved from this automated HRU bypass mode is difficult to determine, as it is depending on complicated factors such as when the bypass hours are accumulated and how it merges with the present ventilation control strategies and internal gains. Energy savings results are further referenced to the findings in the referenced article (Kim and Baldini, 2016), and not included in the present work, although Norway is not part of the study and the boundary conditions are different, the general findings are still of value for Norway climate in combination with the DV technology.

M AM 150 with manufacturer datasheet specifications

Analyzing the AM 150 DV unit with SFP, HRU efficiency, and sound generation-specific air rates extracted directly from the manufacturer Airmaster datasheet in combination with the DV S-CO_2 + temperature control strategy is conducted to investigate how an increased HRU efficiency, SFP value and a higher tolerance for air rates impact the primary energy consumption of the system, although the accuracy of the extracted specifications cannot be given. The results are compared to the centralized CAV system and the representative DV unit results which are based on scientific data and field measurements to analyze the improvement of energy performance the AM 150 DV unit would achieve using Airmaster specifications. All datasheet specifications which are relevant for energy calculations are extracted from the official datasheet given by Airmaster (Airmaster, 2020a).

The relevant specifications which are to be extracted are the max air rate concerning sound level $L_{p,Aeq}$, which should not exceed 35 dB(A) according to Byggforsk 421.421, the HRU efficiency of the recuperative HRU and the SFP of the fans. There are some limitations present in the datasheet, these being that the minimum air rate tested under their specific test conditions is 50 $\frac{m^3}{h}$, so that a constant value will have to be used for all air rates as a simplification since there are no values for < 50 $\frac{m^3}{h}$. All specifications are extracted under the condition of the strictest air filter combination, ePM1 80 % supply filter / ePM10 75 % exhaust filter which yields the highest pressure drop of the filter combinations.

The testing was done concerning the Airmaster specific conditions and in accordance to Norwegian standard test conditions. The sound level $L_{p,Aeq}$ was measured at a height of 1.2 meters above floor level and a horizontal distance of 1 meter away from the AM 150 unit. The HRU efficiency was tested according to EN 308:1997 conditions, which describes a balanced supply and exhaust flow, room air temperature of 25 °C, and an outside temperature of 5 °C. The SFP is measured by measuring the electric power with its respective air rate.

The sound level is read at 35 dB(A) at 115 $\frac{m^3}{h}$ concerning the Airmaster reference test conditions, so this air rate is therefore further used as the max air rate in the building simulation. The HRU efficiency is assumed constant at 85 %, as the HRU efficiency is 85 % at 60 $\frac{m^3}{h}$ and further rises as the air rate is reduced, and reaches 80 % at 150 $\frac{m^3}{h}$. The SFP is assumed constant at 0.700 $\frac{kWs}{m^3}$ since the global minimum of SFP is 0.550 $\frac{kWs}{m^3}$ at 60 $\frac{m^3}{h}$, and is further symmetrically increased in each direction. The SFP value of 0.700 $\frac{kWs}{m^3}$ is chosen as the S-CO_2 + temperature control strategy varies quite a lot within the minimum and maximum air rate interval, so that lower and more optimistic SFP values could be inaccurate.